Cellular mechanisms underlying the ACE inhibitor capacity to stimulate kidney self-repair

Thesis

CELLULAR MECHANISMS UNDERLYING THE ACE INHIBITOR CAPACITY TO STIMULATE KIDNEY SELF-REPAIR

Thesis submitted by

Paola Rizzo

for the degree of

Doctor of Philosophy

Discipline of Life Sciences

Open University Research School, London, UK

IRCCS – Istituto di Ricerche Farmacologiche Mario Negri, Bergamo, Italy

Director of Studies

Dr. Ariela Benigni

Second Supervisor

Prof. Malcolm R. Alison

February 2014

CELLULAR MECHANISMS UNDERLYING THE ACE INHIBITOR CAPACITY TO STIMULATE KIDNEY SELF-REPAIR

Paola Rizzo

IRCCS – Istituto di Ricerche Farmacologiche Mario Negri
Open University Research School, London
Doctor of Philosophy
March 2014

ABSTRACT

Bowman's capsule parietal epithelial cell activation occurs in several human proliferative glomerulonephritides. The cellular composition of the resulting crescentic lesions is controversial, although a population of renal progenitor cells, which in adult healthy kidney contributes to the physiological cell turnover, has been proposed to be a major constituent. In this study we try to get light into the mediators involved in the aberrant progenitor cell proliferation and migration into the Bowman's space, which occurs in presence of an extended glomerular injury.
To this aim, we studied 36 renal biopsies of patients with proliferative and non proliferative glomerulopathies. In parallel, we also analyzed the Munich Wistar Frömter rats with proliferative glomerulonephritis, characterizing for the first time a population of renal progenitor cells also in rodents. We demonstrated that dysregulated progenitor cells of the Bowman's capsule invade the glomerular tuft exclusively in proliferative disorders. In both humans and rats, up-regulation of the CXCR4 chemokine receptor on progenitor cells was accompanied by high expression of its ligand, stromal-derived factor-1 (SDF-1) in podocytes. Parietal epithelial cell proliferation might be sustained by increased expression of the angiotensinII type1 (AT_1) receptor. Treatment with the antihypertensive drug angiotensin-converting enzyme (ACE) inhibitor, reduces the number and the extension of crescents, limiting progenitor cell proliferation and migration. Moreover, ACE inhibitor normalized the expression of CXCR4, SDF-1 and AT_1 receptor on progenitor cells.
These results suggest that glomerular crescents derive from the proliferation and migration of renal progenitors in response to injured podocytes. The SDF-1/CXCR4 axis, together with the AngII/AT_1 receptor pathway, contributes to the dysregulated response of renal progenitors. Targeting the AngII/AT_1/CXCR4 pathway may be beneficial in severe forms of glomerular proliferative disorders.

CONTENTS

LIST OF ABBREVIATIONS ..... i-ii

CHAPTER 1 1
INTRODUCTION

1.1 Chronic kidney disease 2

1.2 The MWF rat model 4

1.3 Extracapillary glomerulonephritis 7

1.4 Role of chemokines in the proliferative pathway 10

1.5 Role of ACE inhibitors in renal disease remission and regression 12
1.5.1 Evidence in animal models 12
1.5.2 Evidence in humans 14

1.6 Role of renal progenitor cells in kidney repair 16
1.6.1 De-differentiation of tubular cells 17
1.6.2 Recruited extra-renal stem cells 17
1.6.3 Resident renal progenitor cells 18

Table 1 24

CHAPTER 2 25
MATERIALS

2.1 Rats 26

2.2 Cells 26

2.3 Fixatives 26

2.4 Media, supplements and reagents for *in vitro* study 27

2.5 Chemicals 27

2.6 Buffers and solutions 28

2.7 Antibodies 30
2.7.1 Primary antibodies 30
2.7.2 Secondary antibodies 31

2.8 Other reagents 32

2.9 Disposable material....33

2.10 Instruments....34

CHAPTER 3....35
METHODS

Methods for *in vivo* studies in the experimental rat model

3.1 Munich Wistar Fromter rats....36

3.2 Renal function measurement....37

3.3 Sacrifice and tissue collection....38

3.4 Renal morphology by light microscopy....39

3.5 Immunohistochemistry....41
3.5.1 Immunofluorescence....41
3.5.2 Immunoperoxidase....45

3.6 Immunogold....47

3.7 Statistical analysis....48

Methods for *in vitro* studies in the experimental rat model

3.8 Cells and cell culture....50

3.9 Immunofluorescence....51

3.10 Statistical analysis....54

Methods for *in vivo* studies in human tissue

3.11 Patients....55

3.12 Demographic and clinical characteristics of patient populations....56
3.12.1 Evaluation of systemic blood pressure....57
3.12.2 Assessment of urinary protein concentrations....57
3.12.3 Assessment of serum creatinine concentrations....58

3.13 Biopsy and tissue collection 58

3.14 Renal morphology by light microscopy 58

3.15 Immunohistochemistry 59
3.15.1 Immunofluorescence 59
3.15.2 Immunoperoxidase 62

3.16 Statistical analysis 63

3.17 Principles of the main instruments 64
3.17.1 Light microscopy 64
3.17.2 Immunofluorescence technique and confocal microscopy 65
3.17.2 Transmission electron microscopy 67

CHAPTER 4 69
RESULTS IN MWF RATS

4.1 Introduction 70

4.2 A population of renal progenitor cells exists within the Bowman's capsule of normal adult rat kidney 71

4.3 Time-dependent evolution of glomerular lesions in Wistar and MWF rats 73

4.4 Phenotype of cell population involved in crescentic lesions in MWF rats. 74

4.5 Treatment with ACE inhibitor reduces proteinuria and induces regression of crescentic lesions 75

4.6 ACE inhibitor limits cell proliferation in crescents 76

4.7 ACE inhibitor preserves Bowman's capsule architecture 77

4.8 Mechanism underlying the renoprotective effect of ACEi 79
4.8.1 Role of the transcription factor C/EBPδ 79
4.8.2 Role of the chemokine receptor CXCR4 79
4.8.3 Role of AT_1 receptor 80

4.9 *In vitro* characterization of PECs 81

Figure 1 83
Figure 2 84

Figure 3. 85
Figure 4 86
Figure 5 87
Figure 6 88
Figure 7. 89
Figure 8 90
Figure 9 91
Figure 10 92
Figure 11 93
Figure 12 94
Figure 13 95
Figure 14 96

CHAPTER 5 97
RESULTS IN HUMAN TISSUE

5.1 Introduction 98

5.2 Clinical and histopathologic characteristics of patient populations..99

5.3 $CD133^{+}CD24^{+}$ renal progenitor cells are major constituents of hyperplastic lesions....101

5.4 CXCR4 is overexpressed in progenitor cells within extracapillary lesions....102

5.5 Podocytes express the CXCR4 ligand SDF-1....102

5.6 AT_1 receptor overexpression on progenitor cells in human proliferative disorders....103

5.7 ACE inhibitor therapy limits the formation of crescentic lesions in a patient with extracapillary glomerulonephritis....104

5.8 ACEi renoprotection occurs via the restoration of CXCR4 and AT_1 receptor expression 105

Table 2....107
Figure 15 108
Figure 16 109
Figure 17 110
Figure 18 111
Figure 19 112
Figure 20 113

CHAPTER 6.....115
DISCUSSION

Figure 21.....124

CHAPTER 7.....125
BIBLIOGRAPHY

CHAPTER 8.....147
APPENDICES

8.1 Contribution to the thesis by other researchers.....148

8.2 Publications concerining the work described in this thesis.....149

8.3 Full list of publications by the candidate on topics not associated with the work described in the thesis. 149

8.4 Congress presentations related to the work described in this thesis.....152

ACKNOWLEDGMENTS.....153

LIST OF ABBREVIATIONS

ABC	avidin-biotin peroxidase complex solution
ACEi	Angiotensin-converting enzyme inhibitor
ALDH	aldehyde dehydrogenase
ANCA	antineutrophil cytoplasm antibodies
Ang II	Angiotensin II
ARBs	angiotensin II type 1 receptor blockers
AT_1	angiotensin II type 1
BrdU	5-bromo-2-deoxyuridine
BSA	bovine serum albumin
C/EBPδ	CCAAT/enhancer binding protein
CKD	chronic kidney disease
DAB	3,3'-diaminobenzidine
DAPI	4',6'-diamidino-2-phenylindole dihydrochloride hydrate
DBP	diastolic blood pressure
DMEM	Dulbecco's modified eagle's medium
ECM	extracellular matrix
EGF	epidermal growth factor
EGM-MV	endothelial growth medium-microvascular
ESRD	end-stage renal disease
FCS	foetal calf serum
FITC	fluorescein isothiocyanate
FSGS	focal segmental glomerulosclerosis
G-CSF	granulocyte colony stimulating factor
GDNF	glial cell line derived neurotrophic factor
GFR	glomerular filtration rate
H3p	phospho-histone H3
HGF	hepatocyte growth factor
HPF	high power field

HSC	haematopoietic stem cell
MSC	mesenchymal stem cell
MWF	Munich Wistar Frömter
NCAM	neural cell adhesion molecule
PAS	periodic acid-Schiff's reagent
PBS	phosphate buffer saline
PCR	polymerase chain reaction
PEC	parietal epithelial cell
PFA	paraformaldehyde
RAS	rennin-angiotensin system
REIN	Ramipril Efficacy in Nephropathy
RRT	renal replacement therapies
SBP	systolic blood pressure
SCID	severe combined immunodeficiency
SDF-1	stromal cell-derived factor
SP	side population
SYN	synaptopodin
TGF-β	transforming growth factor β
VHL	von Hippel–Lindau
WT-1	Wilm's tumor-1

CHAPTER 1

INTRODUCTION

1.1 Chronic kidney disease

Chronic kidney disease (CKD) is a general term to indicate the slow loss of kidney function over time, and also includes some complications such as hypertension, anemia, malnutrition, bone and mineral disorders, and neuropathy as well as increased risk of cardiovascular disease (Dinneen *et al.*, 1997). The definition of CKD is based on the presence of kidney damage (i.e. albuminuria) or decreased kidney function (i.e. glomerular filtration rate [GFR] below 60 ml/min per 1.73 m^2) over a period of 3 months.

CKD is a worldwide threat to public health since it has been estimated that diseases of the kidney account for 830,000 deaths every year, with the sharp rise of renal replacement therapy now exceeding two million patients for cost of more than a trillion US$ (Just *et al.*, 2008). The burden of CKD is not limited to the demand for renal replacement therapies (RRT), which consists primarily of kidney transplantation, haemodialysis and peritoneal dialysis, since they are also a major determinant of cardiovascular diseases with a direct impact on health (Gridelli *et al.*, 2000; Van Der Meer *et al*, 2010).

Approximately 2 million people are currently treated with RRT, but this likely represents less than 10% of those who need them (Eggers *et al.*, 2011). More than 90% of these individuals live in industrialized countries, while available RRT in developing countries is scarce, and null in underdeveloped areas. Many developed nations spend more than 2-3% of

their annual health-care budget to provide treatment for end-stage renal disease (ESRD), while the population with ESRD represents approximately 0.02-0.03% of the total population (Couser *et al.*, 2011).

The leading causes of CKD leading to kidney failure in the United States are diabetes, hypertension and glomerulonephritis (Collins *et al.*, 2009). The kidney disease tends to worsen over time through a sequence of risk factors (i.e. genetic, developmental or demographic), conditions that can cause kidney damage (i.e. diabetes, hypertension and autoimmune diseases), and progression factors (i.e. elevated blood pressure and proteinuria, and smoking). Once established, CKD progression is influenced by a number of non-modifiable and modifiable risk factors (Taal *et al.*, 2008). The non-modifiable progression risk factors include age, race and genetics, while the modifiable progression risk factors include systemic hypertension, proteinuria and metabolic factors. Moreover, cigarette smoking, alcohol consumption and drug use can influence the progression of CKD (Floege J *et al.*, 2010).

The progression of CKD towards ESRD is characterized by the progressive loss of renal cells through apoptosis or necrosis, and their replacement with scars, fibrotic tissue made of collagenous extracellular matrix (ECM). Scarring, that leads to loss of kidney function, may affect different renal districts such as the glomeruli (glomerulosclerosis), tubules and interstitium (tubulointerstitial fibrosis), and vessels (vascular sclerosis) (Floege J *et al.*, 2010).

Renal outcomes are mostly unfavorable in patients with progressive

kidney disease, showing the kidney's limited capacity to repair chronic damage. However, experimental and clinical evidence indicates that there are drugs able to reduce risk of progression to ESRD, offering new hope for the future of kidney regeneration. In addition, lifestyle intervention (i.e. weight loss or smoking cessation), tight diabetes control, and treatment of other cardiovascular risk factors as dyslipidemia are associated with a slow progression to ESRD (Couser *et al.*, 2011).

1.2 The MWF rat model

In the past years, it has been suggested that a reduced number of nephrons may predispose to systemic hypertension and glomerular injury. A consequence of a low number of nephrons is a reduced ability to secrete sodium. Compensatory hemodynamic changes may develop to compensate this renal abnormality and may predispose to progressive glomerular functional and structural deterioriation. Because of the limitations in estimating the number of nephrons in the living human kidney, the parallelism between the nephron number and the hemodynamic changes has been studied for the first time in the Munich Wistar Frömter (MWF) rat model (Fassi *et al.*, 1998). These animals have been selected from the Munich-Wistar strain by Frömter for having a high number of superficial glomeruli (Hackbart *et al.*, 1980; Hackbart *et al.*, 1983). Male MWF rats had body and kidney weights lower than control

Wistar animals of the same age. This could possibly be attributable to a growth defect, likely related to the defect in growth hormone secretion (Martin *et al.*, 1974) of the Munich-Wistar strain from which the studied strain originated (Fassi *et al.*, 1998). The genetic defect in growth hormone may lead to impaired nephrogenesis, resulting in reduced nephron number, about 50% in average, and in superficial capillary tufts not covered by the peripheral layer of proximal tubules that is normally formed during the last phase of nephrogenesis (Fassi *et al.*, 1998; Macconi *et al.*, 2006).

The MWF rats with a high number of superficial nephrons, show an elevated urinary protein excretion and a high systolic blood pressure. To investigate the possible correlation between the number of superficial glomeruli and these pathological changes, MWF rats have been crossed and backcrossed to Wistar animals with no superficial nephrons in order to produce genotypes with different numbers of superficial glomeruli. The analysis of the 12 available genotypes has demonstrated a positive correlation between the amount of superficial glomeruli, urinary protein excretion and systolic blood pressure levels (Hackbarth *et al.*, 1991). About 50% of the urinary protein consisted of albumin, whereas 35% was a sex-dependent low molecular weight protein. Albumin excretion levels increase with age in male MWF rats, whereas excretion of the sex-dependent protein decreases (Remuzzi A. *et al.*, 1992).

The progressive nephropathy which characterizes the MWF rat model is sex-dependent. Starting from few weeks of life, urinary protein

excretion in male rats is already significantly higher than in females, in which proteinuria level is within the normal range. By comparing animals of the same age, male MWF rats also show a higher glomerular ultrafiltration coefficient, that is the product of hydraulic permeability and the filtering surface area of glomerular membrane, than in female MWF rats (Remuzzi A. *et al.*, 1988).

Studies conducted comparing the effects of the angiotensin-converting enzyme (ACE) inhibitor lisinopril with those of a specific angiotensin receptor antagonist (ZD7155) on the renal function in male MWF rats demonstrated that angiotensin II is the likely mediator of proteinuria and glomerulosclerosis which develop spontaneously with age in this model (Remuzzi A. *et al.*, 1996). ACE inhibitors protect glomerular microcirculation and prevent progressive renal injury in this strain by a mechanism that is not directly related to their antihypertensive action. Indeed, by comparing the ACE inhibitor lisinopril with those of another antihypertensive drug, the calcium channel blocker nitrendipine, a study conducted in our Institute has demonstrated that nitrendipine, despite similar blood pressure control, was ineffective in preventing both proteinuria and glomerulosclerosis (Remuzzi A. *et al.*, 1994).

1.3 Extracapillary glomerulonephritis

Cellular crescents, defined as multilayered accumulation of cells in the glomerular Bowman's space, are feature of different kinds of

glomerulonephritides which, if left untreated, can result in rapidly progressive renal failure (Singh KS *et al.*, 2011). The most harmful and diffuse crescentic lesions are found in kidneys of patients with inflammatory glomerular diseases, typically crescentic glomerulonephritis, but also other proliferative forms including lupus nephritis, IgA nephropathy, and membranoproliferative glomerulonephritis (Kambham *et al.*, 2012 ; Jennette *et al.*, 2003).

The cellular components of glomerular crescents have been extensively studied, with controversial findings as to their possible pathogenetic role. Early studies in immune glomerulonephritis revealed the contribution of macrophages which, by releasing proinflammatory cytokines, could promote self-recruitment and proliferation of glomerular cells (Cattell *et al.*, 1978, Jennette *et al.*, 1986).

Subsequent studies attributed to Bowman's capsule integrity a key role in determining the nature of crescent cells. By examining cellular crescents in different cases of human crescentic glomerulonephritis, Boucher and coworkers found that parietal epithelial cells (PECs) represent the major cell population within crescents with intact Bowman's capsule (Boucher *et al.*, 1987). The same observations have been done in the later time in various animal models (Lan *et al.*, 1992; Ophashcharoensuk *et al.*, 1998; Le Hir *et al.*, 2001).

Different studies also suggested the podocyte contribution to the crescent. By using a genetic cell lineage-mapping approach in an experimental model of crescentic glomerulonephritis, Moeller and

coworkers demonstrated that podocytes actively contribute to crescent formation through proliferation *in situ*. However, immunohistochemistry experiments failed to detect podocyte-specific proteins, including WT-1, synaptopodin and nephrin, within the area of crescentic lesions in mouse kidneys with crescentic glomerulonephritis. The absence podocyte markers was attributed to a profound phenotypic change of podocytes in that nephritis model (Moeller *et al.*, 2004). Subsequent studies have confirmed the podocyte involvement in crescent formation both in humans and in animals (Bariety *et al.*, 2005, Thorner *et al.*, 2008). This theory is supported also by the study by Ding and coworkers, which demonstrated that in mice, the deletion of the product of the von Hippel-Lindau gene (*Vhlh*, encoding VHL) selectively from podocytes causes the formation of crescentic lesions. Although in crescentic glomerulonephritis, VHL has not been directly implicated in the disease, different VHL downstream genes are known to be increased in respect to controls. In that study, loss of *Vhlh* permits terminally differentiated podocytes to reenter the cell cycle, suggesting that *Vhlh* is required by podocytes to maintain glomerular integrity (Ding *et al.*, 2006).

In the last years, different populations of progenitor cells with stem cell characteristics have been identified in different portions of the normal adult kidney. Among them, $CD24^{+}CD133^{+}$ renal progenitor cells normally residing in the inner surface of the human Bowman's capsule have been studied, suggesting their ability to differentiate into podocytes in order to replace the injured cells which are lost during the physiologic turnover

(Ronconi *et al.*, 2009). Besides the role of renal progenitors in the physiologic repair of damaged glomerular cells, increasing interest is aroused in determining the pathogenetic role of these cells in different glomerular diseases. Recently, in a study conducted in collaboration with the group of Dr. Smeets and Dr. Romagnani, we have investigated the localization of $CD24^{+}CD133^{+}$ progenitor cells, which in normal kidneys line the human Bowman's capsule (Sagrinati *et al.*, 2006), in biopsies of patients with different podocytopathies and crescentic glomerulonephritis. By using confocal microscopy, laser capture microdissection, and real-time quantitative reverse transcriptase–PCR, we demonstrated that crescentic lesions of patients are mainly constituted by progenitor cells, which proliferate in the failed attempt to replace the injured glomerular cells (Smeets *et al.*, 2009).

Understanding the mechanisms of crescentic lesion formation is pivotal in the search of therapies to protect patients against high-risk progressive renal failure avoiding the use of currently employed toxic drugs.

1.4 Role of chemokines in the proliferative pathway

Leukocyte trafficking from peripheral blood into affected tissues is an essential component of the inflammatory reaction to virtually all forms of injury and is an important factor in the development of many kidney

diseases. In the past years, evidence have highlighted the central role of a family of chemotactic cytokines called chemokines in this process (Segerer *et al.*, 2000). The chemokine system in humans comprises up to 50 small heparin-binding proteins and 20 transmembrane G protein-coupled receptors that were originally identified by their chemotactic activity on bone marrow-derived cells (Garcìa-Vicuna *et al.*, 2004). According to the position and spacing of N-terminal cysteine residues, chemokines can be divided into C, CC, CXC, and CX3C families, and consequently, their receptors have been designated as CR, CCR, CXCR, and CX3CR (Garcìa-Vicuna *et al.*, 2004). In the kidneys, chemokines and their receptors are expressed by intrinsic renal cells as well as by infiltrating cells during renal inflammation, and help to control the selective migration and activation of inflammatory cells into injured renal tissue (Segerer *et al.*, 2000).

The crescentic glomerulonephritis is a glomerular diseases with an inflammatory nature, characterized by massive extracapillary proliferation of parietal epithelial cells in the Bowman's space. Given the well known ability of chemokines in mediating cell proliferation and migration, we suggested their possible involvement in the development of crescentic lesions. In particular we studied CXCR4, which appears to be the major chemokine receptor expressed on proliferating cancer cells, and stromal-derived factor-1 (SDF-1) which is its lone ligand (Reckamp *et al.*, 2008). SDF-1/CXCR4 interactions and signalling have also been implicated as a principal axis regulating retention, migration and mobilization of

hematopoietic stem cells during steady-state homeostasis and injury (Lapidot *et al.*, 2005). Mice lacking CXCR4 or SDF-1 have a lethal defect of colonization of embryonic bone marrow by hematopoietic stem cells and impaired vascular development (Ratajczak *et al.*, 2006). In a previous study, the expression of CXCR4 has been observed in $CD24^{+}CD133^{+}$ progenitor cells isolated from healthy human glomeruli (Mazzinghi *et al.*, 2008). In SCID mice with acute renal failure, intravenously injected renal progenitor cells engraft into injured renal tissue and prevent renal fibrosis. Migration of $CD24^{+}CD133^{+}$ cells into the graft was dramatically reduced by blocking CXCR4 with a neutralizing antibody, suggesting the essential role of CXCR4 in the therapeutic homing of human renal progenitor cells (Mazzinghi *et al.*, 2008).

Given the key role of CXCR4 in mediating cell proliferation in various cell types, CXCR4 inhibition may be a potential therapeutic approach to decrease cell proliferation and migration, possibly limiting the formation of extracapillary crescentic lesions.

1.5 Role of ACE inhibitors in renal disease remission and regression

1.5.1 Evidence in animal models

Nephron loss which characterizes the progression of renal diseases, leads to an adaptation process of the remaining nephrons including glomerular hypertension and enlargement of the pores perforating the

glomerular barrier. The consequent loss of size-selective properties leads to an excessive accumulation of ultrafiltered proteins in the Bowman's space and in the lumen of tubules, contributing to exacerbate renal damage through the recruitment of inflammatory cells and activation of apoptotic pathways (Perico *et al.*, 2008).

Pharmacological treatments aimed at reducing glomerular hypertension and protein trafficking through the glomerular filtration barrier, are effective in limiting renal function deterioration and thus promoting kidney repair. The cornerstone of current treatment is represented by the inhibition of angiotensin II (Ang II), which is the key player of the renin-angiotensin system (RAS). Ang II inhibition may occur through two different classes of drugs. The first class is represented by ACE inhibitors, which prevent the synthesis of Ang II by blocking the action of the enzyme which converts Ang I into Ang II (Tsukamoto *et al.*, 2011). The second class includes the Ang II type I receptor blockers (ARBs), which conversely inhibit the activity of Ang II by blocking its chemical receptors on the small arteries.

Evidence in animal models of non-diabetic and diabetic nephropathies has clearly shown that treatment with ACE inhibitors, ARBs or the combination of the two drugs, not only prevents progressive renal damage, but also promotes regression of glomerulosclerosis and vascular lesions (Marinides *et al.*, 1990; Remuzzi *et al.*, 1999; Remuzzi *et al.*, 2002; Adamczak *et al.*, 2003; Boffa *et al.*, 2003; Remuzzi *et al.*, 2006). In MWF rats, which are genetically programmed to develop renal injury with

age, three-dimensional reconstruction of the glomerular capillary tuft based on serial section analysis of hundreds of glomeruli, has demonstrated that ACE inhibitor reduced the glomerular volume occupied by sclerosis in parallel with a substantial increase in the volume occupied by intact capillaries, suggesting a remodelling of the glomerular architecture and generation of new capillary network (Remuzzi *et al.*, 2006). The effectiveness of Ang II antagonists to promote regression of glomerulosclerosis may be attributable to a decreased extracellular matrix deposition through a reduced expression of plasminogen activator inhibitor-1 (Ma *et al.*, 2000), collagen I and IV and transforming growth factor-β (TGF- β) (Remuzzi *et al.*, 2006), and an increased metalloproteinase activity (Boffa *et al.*, 2003). Conversely, the recovery of glomerular lesions could be due to an effect of ACE inhibitor in modulating glomerular cell proliferation and survival. Accordingly, previous data have described regeneration of glomerular capillaries as a result of limited mesangial cell proliferation and endothelial cell repopulation induced by pharmacological treatment with ACE inhibitor (Adamczak *et al.*, 2003). More recent evidence indicates that ACE inhibitor halts mesangial cell hyperplasia, induces glomerular endothelial cell remodelling, and increases the number of podocytes (Macconi *et al.*, 2009). These data indicate the effectiveness of ACE inhibitor to induce neoformation of healthy glomerular tissue.

1.5.2 Evidence in humans

The effectiveness of ACE inhibitor to limit renal disease progression has been also described in patients with proteinuric non-diabetic and diabetic nephropathies. The Ramipril Efficacy in Nephropathy (REIN) study showed that ACE inhibitor halves the rate of renal function loss in patients with non-diabetic chronic nephropathies (The GISEN group, 1997; Ruggenenti *et al.*, 1998; Ruggenenti *et al.*, 1999). Renoprotection is a function of time and in patients on continued ramipril therapy for at least 5 years, the rate of GFR decline progressively improved (Ruggenenti *et al.*, 1999) to levels comparable to physiologic, age-related loss of GFR observed in subjects with no evidence of renal disease. In ten of these patients, there was a breakpoint indicating the transition from an initial phase of progressive GFR loss to a second phase of progressive function improvement, suggesting the possibility of regression of renal lesions combined to some degree of kidney regeneration (Remuzzi A *et al.*, 2006).

Wilmer and coworkers demonstrated that 8-year treatment with ACE inhibitor stabilizes kidney function in patients with type 1 diabetes and nephrotic syndrome, who generally progress to ESRD. The possibility to promote kidney repair in patients with type 1 diabetes has been suggested long time ago in a study which demonstrated the improvement of typical lesions of diabetic glomerulopathy after ten years of normoglycemia following pancreas transplantation (Fioretto *et al.*, 1998).

The efficacy of combined therapy with high dose of ACE inhibitor with ARB and diuretics in improving clinical outcome was demonstrated

for the first time in a single individual with rapidly worsening renal function (Ruggenenti *et al.*, 2001). Subsequently, multimodal therapy was formally compared with treatment with ACE inhibitor alone in a large cohort of patients with severe chronic kidney disease (Ruggenenti *et al.*, 2008). Over a seven-year follow up, only two out of 56 patients on the integrated protocol have progressed to ESRD compared to 17 out of 56 reference patients. Moreover, GFR has been stabilized in 26 patients, and this was taken to indicate remission of the disease and the possibility of kidney repair in this population (Ruggenenti *et al.*, 2008). This therapeutic program has been named *Remission Clinic* and is currently implemented at least to some extent even in "emerging" countries (Limesh *et al.*, 2012) where dialysis and transplantation are simply not available to most patients.

1.6 Role of renal progenitor cells in kidney repair

In a physiological setting, the kidney has been considered as an organ with minimal cell turnover and with a consequent limited ability for self-repairing. However, after ischemia/reperfusion injury, an increased tubular cell proliferation occurs resulting in regeneration of tubules starting from the third day. After 10 days, 50% of the tubules have been regenerated (Ysebaert *et al.*, 2000) whereas the complete tubular structure restoration has been reached after 4 weeks (Humes *et al.*, 1994; Witzgall R

et al., 1994). This ability of the kidney to self-regenerate supports the hypothesis that resident cells may be involved in normalizing structure and function after an insult.

Different theories are trying to elucidate whether reparative programme depends on cells originating from de-differentiation of tubular cells, from extrarenal stem cells that are recruited to the kidney following damage, or from progenitor cells residing in specific niches in the kidney.

1.6.1 De-differentiation of tubular cells

Terminally differentiated tubular cells that survive to damage might proliferate and generate identical cells or de-differentiate and subsequently re-enter the cell cycle. After the insult, renal tubular cells rapidly lose their brush border and de-differentiate into cells with mesenchymal phenotype, with re-expression of Vimentin, Pax-2 and neural cell adhesion molecule (NCAM), that normally are not expressed in mature tubules (Witzgall *et al.*, 1994; Imgrund *et al.*, 1999; Abbate M *et al.*, 1999). The loss of the highly specialized phenotype is reflected also by decreased expression of the apical brush border markers, gp330 and DPP-IV. De-differentiated tubular cells seem to migrate into regions where tubular basement membrane is denudated following to detachment of necrotic and apoptotic cells. There, the release of growth factors such as insulin-like growth factor-1 and hepatocyte growth factor, promotes cell

proliferation and re-differentiatiation into an epithelial phenotype (Schena *et al.*, 1998), completing the repair process (Cantley *et al.*, 2005).

1.6.2 Recruited extra-renal stem cells

In addition to the ability of tubular cells to self-repairing, emerging theories have shown that bone marrow-derived stem cells contribute to cell turnover and regeneration after injury of several regions of the kidney (De Broe *et al.*, 2005). Poulsom *et al.* have demonstrated that kidney of female mice, that has received a male bone marrow transplant, shows co-localization of Y chromosomes and the tubular epithelial marker *Lens Culinaris* lectin. Moreover, Y chromosome-containing tubular epithelial cells has been observed in kidney suffering damage in male patients who had received kidney transplants from female donors (Poulsom *et al.*, 2001). More recently, it has been demonstrated that in female mice lethally irradiated and transplanted with male bone marrow cells, the number of Y chromosome-positive tubular cells increases following folic acid-induced tubular injury in the recipient mouse, and that some of these cells undergo division within the tubule. However, they note that renal tubular regeneration mainly came from female resident cells, as the cells involved in tubule repair seem to be Y-chromosome-negative (Fang *et al.*, 2005).

Conflicting results are reported by different groups, and nowadays it is not clear whether these cells, coming from the bone marrow, are already present in the kidney prior to injury, functioning as resident stem

cells, or whether they are recruited to the kidney at the time of injury (Poulsom *et al.*, 2002).

1.6.3 Resident renal progenitor cells

A stem cell is defined as a cell that, upon division, can self-renew and give rise to a transit-amplifying progenitor, that subsequently acquires a more differentiated state. Stem cells residing in adult organs formerly believed to have no regenerative potential, have been considered as multipotent precursors having the ability to maintain, generate and replace mature cells which have been lost as a consequence of physiological cell turnover or tissue injury (Blau *et al.*, 2001).

In the adult kidney, resident stem/progenitor cells have been identified through the expression of stem-cell markers or for the presence of functional properties of stem cells, as the low cell cycle. In the recent years several studies have been focused on the search of renal multipotent progenitor cells in the adult kidney, revealing the presence of different population of immature cells in distinct sites of the nephron, including the glomeruli, the tubuli, the interstitium and the renal papilla (Table 1) (Benigni *et al.*, 2010).

The presence of a subset of multipotent progenitor cells in the adult human glomeruli has been demonstrated for the first time by the group of Dr. Romagnani. These cells, located in the inner surface of the Bowman's capsule, express the stem cell markers CD24 and CD133, and the

transcription factors Oct-4 and BmI-1 (Sagrinati *et al.*, 2006). Isolated $CD24^{+}CD133^{+}$ PECs exhibited clonogenic self-renewal and are able to generate podocytes and tubular cells *in vitro*. Moreover, when injected into SCID mice with acute kidney injury, these cells induce tubular regeneration and amelioration of kidney structure (Sagrinati *et al.*, 2006). The Bowman's capsule of healthy glomeruli is not only composed by $CD24^{+}CD133^{+}$ PECs, but three distinct subpopulation of PECs has been described, expressing variable levels of stem cell and podocyte markers (Ronconi *et al.*, 2009). A hierarchical organization have been proposed, with immature progenitor cells (expressing CD24 and CD133 in the absence of podocyte markers nestin and podocalyxin) present closest to the urinary pole, transitional cells (expressing both stem cell and podocyte markers) located between the urinary and the vascular pole, and differentiated podocytes only expressing nestin and podocalyxin near the vascular pole (Ronconi *et al.*, 2009). Genetic labelling has been subsequently used to mark the cells of the Bowman's capsule and irreversibly track their progeny in newborn and adolescent mice, demonstrating that PECs migrate into the glomerular tuft to become podocytes. These finding provide evidence that these cells are responsible for podocyte renewal (Appel *et al.*, 2009).

A different theory has attributed to cells of the renin lineage, normally residing in the juxtaglomerular compartment alongside the glomerular capillaries, the capacity to enhance glomerular regeneration after podocyte depletion (Pippin *et al.*, 2013). After a decreased podocyte

number, a significant increase in the number of renin-expressing cells have been observed in glomeruli in a focal distribution along the Bowman's capsule or within the glomerular tuft, re-expressing the podocyte markers WT-1, nephrin podocin and synaptopodin (Pippin *et al.*, 2013).

A microarray analysis conducted on glomerular and tubular fractions of human kidneys has allowed the identification of $CD24^{+}CD133^{+}$ progenitor cells not only in the Bowman's capsule but also in proximal tubules (Sallustio *et al.*, 2010). The characterization of these cells has been subsequently performed by Lindgren and coworkers on human cells isolated on the basis of the high aldehyde dehydrogenase (ALDH) activity (Lindgren D *et al.*, 2011). Kidney cells with $ALDH^{high}$ activity isolated from the renal cortex, display sphere formation and anchorage-independent growth, two classic stem cell fuctional properties. The analysis of the whole-genome expression profile of $ALDH^{high}$ cells shows high levels of CD24, CD133, vimentin and cytokeratins 19, markers that are also expressed in the metanephric mesenchyme during nephrogenesis (Lindgren D *et al.*, 2011). Whether these tubular-committed progenitor cells can be distinguish from $CD24^{+}CD133^{+}$ progenitors lining the inner surface of the Bowman's capsule has been recently studied by Angelotti and coworkers (Angelotti *et al.*, 2012). A screening of hundreds of genes has been performed on $CD24^{+}CD133^{+}$ cells isolated from the glomerular or from the tubular compartments. The analysis has revealed that some genes were differentially expressed, and among these, the expression of CD106 was approximately 300-fold higher in cells obtained

from glomerular outgrowths than in cells obtained from tubular tissue (Angelotti *et al.*, 2012). While $CD24^+CD133^+CD106^+$ progenitor cells of the Bowman's capsule exhibit an high proliferative rate and could differentiate towards both the podocyte and the tubular lineages, $CD24^+CD133^+CD106^-$ scattered cells of the tubules show a lower proliferative capacity and display a committed phenotype towards the tubular lineage. When injected into SCID mice with acute tubular injury, both of these cell populations engraft the kidney and integrate in tubules (Angelotti *et al.*, 2012).

A different strategy for the identification of progenitor cells in the adult kidney has been based on the property of stem cells to cycle infrequently to maintain the pool of cells for tissue turnover and repair. Cycling cells can be identified by the ability to retain the proliferative marker bromodeoxyuridine (BrdU), previously injected to the animals. On the basis of this concept, Maeshima *et al.* demonstrated the existence of label-retaining cells in proximal and distal tubules of healthy rat kidneys (Maeshima *et al.*, 2003). Further studies showed the presence also in the interstitium of slow-cycling cells, which after ureteral obstruction re-expressed the mesenchymal cell markers vimentin and e-cadherin (Yamashita et al., 2005). The same approach has been used by Oliver and coworkers to demonstrate that the renal papilla is a niche for adult kidney stem cells. In mice and rats pulse-chased with BrdU, low cycling cells have been found very sparse in the kidney except for the renal papilla (Oliver *et al.*, 2004). During the repair phase of transient renal ischaemia, these cells

enter the cell cycle and the BrdU signal quickly disappears from the papilla, suggesting that they can be involved in kidney repair. Isolated renal papillary cells display a plastic phenotype and have the ability to form spheres like other stem cell types. In addition, once injected into the renal cortex they incorporate into the renal parenchyma (Oliver *et al.*, 2004).

The last approach that has been used to identify and isolate progenitor cells in the adult kidney is based on the ability of stem cells to extrude a Hoechst dye (Goodell *et al.*, 1996). Several populations of Hoechst^{low} stem cells, termed side populations, have been found located in renal interstitium (Iwatani *et al.*, 2004). Different studies have documented the beneficial effect of side populations in animal models of kidney diseases as adriamycin nephropathy (Challen *et al.*, 2006), cisplatin-induced acute kidney injury (Hishikawa *et al.*, 2005) and chronic kidney disease (Imai *et al.*, 2007), but probably this phenomenon might be only due to a paracrine effect of the cells.

Species	Markers	Localization	Reference
Human	$CD133^{+}CD24^{+}$	Bowman's capsule	Sagrinati *et al.*, 2006
Mouse	Renin	Juxtaglomerular compartment	Pippin *et al.*, 2013
Human	$CD133^{+}CD24^{+}$	Bowman's capsule Proximal and distal tubule	Sallustio *et al.*, 2010
Human	$CD133^{+}CD24^{+}CD106^{+}$ $CD24^{+}CD133^{+}CD106^{-}$	Bowman's capsule Proximal and distal tubule	Angelotti *et al.*, 2012
Human	Aldehyde $dehydr^{high}CD24^{+}CD133^{++}$	Proximal tubules	Lindgren *et al.* 2011
Rat	BrdU (slow-cycling cells)	Proximal and distal tubules	Maeshima *et al.*, 2003
Rat	slow-cycling cells	Interstitium	Yamashita *et al.*, 2005
Rat	$Hoechst^{low}$ (side population)	Interstitium	Iwatani *et al.*, 2004
Rat/Mouse	BrdU (slow-cycling cells)	Papilla	Oliver *et al.*, 2004

Table 1. Localization of renal progenitor cells in the adult kidney

CHAPTER 2

MATERIALS

2.1 Rats

- Male Wistar and MWF rats were bred at the IRCCS - Istituto di Ricerche Farmacologiche Mario Negri, starting from animals initially purchased from Charles River Italia s.p.a., Calco, Italy.

2.2 Cells

- Rat progenitor cells were isolated from the outgrowth of control Wistar rats (Methods, section 3.8).

2.3 Fixatives

- **Duboscq-Brazil solution** ready to use, was purchased from DiaPath, Martinengo, Bergamo, Italy.
- **Paraformaldehyde** was purchased from Electron Microscopy Sciences, Hatfield, PA, USA. In order to prepare a 4% solution, we diluted 8% aqueous solution in PBS 2X under a fume hood.
- **Immunogold fixative:** 3.5% paraformaldehyde plus 0.01% glutaraldehyde. Glutaraldehyde was purchased from Sigma Aldrich, St Louis, MO, USA.
- **Fixative for *in vitro* cells:** 2% paraformaldehyde + 4% sucrose.

2.4 Media, supplements and reagents for *in vitro* study

- **medium plus endothelial growth medium-microvascular (EGM-MV)** was purchased from Lonza Walkersville, USA

- **DMEM** was purchased from Sigma-Aldrich

- **VRAD medium:** DMEM/F12 supplemented with vitamin D3 100 nmol/L and retinoic acid 100 μmol/L

- **Fetal bovine serum** was purchased from Thermo Scientific, Rockford, IL, USA.

- **Blocking solution:** 2% BSA, 0.2% gelatin bovine, and 2% FBS in PBS

- **Fibronectin** from rat plasma was purchased from Sigma-Aldrich

- **Goat anti-rabbit IgG MicroBeads** was purchased from Miltenyi Biotech Inc, Auburn, CA, USA

- **Angiotensin II** was purchased from Sigma-Aldrich and used at a final consentration of 10^{-7} mol/L.

- **Permeabilizing solution:** TRITON X100 was purchased from Sigma-Aldrich and was diluted to a final concentration of 0.3% in PBS 1X.

2.5 Chemicals

- **Paraffin,** Bioplast Plus, was purchased from Bio Optica, Milan, Italy.

- **Unyhol Plus** Bioplast Plus, was purchased from Bio Optica.

- **Ethanol** was purchased from Carlo Erba, Milan, Italy.

- **Methanol** was purchased from Carlo Erba.

- **Acetone** was purchased from Carlo Erba.

- **Periodic acid** was purchased from Diapath, Martinengo, Bergamo, Italy

- **Schiff's reagent** was purchased from Kaltek srl, Padova, Italy

- **Sodium hyposolfite** was purchased from Merck, Milan, Italy. A 5% solution was prepared by dissolving the powder in water.

- **Picro Indigo Carmine** was purchased from Bio-Optica.

- **Sucrose** was purchased from Sigma Aldrich.

- **Coomassie brilliant blue dye** was purchased from Sigma-Aldrich.

- **Carazzi haematoxylin** was purchased from Bio-Optica.

- **Harris haematoxylin** was purchased from Bio-Optica.

- **Orthophosphoric acid** was purchased from Merck, Milan, Italy.

- **Hydrogen peroxide (H_2O_2)** solution was purchased from Sigma-Aldrich.

- **Propylene oxide** (1,2-epoxypropane), Electron Microscopy Sciences, EMS, Rome, Italy.

- OsO_4 was purchased from Electron Microscopy Sciences.

- **Uranyl acetate** was purchased from Electron Microscopy Sciences.

2.6 Buffers and solutions

- **Phosphate buffer saline (PBS) 10X** (for cell culture and immunohistochemistry) was purchased from Ambion-Invitrogen. Finally, PBS 1X is prepared diluting 1:10 PBS 10X in water.

- **Citrate buffer** 10% concentrated pH 6.0, was diluted 1:10 in PBS 1X and was purchased from DiaPath.

- **Blocking buffer.** Bovine serum albumin (BSA) (Sigma-Aldrich) was added to PBS to obtain a final BSA concentration of 1%. The solution was maintained on ice for few minutes to facilitate albumin solubilisation. The solution was then filtered with a 0.2 μm sterile filter.

- **3,3'-diaminobenzidine (DAB).** One tablet of DAB was put into 25 ml of distilled water. Solution was mixed and 6.5 μl of 30% H_2O_2 was added. DAB was purchased from Merck.

- **Cacodylate buffer 0.2 M.** Sodium cacodylate trihydrate 12.84 g, Sigma-Aldrich, + 300 ml of water. pH was stabilized at 7.4 with HCl 0.2 N (Merck).

- **Cacodylate buffer 0.1M pH 7.4.** Prepared by diluting (1:1) in water cacodylate buffer 0.2 M, pH 7.4

- **Epon resin.** Solution 1: 5 ml of Durcupam ACM, Fluka (Sigma-Aldrich) + 18 ml of Epoxy Embedding Medium, Hardener DDSA, Fluka. Solution 2: 6 ml of Epoxy Embedding Medium, Fluka + 300 μl of Epoxy Embedding Medium Accelerator, Fluka. Finally, solution 1 and 2 were mixed.

2.7 Antibodies

For all antibodies, preliminary experiments were performed following

manufacturer's suggestions in order to identify the most appropriate experimental protocol and concentration.

2.7.1 Primary antibodies:

- Rabbit anti-**Wilm's tumor 1**, purchased from Santa Cruz Biotechnology, Santa Cruz, CA, USA. Final concentration: 1:50.

- Rabbit anti-**claudin1**, purchased from Thermo Scientific. Undiluted.

- Mouse or goat anti-**CD24**, purchased from Santa Cruz Biotechnology. Final concentration: 1:25.

- Mouse anti-**Thy1.1** antibody was purchased from BD Biosciences. Final concentration 1:100.

- Mouse anti-**ED1** antibody, purchased from Chemicon International, Temecula, CA, USA. Final concentration 1:100.

- Mouse anti-**BrdU** antibody was purchased from BD Biosciences. Final concentration 1:100.

- Mouse anti-**NCAM**, purchased from Developmental Studies Hybridoma Bank, University of Iowa, USA. Final concentration: 1:2.

- Rabbit anti- human **CXCR4** antibody purchased from Abcam, and used at the concentration of 1:50.

- Rabbit anti-**AT_1 receptor** purchased from Santa Cruz Biotechnology. Final concentration: 1:25.

- Rabbit anti-**SDF-1** antibody was purchased from Abcam. Final concentration 1:200.

- Goat anti-**Nephrin**, purchased from Santa Cruz Biotechnology. Final

concentration: 1:400.

- Rabbit anti-**Type III collagen** antibody was purchased from Chemicon International. Final concentration 1:100.

- Rabbit anti-**C/EBPδ**, purchased from Santa Cruz Biotechnology. Final concentration: 1:25.

- Mouse anti-**Synaptopodin** purchased from Progen Biotechnik GmbH. Undiluted.

- Rabbit anti-**Phospho-histone H3** was purchased from Cell Signalling Technology. Final concentration 1:100.

- Mouse anti-**CD133** was purchased from Miltenyi Biotech Inc. Final concentration 1:100.

- Mouse anti-**CD68** was purchased from DakoCytomation, Glostrup Denmark. Final concentration 1:100.

2.7.2 Secondary antibodies:

- **Cy3-conjugated goat anti rabbit IgG**, purchased from Jackson ImmunoResearch Laboratories and used at final concentration of 1:50.

- **Cy3-conjugated donkey anti mouse IgG**, purchased from Jackson ImmunoResearch Laboratories and used at final concentration of 1:150.

- **Cy3-conjugated donkey anti goat IgG**, purchased from Jackson ImmunoResearch Laboratories and used at final concentration of 1:300.

- **FITC-conjugated goat anti mouse IgG**, purchased from Jackson ImmunoResearch Laboratories and used at final concentration of 1:50.

- **FITC-conjugated goat anti rabbit IgG,** purchased from Jackson ImmunoResearch Laboratories and used at final concentration of 1:50.

- **FITC-conjugated rabbit anti goat IgG,** purchased from Jackson ImmunoResearch Laboratories and used at final concentration of 1:50.

- **Cy5-conjugated donkey anti-rabbit** antibody purchased from Jackson ImmunoResearch Laboratories and used at final concentration of 1:50.

- **Biotinylated sheep anti-mouse IgG,** purchased from Jackson ImmunoResearch Laboratories and used at final concentration of 1:75.

- **Biotinylated goat anti-rabbit IgG,** purchased from Jackson ImmunoResearch Laboratories and used at final concentration of 1:150.

- **12-nm gold-conjugated donkey anti-goat IgG,** purchased from Jackson ImmunoResearch Laboratories and used at final concentration of 1:20.

2.8 Other reagents

- **Lisinopril** was dissolved in drinking water at concentration of 80mg/L.

- **Ramipril** was used at increasing doses starting from 2.5 to 7.5 mg/day.

- **Azathioprine** was used at a concentration of 50 mg/day.

- **5-bromo-2-deoxyuridine (BrdU)** was purchased from Sigma-Aldrich. It was injected to the animals at concentration of 50 mg/kg dissolved in saline, 5 days before sacrifice.

- **Tissue-Tek OCT Compound** was purchased from Sakura Finetek, Torrance, CA, USA.

- **Eukitt** was purchased from Bio Optica.

- **Vectastain avidin-biotin peroxidase complex solution (ABC) kit** purchased from Vector Laboratories, Burlingame, CA, USA.

- **Fluorescence mounting medium** was purchased from DakoCytomation.

- **FITC-labeled lectin Wheat Germ Agglutinin (WGA)** was purchased from Vector Laboratories. Final concentration 1:400.

- **Rhodamine-labelled Lectin Lens Culinaris Agglutinin** (LCA) was purchased from Vector Laboratories.. Final concentration 1:400.

- **DAPI:** 4',6'-diamidino-2-phenylindole dihydrochloride hydrate was purchased from Sigma-Aldrich.

2.9 Disposable materials

- **Filter paper 3MM**, purchased from Whatman.

- **Plastic cuvettes** were purchased from DISA RAffaele e F.lli s.a.s.

- **Polyethylene labelled-cone shaped capsules** were purchased from Electron Microscopy Sciences.

- **Formvar** were purchased from Electron Microscopy Sciences.

2.10 Instruments

- **Autoanalyzer for serum creatinine and urinary protein concentration measurement:** Synchron CX9 system was purchased from Beckman Coulter, Fullerton, USA.

- **Microtome,** RM2255, was purchased from Leica Microsystems.

- **Cryostat, CM1950,** was purchased from Leica Microsystems.

- **Ultramicrotome** EM UC7, was purchased from Leica Microsystems.

- **ApoTome** Mod Axio Imager Z2, was purchased from Zeiss, Jena, Germany.

- **Confocal laser-scanning microscope** LS 510 Meta; was purchased from Zeiss.

- **Electron microscope Morgagni 268D** was purchased from Philips, Bmo, Czech Republic.

CHAPTER 3

METHODS

Methods for *in vivo* studies in the experimental rat model

3.1 Munich Wistar Frömter rats

Male Wistar and Munich Wistar Frömter (MWF) rats (Materials, section 2.1) were used. Sixty MWF rats were divided into different groups as follows:

- group 1 (n = 50) received saline and were sacrificed at different time points, 10, 25, 40, 50, and 60 weeks of age (n = 10 rats for each time point);
- group 2 (n = 10) received lisinopril (Materials, section 2.8, 80 mg/L in drinking water) from 50 to 60 weeks of age;
- group 3 (n = 20) 10, 25, 40, 50, and 60-week-old Wistar rats were used as controls.

To study cell proliferation, Wistar and MWF rats given vehicle or lisinopril from 50 to 60 weeks of age (n = 4 for each group) were injected intraperitoneally with an S-phase labeled 5-bromo-2-deoxyuridine (BrdU, Materials, section 2.8, 50 mg/kg dissolved in saline) for 5 days before sacrifice. Animals were housed in a constant temperature room with a 12-hour dark 12-hour light cycle and fed a standard diet. Animal care and treatment were in accordance with institutional guidelines in compliance with national (D.L. n.116, G.U., suppl 40, 18 February 1992, Circolare No. 8, G.U., 14 July 1994) and international laws and policies (EEC Council

Directive 86/609, OJL 358, Dec 1987; NIH Guide for the Care and Use of Laboratory Animals, U.S. National Research Council, 1996). Animal studies were submitted to and approved by the Institutional Animal Care and Use Committee of the "Mario Negri" Institute, Milan, Italy.

3.2 Renal function measurement

To assess renal function, we measured total urinary protein excretion rate by using the Coomassie brilliant blue dye-binding assay. Coomassie brilliant blue (50 mg; Materials, section 2.5) was dissolved in 50 ml orthophosphoric acid 99% 16 M (Materials, section 2.5) and 46.7 ml absolute ethanol (Materials, section 2.5) then diluted to 1 L with water. The solution was filtered through Whatman paper (Materials, section 2.9) and stored in dark-colour glass bottles, maintaining rigorous cleanliness. The half-life of the solution is several weeks, but refiltering may be required if precipitation of dye occurs. The assay was performed in plastic cuvettes (Materials, section 2.9). Coomassie brilliant blue dye-reagent (2 ml) was added to 50 μl of urine samples. In each evaluation 1 sample of water alone and 3 samples with bovine serum albumin (BSA) (Materials, section 2.6) at known concentrations (50, 100 and 200 μg/ml) were included to obtained the standard curve. Samples were always assayed in triplicate. The colour development is essentially complete at 5 minutes and

remains stable for a period of 2 hours. The absorbance at 578 nm was measured at the spectrophotometer. The concentration of proteins present in the samples of interest was obtained taking into account the absorbance values derived from the standard curve in which the BSA concentrations were known.

Creatinine is an endogenous substance mainly produced in muscle cells from creatine and phosphocreatine. The serum creatinine concentration rises with the decline of GFR, because creatinine is excreted mainly by glomerular filtration. Here the serum creatinine concentration was measured using an automatic device with a quantitative, colorimetric assay based on a modified Jaffè method where alkaline picrate forms a reddish colored solution in the presence of creatinine. The measurement was performed immediately after the taking of the sample. Blood pressure was evaluated by tail plethysmography in awake animals.

3.3 Sacrifice and tissue collection

Wistar and MWF rats were sacrificed by exposure to CO_2 at 10, 25, 40, 50 or 60 weeks of age. Kidneys were weighed and in order to take samples representative of the different structural components of the kidney, sections were cut in the axial coronal plane. Depending on the type of procedure that would have been applied (immunohistochemistry, immunofluorescence, electron microscopy), samples were differently fixed

as described in each specific chapter.

3.4 Renal morphology by light microscopy

Immediately after collection, kidney fragments were fixed overnight in Duboscq-Brazil solution (Materials, section 2.3) and then dehydrated by ascending concentrations of ethanol (Materials, section 2.5) (70% and 100% for 2 hours each). Once dehydrated, samples were dipped in Unyhol Plus (Materials, section 2.5) for 1 hour, transferred to stainless steel base moulds, covered by paraffin (Materials, section 2.5), and finally incubated for 2 hours at 60°C. During this period of time paraffin infiltrates the sample. Samples were then placed at room temperature to allow paraffin to solidify. Embedded samples were cut in 3 μm thickness slices by using a microtome (Materials, section 2.10).

For the histologic staining, sections were deparaffinised in Unyhol Plus (Materials, section 2.5) for 20 minutes and then rehydrated in decreasing concentrations of ethanol (Materials, section 2.5, 100% for 10 minutes, followed by 90 and 80% for 5 minutes each) and water. Samples were than incubated for 10 minutes with 1% periodic acid (Materials, section 2.5) and washed 5 minutes in distilled water. Slides were then stained with periodic acid-Schiff's (PAS) (Materials, section 2.5) reagent for 1 hour and washed three times for 5 minutes each with sodium

hyposulphite (Materials, section 2.5), rinsed in tap water for 5 minutes, and then in distilled water for another 5 minutes. Nuclei were stained by placing glass slides in Carazzi haematoxylin (Materials, section 2.5) for 10 minutes. After rinsing in water, samples were quickly immersed in Picro Indigo Carmine (Materials, section 2.5) followed by 100% ethanol and Unyhol Plus, and finally mounted with Eukitt (Materials, section 2.8).

Slides were scored for the following changes: synechiae (thin connections between glomerular Bowman's capsule and the capillary tuft), and crescents (multilayers of cells accumulating in the inner surface of the Bowman's capsule, which obliterate the Bowman's space).

To evaluate the extent of glomerular lesions, an average of 35 glomeruli was examined and data were expressed as index. Each glomerulus was scored according to the extension of glomerular lesions as follows: 0 = absence of lesions; 1 = lesions affecting less than 25% of glomerulus; 2 and 3 = lesions affecting >25 to 50% and >50 to 75% of the glomerulus, and 4 = lesions exceeding 75% of the glomerulus. The index for synechiae and crescents were calculated by using the following formula:

$$\text{index} = (1 \times n_1) + (2 \times n_2) + (3 \times n_3) + (4 \times n_4) / n_0 + n_1 + n_2 + n_3 + n_4$$

Where nx = number of glomeruli in each grade of lesions (Davis *et al.*, 2004). Sections were analysed in a single-blind fashion. Renal histology pictures were acquired with a fluorescence and optical microscope

(ApoTome, Materials, section 2.10).

3.5 Immunohistochemistry

3.5.1 Immunofluorescence

For all immunofluorescence experiments, kidney samples collected immediately after rat sacrifice, were fixed in 4% paraformaldehyde (PFA, Materials, section 2.3) overnight at 4°C, washed twice for 10 minutes in PBS, infiltrated with 30% sucrose (Materials, section 2.5), embedded in Tissue-Tek OCT Compound (Materials, section 2.8) and finally frozen in liquid nitrogen. Three-micrometer-thick sections were cut by using a cryostat (Materials, section 2.10) and stored at -80°C. The antigen retrieval was performed in citrate buffer (Materials, section 2.6) 10 mmol/L (pH 6.0) at boiling temperature for 20 minutes, followed by incubation with citrate buffer (20 minutes) at room temperature to enhance the reactivity of antibodies to antigens. To block nonspecific sites, sections were treated with 1% BSA (Materials, section 2.6) for 30 minutes at room temperature and then incubated with the following primary antibodies.

WT1. Sections were incubated overnight at 4°C (or 3 hours at room temperature in case of co-incubation with other antibodies) with rabbit anti-Wilm´s tumor 1 antibody (Materials, section 2.7.1) diluted 1:50 in PBS1X. Subsequently, kidney samples were treated with goat anti rabbit-Cy3 antibody (Materials, section 2.7.2), Donkey anti rabbit-Cy5 antibody

(Materials, section 2.7.2), or goat anti rabbit-FITC antibody (Materials, section 2.7.2), for 1 hour at room temperature.

Claudin1. Sections were incubated overnight at 4°C with undiluted rabbit anti-claudin1 antibody (Materials, section 2.7.1). Subsequently, kidney samples were treated with goat anti rabbit-Cy3 antibody (Materials, section 2.7.2) or goat anti rabbit-FITC antibody (Materials, section 2.7.2), for 1 hour at room temperature.

CD24. Sections were incubated overnight at 4°C with mouse anti-CD24 antibody (Materials, section 2.7.1) diluted 1:25 in PBS1X. Subsequently, kidney samples were treated with goat anti mouse-FITC antibody (Materials, section 2.7.2) for 1 hour at room temperature.

Thy1.1. Sections were incubated overnight at 4°C with mouse anti-Thy1.1 antibody (Materials, section 2.7.1) diluted 1:50 in PBS1X. Subsequently, kidney samples were treated with donkey anti mouse-Cy3 antibody (Materials, section 2.7.2) for 1 hour at room temperature.

ED1. Sections were incubated overnight at 4°C (or 3 hours at room temperature in case of co-incubation with other antibodies) with mouse anti-ED1 antibody (Materials, section 2.7.1) diluted 1:100 in PBS1X. Subsequently, kidney samples were treated with Donkey anti mouse-Cy3 antibody (Materials, section 2.7.2) or goat anti mouse-FITC antibody (Materials, section 2.7.2), for 1 hour at room temperature.

BrdU. Sections were incubated 1 hour at room temperature with mouse anti-BrdU antibody (Materials, section 2.7.1) diluted 1:50 in PBS1X.

Subsequently, kidney samples were treated with Donkey anti mouse-Cy3 antibody (Materials, section 2.7.2) for 1 hour at room temperature.

NCAM. Sections were incubated 1 hour at room temperature with mouse anti-NCAM antibody (Materials, section 2.7.1) diluted 1:2 in PBS1X. Subsequently, kidney samples were treated with Donkey anti mouse-Cy3 antibody (Materials, section 2.7.2), or goat anti mouse-FITC antibody (Materials, section 2.7.2), for 1 hour at room temperature.

CXCR4. Sections were incubated overnight at 4°C with mouse anti-CXCR4 antibody (Materials, section 2.7.1) diluted 1:25 in PBS1X. Subsequently, kidney samples were treated with Donkey anti mouse-Cy3 antibody (Materials, section 2.7.2) for 1 hour at room temperature.

AT_1 receptor. Sections were incubated overnight at 4°C with rabbit anti-AT_1 receptor antibody (Materials, section 2.7.1) diluted 1:25 in PBS1X. Subsequently, kidney samples were treated with goat anti rabbit-FITC antibody (Materials, section 2.7.2) for 1 hour at room temperature.

SDF-1. Sections were incubated 1 hour at room temperature with rabbit anti-SDF-1 antibody (Materials, section 2.7.1) diluted 1:100 in PBS1X. Subsequently, kidney samples were treated with goat anti rabbit-Cy3 antibody (Materials, section 2.7.2) for 1 hour at room temperature.

Nephrin. Sections were incubated overnight at 4°C with goat anti-nephrin antibody (Materials, section 2.7.1) diluted 1:100 in PBS1X. Subsequently, kidney samples were treated with rabbit anti goat-FITC antibody (Materials, section 2.7.2) for 1 hour at room temperature.

Slides were then washed with PBS1X and incubated for 15 minutes at room temperature with FITC- or rhodamine-conjugated lectin Wheat Germ Agglutinin (WGA, Materials, section 2.8), which by binding membrane glycoproteins and sialic acid, was used to better identify renal structures. Nuclei were subsequently stained with 4',6'-diamidino-2-phenylindole dihydrochloride hydrate for 15 minutes at room temperature (DAPI, Materials, section 2.8). Sections were finally washed with PBS 1X and mounted with the DAKO fluorescence mounting medium (Materials, section 2.8). Negative controls were obtained by omitting the primary antibody on adjacent sections. During the experiment, slides were always kept in a moist chamber to avoid the hydration of the sections. Slides were analyzed by an inverted confocal laser-scanning microscope (Materials, section 2.10). Quantification of cells positive for the different markers was performed in at least 30 randomly selected glomeruli per each animal.

3.5.2 Immunoperoxidase

For immunoperoxidase experiments, renal tissues were fixed overnight in Duboscq-Brazil, dehydrated in alcohol and embedded in paraffin as previously described (Methods, section 3.4). Three-micrometers thick sections were deparaffinized in Unyhol Plus, rehydrated and incubated for 30 minutes at room temperature with 0.3% H_2O_2 (Materials, section 2.5) diluted in methanol (Materials, section 2.5). This step is necessary to quench endogenous peroxidase found in many

tissues and avoid aspecific signal. Antigen retrieval was performed using a microwave (2x5 minutes in citrate buffer at an operating frequency of 2450 MHz and a 600 W power output) and citrate buffer incubation (15 minutes at room temperature, Materials, section 2.6) to increase the reactivity of antibodies to antigens. To block nonspecific sites, sections were treated with 1% BSA (Materials, section 2.6) for 30 minutes at room temperature and then incubated overnight at 4°C with the following primary antibodies.

Type III collagen. Sections were incubated overnight at 4°C with rabbit anti-type III collagen antibody (Materials, section 2.7.1) diluted 1:100 in PBS1X. Subsequently, kidney samples were treated with goat anti rabbit-biotinylated antibody (Materials, section 2.7.2) for 1 hour at room temperature.

C/EBPδ. Sections were incubated overnight at 4°C with rabbit anti-C/EBPδ antibody (Materials, section 2.7.1) diluted 1:100 in PBS1X. Subsequently, kidney samples were treated with goat anti rabbit-biotinylated antibody (Materials, section 2.7.2) for 1 hour at room temperature.

After washing in PBS 1X, slides were incubated with avidin-biotin peroxidase complex solution (ABC) (Materials, section 2.8) linking the biotinylated secondary antibody, for 30 min at room temperature. The staining was visualized using diaminobenzidine (DAB) (Materials, section

2.6) substrate solution, that reacts with the peroxidase producing a brown end product. The reaction of the substrate was monitored by observing sections at light microscopy, and then blocked by immersing slices in distilled water. This step is important to determine the right period of reaction that was then applied to all slices. After rinsed in water, samples were counterstained with Harris haematoxylin (Materials, section 2.5), quickly dehydrated with 100% ethanol (Materials, section 2.5) and Unyhol Plus (Materials, section 2.5), and finally mounted with Eukitt (Materials, section 2.8). Negative controls were obtained by omitting the primary antibody on adjacent sections. During the experiment, the slides were always kept in a moist chamber to avoid that the sections could dehydrate. Quantification of cells positive for the markers was performed in at least 30 randomly selected glomeruli per each animal.

C/EBPδ signal on the Bowman's capsule was graded on a scale of 0 to 3 (0: no C/EBPδ -positive cells, 1: <25% positive cells, 2: 25% to 50% positive cells, 3: >50% positive cells in the Bowman's capsule).

3.6 Immunogold

For immunogold staining, small fragments of kidney tissue that averaged 0.5-1 mm thickness, were fixed overnight at 4°C in 3.5% paraformaldehyde plus 0.01% glutaraldehyde (Materials, section 2.3)

overnight at 4°C, and washed repeatedly in 0.1 M cacodylate buffer, pH 7.4 (Materials, section 2.6) in order to stabilize the sample and prevent degradation. Specimens were post-fixed in 1% OsO_4 (Materials, section 2.5) for 1 hour. This step confers stability during the following steps of dehydration and embedding and provides electron contrast.

Specimens were dehydrated through ascending grades of alcohol: 10% for 10 minutes, 50% and 70% for 10 minutes each, 90% and 100% for 15 minutes each. Samples were then placed in propylene oxide (1,2-epoxypropane) (Materials, section 2.5), a fluid miscible with both alcohol and epoxy resin, and embedded in Epon resin (Materials, section 2.6) overnight at room temperature that maintains the resin in a liquid state to better infiltrate the sample. Polyethylene labelled-cone shaped capsules (Materials, section 2.9) containing freshly prepared resin was used to contain the samples. Tissue fragments were placed at the tip of the truncated cone that was filled with embedding thermosetting synthetic resins. After 3 days during which time the samples were incubated at 60°C to allow polymerisation and solidification of the resin, the blocks of resin were cut by ultramicrotome (Materials, section 2.10) and then transferred to nickel grids coated with Formvar (Materials, section 2.9). After blocking with 1% BSA for 15 minutes, sections were incubated overnight with goat anti-nephrin (Materials, section 2.7.1) followed by 12-nm gold-conjugated donkey anti-goat secondary antibody (Materials, section 2.7.2) for 1 hour at room temperature. The grids were washed with PBS1X, stained for 5 minutes with 2% aqueous uranyl acetate (Materials, section 2.5), and

examined with a Morgagni 268D electron microscopy (Materials, section 2.10).

3.7 Statistical analysis

Results are expressed as means ±SE. Correlation analysis between index of crescents and proteinuria was performed by evaluating Pearson's *r* coefficient, using a Microsoft Excel spreadsheet. Statistical analysis of AT_1 receptor quantification was performed using analysis of variance with the Bonferroni post hoc analysis for multiple comparisons. Proteinuria levels, synechiae, and crescents were analyzed using 2-way ANOVA. The nonparametric Kruskal-Wallis and Mann-Whitney tests were applied, as appropriate. The statistical significance level was defined as $P<0.05$.

Methods for *in vitro* studies in the experimental rat model

3.8 Cells and cell culture

Kidneys of adult Wistar rats were quickly removed, and the cortex homogenate was gently pressed through a 105-μm (140 mesh) sieve and then over a 75-μm (140 mesh) sieve that retains glomeruli. Glomeruli were then centrifuged, resuspended in medium plus endothelial growth medium-microvascular (EGM-MV, Materials, section 2.4) and 20% fetal bovine serum (FBS, Materials, section 2.4), and plated on fibronectin-coated dishes (10 μg/mL, Materials, section 2.4) at a density of 200 glomeruli/100-mm plate. After 5 to 7 days of culture, cellular outgrowth observed on adherent capsulated glomeruli, was harvested and cultured in EGM-MV 20% FBS on glass coverslips coated with fibronectin.

For differentiation and proliferation experiments, cells from glomerular outgrowth have been expanded and claudin1-positive cells were obtained by immunomagnetic separation using goat anti-rabbit IgG MicroBeads (Materials, section 2.4) according to the manufacturer's protocol. The cells obtained from the second passage of claudin1$^+$ cell fraction were used for all experiments. For podocyte differentiation, claudin1$^+$ PECs were treated for 7 days with DMEM/F12 supplemented with vitamin D3 100 nmol/L and retinoic acid 100 μmol/L (VRAD medium, Materials, section 2.4). The proliferation rate of immunoisolated

claudin1$^+$ PECs was assessed by evaluating the phosphorylation at Ser10 of histone H3 in cells maintained overnight in medium plus 1% FBS and then exposed to medium or to angiotensin II (10^{-7} mol/L, Materials, section 2.4) for 24 hours.

The expression of C/EBPδ was evaluated in PECs incubated in DMEM (Materials, section 2.4) plus 2% BSA, exposed or not with 10^{-7} mol/L angiotensin II (Materials, section 2.4). After 6 hours, the cells were fixed and processed as described in Methods, section 3.9.

3.9 Immunofluorescence

For immunofluorescence analysis, cells were fixed in 2% paraformaldehyde plus 4% sucrose (Materials, section 2.3) and permeabilized with 0.3% Triton- X100 (Materials, section 2.4). After blocking the non-specific sites with 2% BSA plus 0.2% gelatin bovine and 2% FBS in PBS, cells were incubated with the following primary antibodies:

Claudin1. The expression of claudin1 was evaluated in cells obtained from the outgrowth of capsulated glomeruli. Cells were incubated 1 hour at room temperature with undiluted rabbit anti-claudin1 antibody (Materials, section 2.7.1). Subsequently, cells were treated with goat anti

rabbit-Cy3 antibody (Materials, section 2.7.2), for 1 hour at room temperature.

NCAM. The expression of NCAM was evaluated in cells obtained from the outgrowth of capsulated glomeruli. Cells were incubated 1 hour at room temperature with mouse anti-NCAM antibody (Materials, section 2.7.1) diluted 1:2. Subsequently, cells were treated with goat anti mouse-FITC antibody (Materials, section 2.7.2), for 1 hour at room temperature.

CD24. The expression of CD24 was evaluated in cells obtained from the outgrowth of capsulated glomeruli. Cells were incubated with mouse anti-CD24 antibody (Materials, section 2.7.1) diluted 1:25, overnight at 4°C. Subsequently, cells were treated with goat anti mouse-FITC antibody (Materials, section 2.7.2), for 1 hour at room temperature.

Synaptopodin. The expression of synaptopodin (SYN) was evaluated in claudin1-positive cells obtained by the immunomagnetic separation using MicroBeads. Cells were incubated with undiluted mouse anti-SYN antibody (Materials, section 2.7.1), overnight at 4°C. Subsequently, cells were treated with goat anti mouse-FITC antibody (Materials, section 2.7.2), for 1 hour at room temperature.

Phospho-histone H3. The expression of phospho-histone H3 (H3p) was evaluated in claudin1-positive cells obtained by the immunomagnetic separation using MicroBeads. Cells were incubated with undiluted rabbit anti-H3p antibody (Materials, section 2.7.1), overnight at 4°C. Subsequently, cells were treated with goat anti rabbit-FITC antibody (Materials, section 2.7.2), for 1 hour at room temperature.

C/EBPδ. The expression of C/EBPδ was evaluated in cells obtained from the outgrowth of capsulated glomeruli, treated or not with Angiotensin II. Cells were incubated 3 hours at room temperature with rabbit anti-C/EBPδ antibody (Materials, section 2.7.1) diluted 1:25. Subsequently, cells were treated with goat anti rabbit-FITC antibody (Materials, section 2.7.2), for 1 hour at room temperature.

Nuclei were then stained with DAPI (Materials, section 2.8) for 15 minutes at room temperature. Finally, cells were washed with PBS 1X and mounted with the DAKO mounting medium (Materials, section 2.8). Representative images were acquired using an inverted confocal laser scanning microscope (Materials, section 2.10).

The quantification of cells positive for SYN or H3p was assessed evaluating fluorescent cells per total $DAPI^+$ cells in each high-power field (HPF) (five to 10 fields/slide; n = 3 experiments). Data were expressed as percentage of SYN+H3p+ cells on total DAPI+ cells, per each HPF.

3.10 Statistical analysis

Results are expressed as means ±SE. Statistical analysis was performed using student's t-test. The statistical significance level was defined as $P<0.05$.

Methods for *in vivo* studies in human tissue

3.11 Patients

Thirty six patients with proliferative and non proliferative glomerulopathies from the archives of the Unit of Nephrology, Ospedali Riuniti of Bergamo, Italy, were enrolled in the study. Patients were divided into different groups as follows:

- Patients with extracapillary proliferative lesions as:
  1) extracapillary glomerulonephritis (n=9)
  2) IgA nephropathy (n=9).
- Patients with non proliferative diseases as:
  1) membranous nephropathy (n=7)
  2) diabetic nephropathy (n=11).

Written informed consent was obtained from all these patients. In addition, to further address the possible participation of the Ang II/AT_1 receptor pathway and renal progenitor cells in the development of glomerular hyperplastic lesions, we analyzed in-depth renal tissue specimens from one of these patients with antineutrophil cytoplasm antibodies (ANCA)-positive crescentic glomerulonephritis from whom two biopsies were collected, before and after 8 months therapy with the ACE inhibitor ramipril (titrating up the dose from 2.5 to 7.5 mg/day, Materials, section 2.8) associated with the immunosuppressant

azathioprine (50 mg/day). All kidney biopsy specimens considered for the present study had been originally obtained for the diagnosis of renal disease. In addition to specimens from patients with proliferative and non proliferative diseases, renal biopsies from an uninvolved portion of kidney collected from tumor nephrectomy specimens were obtained from 10 patients and used as controls.

3.12 Demographic and clinical characteristics of patient populations

For all patients enrolled in the study, demographic, clinical and hematochemical parameters at the time of renal biopsy were retrieved from the Hospital database. Demographic parameters taken into account were the age of patients reported as range of years-old, and the gender expressed as ratio between male and female (M:F). The clinical parameters evaluated in the patients, quantified by the Laboratories of the Division of Nephrology and Dialysis of the hospital, were systolic and diastolic blood pressure, proteinuria and serum creatinine.

3.12.1 Evaluation of systemic blood pressure

Systemic blood pressure was measured by sphygmomanometer. The blood pressure levels reflect the values of systolic and diastolic pressure. Systolic pressure refers to systole, the phase when the heart pumps blood out into the aorta. Diastolic pressure refers to diastole, the resting period when the heart refills with blood. A typical blood pressure reading of a healthy adult should be 120 millimeters of mercury (mmHg) of systolic blood pressure and 80 mmHg of diastolic blood pressures. The values vary depending on age and many other factors.

3.12.2 Assessment of urinary protein concentrations

Urinary protein concentration, collected for 24 hours (h), was measured using an autoanalyzer (Materials, section 2.10). The test used is based on the procedure developed by Watanabe *et al* (Watanabe *et al.*, 1986). This is a dye-binding method that generate a complex of purple colour with the proteins content in the sample. The resulting complex has a maximum absorbance at 600 nanometers (nm). The system automatically apportions the sample and reagent into a cuvette at a ratio of 1:30 for urine samples. The system monitors the change in absorbance at 600 nm at a fixed-time interval. The change in absorbance is directly proportional to the concentration of protein in the sample and is used by the system to calculate and express the protein concentration.

3.12.3 Assessment of serum creatinine concentrations

The serum creatinine concentration was measured in patients using an automatic device (Materials, section 2.10) with a quantitative, colorimetric assay based on a modified Jaffè method where alkaline picrate forms a reddish colored solution in the presence of creatinine. A precise volume of sample is automatically introduced by Synchron CX System into a reaction cup containing the alkaline picrate solution in the ratio of 1:11. The system reads the alterations of the absorbance at both 520 nm and 560 nm. These alterations are directly proportional to the creatinine concentration of the samples.

3.13 Biopsy and tissue collection

Depending on the type of procedure that would have been applied (immunohistochemistry or immunofluorescence), samples were frozen in liquid nitrogen or embedded in paraffin as described in each specific chapter.

3.14 Renal morphology by light microscopy

Immediately after collection, kidney fragments were fixed overnight in Duboscq-Brazil solution (Materials, section 2.3), dehydrated and

embedded in paraffin (Materials, section 2.8) as previously described (Methods, section 3.4). Embedded samples were cut at 2 μm thickness slices by using a microtome (Materials, section 2.10).

For the histologic staining, sections were deparaffinised, rehydrated and undergone to PAS (Materials, section 2.5) staining as previously described (Methods, section 3.4). Slides were observed with light microscopy (Materials, section 2.10), and quantified as the percentage of glomeruli affected by different glomerular lesions: extracapillary proliferation (multilayers of cells accumulating in the inner surface of the Bowman's capsule, which obliterate the Bowman's space), global sclerosis (accumulation of PAS-positive materials in the entire glomerular tuft), segmental sclerosis (accumulation of PAS-positive materials in a restricted area of the glomerular tuft), other glomerular changes (capillary loop thickening, mesangial hypercellularity and matrix expansion, epithelial vacuolization). In addition, the percentage of normal glomeruli has been also quantified.

3.15 Immunohistochemistry

3.15.1 Immunofluorescence

For all immunofluorescence experiments, samples collected immediately after renal biopsy, were embedded in Tissue-Tek OCT

Compound (Materials, section 2.8) and frozen in liquid nitrogen. Two-micrometer-thick sections were cut by using a cryostat (Materials, section 2.10) and stored at -80°C. Sections were air dried, fixed in cold acetone (Materials, section 2.5), and washed in PBS 1X and incubated with 1% BSA as previously described (Methods, section 3.5.1). Slides were then incubated with the following primary antibodies.

CD24. Sections were incubated 1 hour at room temperature with goat or mouse anti-CD24 antibody (Materials, section 2.7.1) diluted 1:25 in PBS1X. Subsequently, kidney samples were treated with donkey anti goat-Cy3 antibody (Materials, section 2.7.2) or goat anti mouse-FITC antibody (Materials, section 2.7.2), for 1 hour at room temperature.

CD133. Sections were incubated 1 hour at room temperature with mouse anti-CD133 antibody (Materials, section 2.7.1), diluted 1:50. Subsequently, kidney samples were treated with donkey anti mouse-Cy3 antibody (Materials, section 2.7.2) for 1 hour at room temperature.

CXCR4. Sections were incubated overnight at 4°C with rabbit anti-CXCR4 antibody (Materials, section 2.7.1) diluted 1:50 in PBS1X. Subsequently, kidney samples were treated with goat anti rabbit-FITC antibody (Materials, section 2.7.2) for 1 hour at room temperature.

SDF-1. Sections were incubated overnight at 4°C with rabbit anti-SDF-1 antibody (Materials, section 2.7.1) diluted 1:200 in PBS 1X. Subsequently, kidney samples were treated with goat anti rabbit-Cy3 antibody (Materials, section 2.7.2) for 1 hour at room temperature.

CD68. Sections were incubated 1 hour at room temperature with mouse anti-CD68 antibody (Materials, section 2.7.1), diluted 1:100. Subsequently, kidney samples were treated with goat anti mouse-FITC antibody (Materials, section 2.7.2) for 1 hour at room temperature.

Nephrin. Sections were incubated overnight at 4°C with goat anti-nephrin antibody (Materials, section 2.7.1) diluted 1:100 in PBS1X. Subsequently, kidney samples were treated with rabbit anti goat-FITC antibody (Materials, section 2.7.2) for 1 hour at room temperature.

AT_1 receptor. Sections were incubated overnight at 4°C with rabbit anti-AT_1 receptor antibody (Materials, section 2.7.1) diluted 1:25 in PBS1X. Subsequently, kidney samples were treated with goat anti rabbit-FITC antibody (Materials, section 2.7.2) for 1 hour at room temperature.

Slides were then washed with PBS1X and incubated for 15 minutes at room temperature with FITC- or rhodamine-conjugated lectin Wheat Germ Agglutinin and with DAPI (Materials, section 2.8) as previously described (Methods, section 3.5.1). Sections were finally washed with PBS 1X and mounted with the mounting medium DAKO (Materials, section 2.8). Negative controls were obtained by omitting the primary antibody on adjacent sections. Slides were analyzed by an inverted confocal laser-scanning microscope (Materials, section 2.10). For SDF-1 expression in patients with extracapillary glomerulonephritis and in normal kidneys, all glomeruli of the section were acquired and subjected to semi-quantitative

analysis. Glomerular SDF-1 expression was scored on a scale of 0 to 3 (0: no staining, 1: mild, 2: moderate, 3: strong diffuse staining).

3.15.2 Immunoperoxidase

For AT_1 receptor evaluation, Duboscq-Brazil-fixed kidney biopsies were embedded in paraffin (Materials, section 2.8), and sections were subsequently deparaffinized, rehydrated and incubated for 30 minutes at room temperature with 0.3% H_2O_2 (Materials, section 2.5) diluted in methanol as described (Methods, section 2.5). Antigen retrieval was performed using a microwave, and 1% BSA was applied to block nonspecific sites (Methods, section 2.6). Sections were then incubated overnight at 4°C with rabbit anti-AT_1 receptor antibody (Materials, section 2.7.1) diluted 1:25 in PBS1X. Subsequently, kidney samples were treated with goat anti-rabbit biotinylated antibody (Materials, section 2.7.2) for 1 hour at room temperature.

After washing in PBS 1X, slides were incubated with ABC (Materials, section 2.8), and the staining was visualized using DAB (Materials, section 2.6) substrate solution as described (Methods, section 3.5.2). Samples were counterstained with Harris haematoxylin (Materials, section 2.5), quickly dehydrated with 100% ethanol (Materials, section 2.5) and Unyhol Plus (Materials, section 2.5), and finally mounted with Eukitt (Materials, section 2.8). Negative controls were obtained by omitting the primary antibody on adjacent sections.

3.16 Statistical analysis

Results are expressed as mean ± SD. Statistical analysis of AT_1 receptor quantification in experimental animals was performed using ANOVA with the Bonferroni post hoc analysis for multiple comparisons. The Student's t-test was applied for SDF-1 quantification in patients. Statistical significance was defined as $P<0.05$.

3.17 Principles of the main instruments

3.17.1 Light microscopy

A microscope is an instrument that allows observation of objects that are too small to be seen by the naked eye. In order to visualise objects, the light microscope uses light and magnifying lenses. Most microscopes are composed by two lens systems: the objective lens and the ocular. The final magnification of an object results by the multiplication of the magnifying power of the objective lens (from 4x to 100x) and the magnifying power of the ocular lens (from 8x to 12x). As a result, a standard microscope provides a final magnification range of 40x up to 1000x.

The essential factor for producing a good image is the light. The microscope uses another lens, the condenser, to produce a bright and uniform light illuminating the specimen. A good image is obtained when the resolution is high. The resolution is the ability to distinguish two objects as separate entities. Resolution is best when the distance separating the two tiny objects is small.

In this study the light miscoscopy is used to observe renal specimens labelled with PAS staining (Methods, section 3.14) or immunoperoxidase techniques (Methods, section 3.15.2). The PAS is a staining method used to detect polysaccharides such as glycogen, and mucosubstances such as glycoproteins, glycolipids and mucins in tissues. The Schiff reagent gives a purple-magenta colour, which labels the connective tissue, glycocalyx and

basal laminae. In the kidney, the PAS staining is commonly used to evaluate and quantify the glomerular and tubular damage.

3.17.2 Immunofluorescence technique and confocal microscopy

This technique uses the specificity of antibodies to their antigens to target specific cells with fluorescence dyes, and therefore allows to visualize the distribution of the target cells through the sample. There are two types of immunofluorescence: the direct immunofluorescence and the indirect one. The direct immunofluorescence uses a primary antibody, against the antigen of interest, which is directly conjugated with a fluorophore. The indirect immunofluorescence, which is more frequently used, employs two sets of antibodies: a primary antibody and a subsequent, secondary, dye-coupled antibody, which recognizes the primary antibody.

Immunofluorescent labeled samples are analyzed using fluorescence or confocal microscope.

A fluorescence microscope is an optical microscope used to study properties of organic or inorganic substances using fluorescence and phosphorescence instead of, or in addition to, reflection and absorption. The specimen is illuminated with light of a specific wavelength, which is absorbed by the fluorophores, causing them to emit longer wavelengths of light (of a different colour than the absorbed light). The illumination light is separated from the much weaker emitted fluorescence through the use

of an emission filter. Typical components of a fluorescence microscope are the light source (Xenon or Mercury arc-discharge lamp), the excitation filter, the dichroic mirror (or dichromatic beamsplitter), and the emission filter. The filters and the dichroic are chosen to match the spectral excitation and emission characteristics of the fluorophore used to label the specimen.

The confocal microscopy is an optical imaging technique used to increase micrograph contrast and/or to reconstruct three-dimensional images by using a spatial pinhole to eliminate out-of-focus light or flare in specimens that are thicker than the focal plane. The principle of confocal imaging was patented by Marvin Minsky in 1957 and aims to overcome some limitations of traditional wide-field fluorescence microscopes. In a conventional fluorescence microscope, the entire specimen is flooded in light from a light source. All parts of the specimen throughout the optical path are excited at the same time and the resulting fluorescence is detected by the microscope's photodetector or camera including a large unfocused background part. In contrast, a confocal microscope uses point illumination and a pinhole in an optically conjugate plane in front of the detector to eliminate out-of-focus information. Only the light within the focal plane can be detected, so the image quality is much better than that of wide-field images. As only one point is illuminated at a time in confocal microscopy, 2D or 3D imaging requires scanning over a regular raster in the specimen. The thickness of the focal plane is defined mostly by the

square of the numerical aperture of the objective lens, and also by the optical properties of the specimen and the ambient index of refraction.

3.17.3 Transmission electron microscopy

The transmission electron microscope is a type of microscope that uses beam of electrons to observe the specimen. The beam of electrons, emitted by a high voltage electron emitter situated at the top of the microscope column, pass through the sample and through a series of magnifying magnetic lenses, to reach the viewing screen where they are ultimately focused. In the column, a very high vacuum is created in order to reduce the electron beam interactions with air. Energy produced by an electric source (~2500K) superheats a tungsten wire that emits electrons. Liquid nitrogen is used to cool down the column for easier removal of water vapour. Electrons are sent down the microscope column, across the sample, lenses, and apertures. The lenses are magnetic coils that, set on a specific electron wavelength, focus and direct the electron beam. As it passes through the lens (three primary lenses) the electron beam is split. The topmost lens is the objective and it magnifies and focuses the image. Then there is the intermediate lens that controls the magnification of the image and the diffraction pattern. Finally, the projector lens that focuses and projects the image onto the imaging surface. The image can be visualized on a screen: where fewer electrons were transmitted through the sample, in thicker or denser zones, the image shows dark areas whereas areas where the sample was thinner or less dense more electrons

are transmitted through and the image appears more light. The power of resolution of electron microscopy depends on the lens-systems and on sample preparation method. Usually, in modern microscopes the resolution power ranges from 0.2 - 0.3 nm and magnification up to 180,000x.

CHAPTER 4

RESULTS IN MWF RATS

4.1 Introduction

Until few years ago, the kidney has been considered as an organ with low regenerative properties, and the common thought was that renal cells which were lost following an injury cannot be repaired. In the recent years, robust evidence have documented the beneficial effect of ACE inhibitors to slow the development of proteinuria and limit renal damage, both in humans (The GISEN group, 1997; Ruggenenti *et al.*, 1999 Fioretto *et al.*, 1998) and in experimental models (Marinides *et al.*, 1990; Remuzzi A *et al.*, 1999; Remuzzi A *et al.*, 2002; Adamczak *et al.*, 2003; Boffa *et al.*, 2003; Remuzzi A *et al.*, 2006). By three-dimensional reconstruction of glomerular capillary tufts based on kidney serial section analysis, a group of researchers of our Insitute has found that 10 week treatment with ACE inhibitor, given to MWF rats in the advanced phase of the disease, effectively reduced the extent of sclerosis and induced generation of new capillary tissue (Remuzzi A. *et al.*, 2006). This approach strongly suggests the possibility for the kidney to regenerate, however, has not identified glomerular cellular components. As a follow-up of that study (Remuzzi A. *et al.*, 2006), the same group of researchers showed that, in MWF rats, ACE inhibitor halted the spontaneous podocyte loss and restored podocyte number (Macconi *et al.*, 2009).

The regression of glomerulosclerosis and neoformation of glomerular tissue as been recently linked to progenitor/stem cells of renal or extrarenal origin (Oliver *et al.*, 2004).

Mechanisms and cellular determinants of progressive nephropathies in the context of recent findings of glomerular epithelial cell activation have never been addressed in systematic fashion. Inhibiting ACE can be a selective way to potentiate the regeneration of the glomerulus, shifting the process toward kidney healing. To this end, the spontaneous glomerulopathy of MWF rats represents the most appropriate model in which to study the cellular basis for glomerular restructuring and repair.

4.2 A population of renal progenitor cells existed within the Bowman's capsule of normal adult rat kidney

The phenotype of PECs in the Bowman's capsule of control Wistar rats was assessed by simultaneously staining claudin1, a marker of glomerular PECs that localizes to intercellular tight junctions (Ohse *et al.*, 2008), and the podocyte marker WT1. All of the cells lining the Bowman's capsule express claudin1, and a small fraction co-expressed WT1 (21.9% $\pm$ 0.5%) (Figure 1A). That claudin1$^+$WT1$^+$ cells residing in the inner surface of the Bowman's capsule represent parietal podocytes was confirmed by ultrastructural analysis. Through immunogold approach we clearly identified some PECs exhibiting foot processes in which marked expression of the slit diaphragm protein nephrin has been found (Figure 1B).

Previous studies in humans document that the Bowman's capsule is lined by a subset of parietal epithelial cells with stem cell characteristics (Sagrinati *et al.*, 2006), which in physiological conditions gradually lose their stemness and regenerate podocytes (Ronconi *et al.*, 2009). Since no stem cell population in the Bowman's capsule of rats has been ever described, we search a marker of stemness in rats, by focusing our attention on NCAM. NCAM is a protein expressed during the kidney development in metanephric mesenchyme, which gradually disappears remaining confined in the glomerular capsule in mature kidney (Abbate *et al.*, 1999; Bard *et al.*, 2001). In control rats, NCAM was expressed by the majority of claudin1^{+} cells in the Bowman's capsule (Figure 2A). Cells positive for NCAM also expressed CD24, a surface antigen known to be a marker of renal progenitor cells in mice (Challen *et al.*, 2004; Swetha *et al.*, 2009) and in humans (Ronconi *et al.*, 2009) (Figure 2B). Through a double immunolabeling with NCAM and the podocyte marker WT1, we detected and quantified three distinct populations of cells in the Bowman's capsule (Figure 2C). The most abundant population was constituted by cells only expressing NCAM in the absence of WT1, representing immature progenitor cells. Two minor cell populations were represented by transitional cells co-expressing markers of renal progenitors and podocytes (NCAM+WT1+), and by parietal podocytes, that are more differentiated cells that no longer expressed NCAM but exhibited the marker WT1 (Figure 2C). A schematic representation of the cell

populations identified in the Bowman's capsule of normal rats was given in Figure 2D.

4.3 Time-dependent evolution of glomerular lesions in Wistar and MWF rats

Changes in renal histology as a function of time was assessed in control Wistar rats as well as in MWF rats studied at different time points from 10 to 60 weeks of age (Figure 3).

In Wistar rats, the only morphological abnormalities observed in renal biopsies were synechiae, focal adhesions of glomerular capillaries to the Bowman's capsule (Figure 3A). These early lesions were found between 50 and 60 weeks, while no more severe alterations were observed in control animals at any other time point (Figure 3A).

In MWF rats, synechiae were detected starting from 10 weeks of age, while from 25 weeks multilayers of cells accumulated at the site of synechiae resulting in more severe crescentic lesions, typically found in 40- to 60-week-old animals (Figure 3A). The percentage of glomeruli with crescents was 39% $\pm$ 4% at 40 weeks, 64% $\pm$ 5% at 50 weeks, and 76% $\pm$ 4% at 60 weeks. The index of crescents, which takes into account both the number and the extension of glomerular lesions, positively correlated with the levels of proteinuria (Figure 3A and B, r = 0.94, $p<0.01$), which

developed with time in MWF rats from 10 weeks and reached values of 730 ± 44 mg/day at 60 weeks.

That crescentic lesions may evolve in glomerulosclerosis was supported by the observation that type III collagen deposition was observed later on in respect to the onset of crescents (Figure 4). Histological analysis of 10-week-old MWF rats revealed that early synechiae were not associated with accumulation of type III collagen. From 25 weeks, crescent-like lesions were observed, which increased in number and extension with age. At an early stage, crescents were characterized by cell proliferation in the absence of type III collagen deposition. Lesions in 40-week-old rats were characterized by scanty accumulation of type III collagen, which increased over time in rats from 50 to 60 weeks of age. At the end of the observation period, glomerulosclerosis was so severe as to occupy most of the glomerular tuft in the majority of the glomeruli (Figure 4).

4.4 Phenotype of cell population involved in crescentic lesions in MWF rats

In the past years, different studies analysed the cellular composition of crescents obtaining conflicting results (Cattell *et al.*, 1978, Jennette *et al.*, 1986; Boucher *et al.*, 1987; Lan *et al.*, 1992; Ophashcharoensuk *et al.*, 1998; Le Hir *et al.*, 2001; Moeller *et al.*, 2004; Bariety *et al.*, 2005, Thorner *et al.*,

2008). Here, we assessed the phenotype of cells contributing to glomerular lesions in 60 week-old MWF rats by evaluating the expression of different markers (Figure 5). The most abundant cell population was constituted by claudin1$^+$ PECs, accounting for about 60% of the total cells in crescents. These cells may represent progenitor cells. A high percentage of WT1$^+$ podocytes was also observed within hyperplastic lesions, and on average 12% of these cells co-expressed claudin1 representing transitional cells. Mesangial cells and macrophages, identified respectively by Thy1.1 and ED1 immunolabeling, represented two minor cell populations in crescents (Figure 5).

4.5 Treatment with ACE inhibitor reduced proteinuria and induced regression of crescentic lesions

MWF rats receiving the ACE inhibitor lisinopril from 50 to 60 weeks of age showed proteinuria levels that were markedly reduced in respect to those observed in MWF rats before the beginning of the treatment (Figure 6). In parallel with the decrease of proteinuria, lisinopril limited the number and the extension of crescentic lesions, as demonstrated by the remarkable reduction of the index of crescents, which reflected the degree of severity of the lesions (Figure 6). The extension of glomerular lesions in 60 week-old MWF rats receiving lisinopril was even lower in respect to that observed in 50 week-old rats, suggesting the ability of ACE inhibitor

to induce regression of glomerular injury. At 60 weeks, MWF rats had renal function impairment and developed hypertension (serum creatinine, 2.0 ± 0.3 versus controls: 0.7 ± 0.01 mg/dL, systolic blood pressure: 192.0 ± 5.2 versus controls: 127.0 ± 1.7 mm Hg, $P < 0.01$). Treatment with ACE inhibitor (from 50 to 60 weeks of age) decreased serum creatinine levels (1.3 ± 0.1 mg/dL, $P < 0.05$) and systolic blood pressure (133.0 ± 16.8 mm Hg, $P < 0.05$) with respect to rats receiving saline.

When animals were treated only 2 weeks with ACE inhibitor, from 50 to 52 weeks of age, proteinuria was only mildly affected, and the index of crescents did not change (50 week old: 1.5 ± 0.2 versus treated 52 week old: 1.6 ± 0.3).

4.6 ACE inhibitor limited cell proliferation in crescents

To investigate whether the renoprotection exerted by ACE inhibitor occurs via the limitation of cell proliferation in crescents, we evaluated the number of BrdU-retaining cells in pulsed MWF animals at 60 weeks of age, receiving or not lisinopril (Figure 7A). The number of $BrdU^+$ proliferating cells in crescentic lesions of MWF rats given saline accounted for 9.6% ± 1.5%. The majority of BrdU-labeled cells expressed claudin1 in the absence of podocyte marker WT1, whereas proliferating $claudin1^+WT1^+$ represented a minor cell population in crescents. Finally, differentiated podocytes expressing WT1 in the absence of claudin1

markers were almost absent (Figure 7B and C). Ten week treatment with ACE inhibitor significantly decreased the proliferation of all cell populations in respect to MWF rats receiving saline (Figure 7B).

That claudin1$^+$ cells within the crescents represent a population of progenitor cells was confirmed by immunostaining for NCAM (Figure 8). Consistently with the decreased proliferation of claudin1$^+$WT1$^-$ and claudin1$^+$WT1$^+$ cells, treatment with ACE inhibitor effectively reduced the presence of NCAM$^+$ cells in crescents by limiting progenitor cell activation and migration toward capillary tuft. Of note, following the treatment with lisinopril, the distribution of progenitor cells along the Bowman's capsule was restored to a pattern similar to controls (Figure 8C versus A).

4.7 ACE inhibitor preserved Bowman's capsule architecture

The antiproliferative effect of ACE inhibitor on claudin1$^+$ cells constituting the crescents, prompted us to analyze whether this drug can also influence the proliferative status of claudin1$^+$ cells in the Bowman's capsule. In line with data obtained few years ago by a group of our Institute (Macconi *et al.*, 2009), the total number of PECs lining the Bowman's capsule was comparable in 60-week-old MWF rats (445.8 $\pm$ 19.8 x 10^{-4}/μm of capsule) and controls (427.2 $\pm$ 5.2 x 10^{-4}/ μm of capsule). The characterization of cell phenotype demonstrated that, as compared with

controls, in untreated 60-week-old MWF rats the percentage of claudin1+WT1- PECs was markedly enhanced at the expense of claudin1$^+$WT1$^+$ parietal podocytes that significantly decreased (Figure 9A). The proliferative status of claudin1$^+$ PECs in the Bowman's capsule of MWF rats, as assessed by the quantification of BrdU-retaining cells, was markedly enhanced as compared with controls, in which proliferating claudin1$^+$ PECs were extremely rare (Figure 9B and C).

Consistent with the ability of ACE inhibitor to reduce proliferation of claudin1$^+$ cells in crescents, the treatment with lisinopril also reduced the proliferative status of Bowman's capsule cells (Figure 9B). The effect of ACE inhibitor in limiting cell proliferation paralleled the restoration of the ratio between claudin1$^+$ PECs and parietal podocytes (claudin1$^+$WT1$^+$) in the Bowman's capsule (Figure 9A).

4.8 Mechanism underlying the renoprotective effect of ACE inhibitor:

4.8.1 Role of the transcription factor C/EBPδ

To deepen the mechanism by which ACE inhibitor limits the abnormal proliferation of claudin1$^+$ progenitor cells, we evaluated the role of C/EBPδ, a transcription factor specific for adult cells and mitotically quiescent stem cells of epithelial origin (Barbaro *et al.*, 2007), which regulates cell cycle and selfrenewal potential (O'Rourke *et al.*, 1997, Zhang

et al., 2008). In Wistar rats, C/EBPδ was detectable in the majority of cell nuclei along the Bowman's capsule, indicating the low-cycling status of these cells, whereas it was markedly decreased in untreated 60 week-old MWF rats. ACE inhibitor restored C/EBPδ expression to control levels (Figure 10), suggesting the involvement of C/EBPδ in the antiproliferative effect of this drug.

4.8.2 Role of the chemokine receptor CXCR4

To evaluate the potential role of chemokines in promoting cell proliferation resulting in the formation of crescentic lesions, we analyzed the expression of SDF-1 and its receptor CXCR4 in 60 week-old MWF rats, treated or not with ACE inhibitor. While in Wistar rats SDF-1 was rarely detectable in few cells along the Bowman's capsule, its expression markedly increased in MWF rats specifically in podocytes, as documented by double immunostaining with nephrin (Figure 11A, arrows). Of note, SDF-1 staining showed no co-localization with ED1 macrophages (Figure 11B). The enhanced SDF-1 expression in MWF rats paralleled an increase of its receptor CXCR4, which in 60 week-old animals was mainly localized in the area of hyperplastic lesions (Figure 11C, inset). MWF rats receiving ACE inhibitor treatment showed a normalization of the immunostaining for both SDF-1 and CXCR4 (Figure 11A and C) and no more abundance of ED1 macrophages than in the normal kidney (Figure 11B).

4.8.3 Role of AT_1 receptor

Given the antiproliferative effect of ACE inhibitor on parietal epithelial cells, we wonder to evaluate the expression of AT_1 receptor in Wistar and MWF rats, treated or not with lisinopril. In Wistar rats AT_1 receptor was expressed by few PECs along the Bowman's capsule (Figure 12A). The enhanced cell proliferation observed in MWF rats was associated with an increase in AT_1 receptor expression, which localized in the glomerulus including the Bowman's capsule (Figure 12B, arrows), as well as in the area of hyperplastic lesions (Figure 12B, arrowheads). The MWF rats given the ACE inhibitor lisinopril showed a significant reduction in the number of PECs expressing the AT_1 receptor compared with untreated animals (Figure 12C vs B, arrows), suggesting a key role of the AT_1 receptor in progenitor cell-mediated extracapillary proliferation. A quantification of PECs expressing AT_1 receptor was given in Figure 12D.

4.9 *In vitro* characterization of PECs

Parietal epithelial cells were isolated by the initial outgrowth of capsulated control rat glomeruli, as previously described (Sagrinati *et al.*, 2006, Swetha *et al.*, 2009). Immunofluorescence analysis on cultured cells confirmed data obtained *ex vivo* in renal tissue, shown in Figure 1. Isolated PECs expressed either markers of adult epithelial cells such as claudin-1, or markers of immature progenitors including NCAM, and CD24 (Figure 13A). Immunoisolated claudin1^{+} PECs can differentiate and generate podocytes, as documented by the ability to acquire the podocyte marker synaptopodin when exposed to a specific inductive medium, named VRAD (Ronconi *et al.*, 2009) (Figure 13B to D). After 7 days exposure to VRAD, 29% of cells acquired the specific podocyte marker with the typical localization along cytoskeletal fibers (Figure 13C and D), according with the theory that PECs contain a population of progenitor cells devoted to generate podocytes.

To evaluate the capacity of angiotensin II to induce PEC proliferation, we evaluated the phosphorylated form of Histone H3-serine 10 (H3p) as a marker of mitosis, on immunoisolated claudin1+ PECs, before and after 24 hour incubation with Ang II. After Ang II exposure, a large number of PECs revealed nuclear-positive granular staining for H3p with respect to unstimulated cells (Figure 14B versus A). The percentage of Ang II-induced proliferating cells averaged 39% $\pm$ 6% as compared to 15% $\pm$ 3% observed in unstimulated cells (Figure 14C).

The involvement of the transcription factor C/EBPδ in the regulation of PECs proliferation was also assessed. In line with the above data, incubation with Ang II markedly reduced the expression of C/EBPδ (Figure 14D and E), suggesting that the mitogenic effect of the peptide can be exerted through the down-regulation of the C/EBPδ signalling pathway.

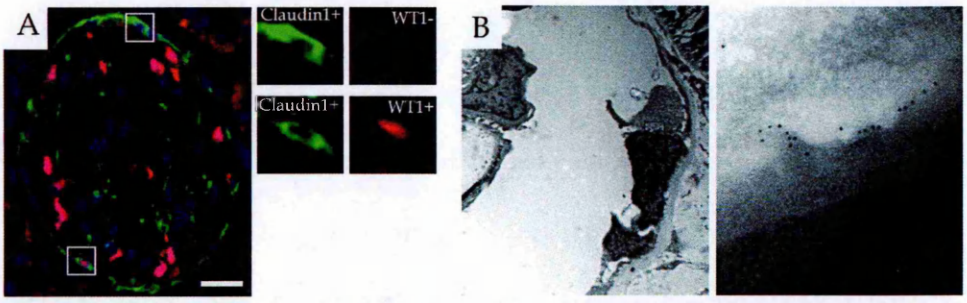

Figure 1. Populations of cells in the Bowman's capsule of normal rat kidney.
(**A**) Representative picture of immunofluorescence stainings of claudin1 and WT1 in the Bowman's capsule of Wistar rats used as controls. High-magnification insets show claudin1+WT1- cell (upper insets) and claudin1+WT1+ cell (lower insets). Scale bars=25 μm (**B**) Representative pattern of immunogold labelling for nephrin in the Bowman's capsule of Wistar rats. Left panel shows the ultrastructure of parietal cells along the Bowman's capsule. High-magnification inset (right panel) shows that gold particles are localized along the foot processes of parietal cells. Original magnifications x4400 (left panel) and x71000 (right panel).

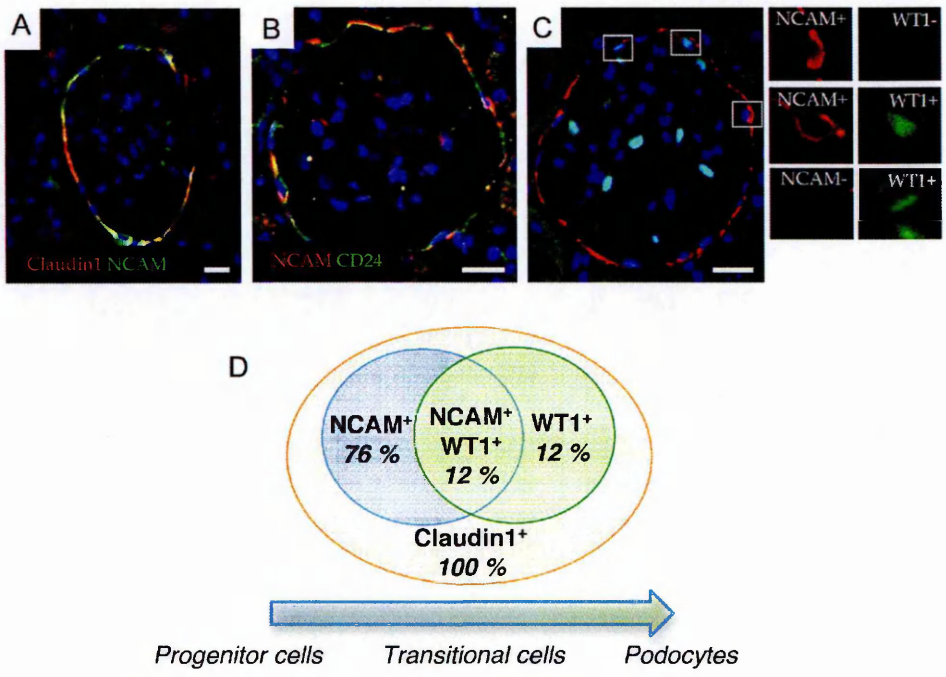

Figure 2. Identification of three progenitor cell populations in the Bowman's capsule of normal rat kidney.

(**A**) Double-immunolabeling for claudin1 and NCAM shows in most of the cells the colocalization of the two markers. (**B**) Double immunofluorescence staining for NCAM and CD24 reveals that in the Bowman's capsule the two antigen are expressed by the same cells. (**C**) Representative photomicrograph showing three distinct cell populations in the Bowman's capsule of Wistar rats, identified by staining of NCAM and WT1: NCAM+WT1- progenitor cells (upper inset), NCAM+WT1+ transitional cells (middle inset) and NCAM-WT1+ parietal podocytes (lower inset). DAPI stains nuclei. Scale bars=25 μm (**D**) Schematic representation of the cell populations identified in the Bowman's capsule of Wistar rats. All the cells were positive for PEC marker claudin1. A gradient of expression of NCAM and WT1 defined three populations of claudin1+ PECs with different degree of differentiation.

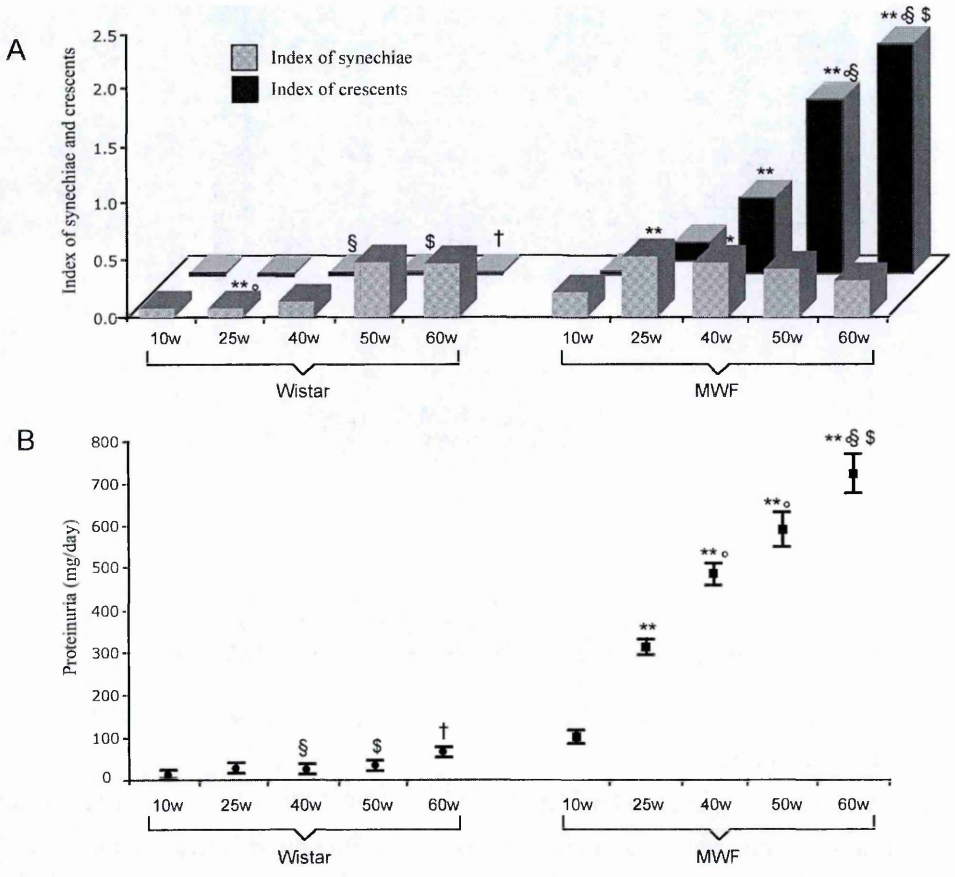

Figure 3. Time course of proteinuria and histologic glomerular lesions in Wistar and MWF rats.

(**A**) Age-related changes of the index of synechiae (striped bars), and crescents (dark grey bars) quantified in Wistar (n=20) and MWF (n=50) rats. ** P<0.01 vs 10w MWF; * P<0.05 vs 10w MWF; °P<0.01 vs 25w MWF; §P<0.01 vs 40w MWF; $ P<0.01 vs 50w MWF; † P<0.01 vs 60w MWF. (**B**) Proteinuria levels progressively increased with age in MWF rats. ** P<0.01 vs 10w MWF; °P<0.01 vs 25w MWF; §P<0.01 vs 40w MWF; $ P<0.01 vs 50w MWF; † P<0.01 vs 60w MWF.

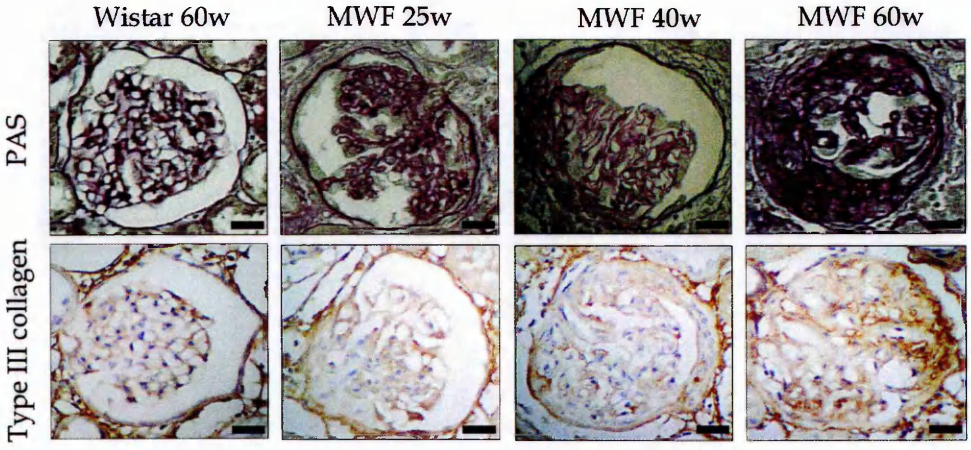

Figure 4. Time-dependent evolution of glomerular lesions in Wistar and MWF rats.

Upper panels show that renal sections of 60 week-old Wistar rats are characterized by few synechiae. In MWF rats, synechiae were present from 10 weeks of age, and more severe crescentic lesions develop from 25 weeks of age and progressively increased with time. Lower panels show representative pictures of type III collagen immunostaining. Synechiae in Wistar rats are not associated with accumulation of type III collagen. Also early crescents found in 25 week-old MWF rats, are negative for type III collagen. In 40 week-old MWF rats, crescents are characterized by scanty accumulation of type III collagen, which progressively increased with time. Scale bars=25 μm

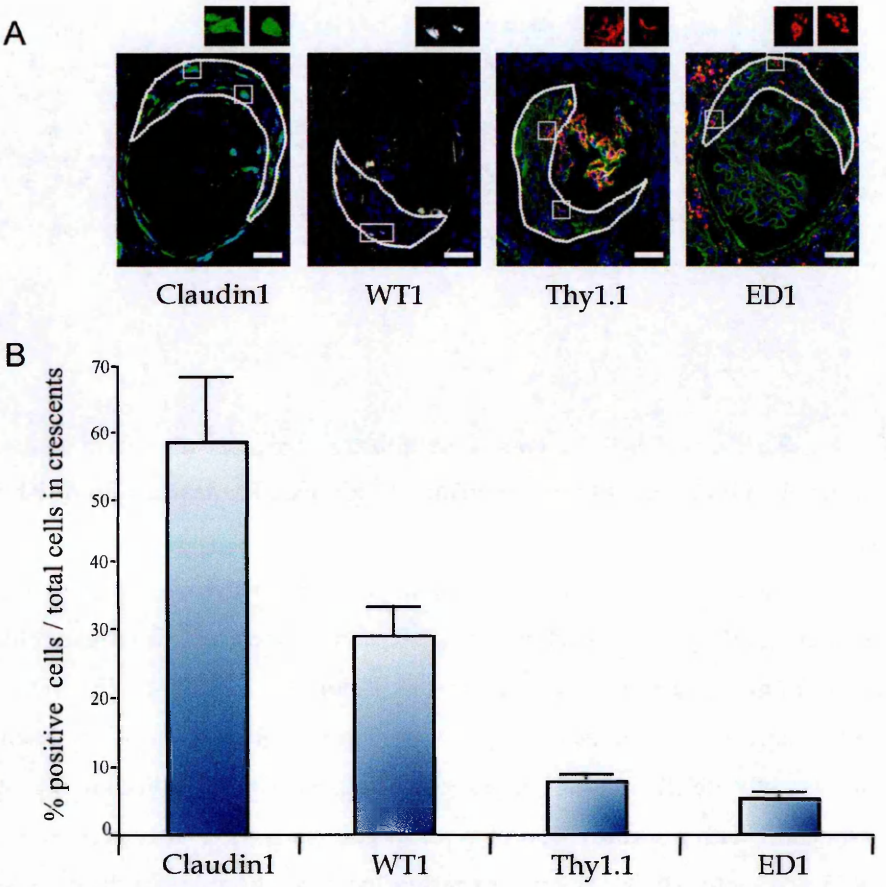

Figure 5. Phenotype of cell populations involved in crescentic lesions. (**A**) Representative pictures of immunofluorescence stainings for claudin1, WT1, Thy1.1 and ED1 in glomeruli of 60 week-old MWF rats. High magnification insets show cells positive for the different markers. Dotted lines define the area of crescents in which positive cells have been quantified. DAPI stains nuclei. Scale bars=25 μm (**B**) Quantitative assessment of cells positive for each marker, reveals that the most represented cell population in crescents consists of claudin1+ cells, and to a lesser extent of WT1+ cells. Thy1.1+ and ED1+ cells represented minor cell populations within the lesions.

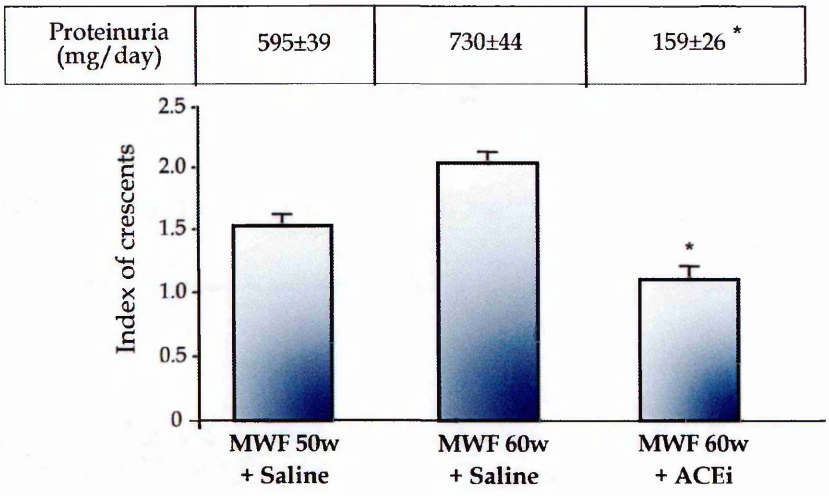

Figure 6. ACE inhibitor lowers proteinuria levels and reduces the number and extension of crescents.

A significant decrease of proteinuria levels and index of crescents was observed in 60 week-old MWF rats receiving ACEi for 10 weeks as compared with animals given saline. * $P<0.01$ vs 60w MWF.

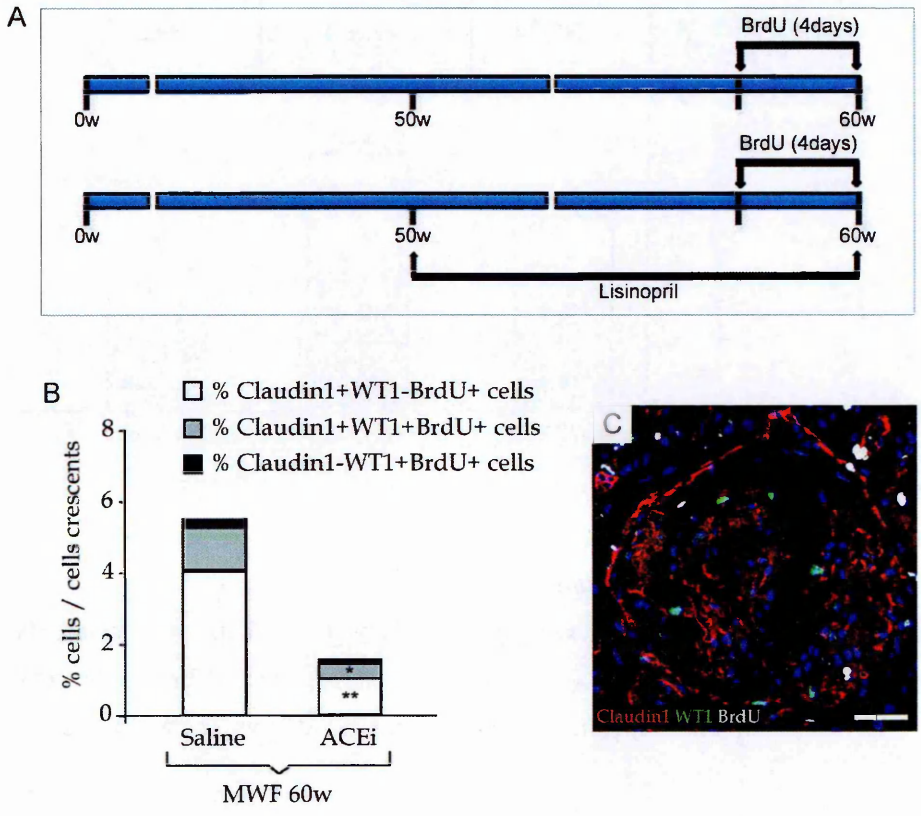

Figure 7. ACE inhibitor limits progenitor cell proliferation and migration.

(**A**) Experimental design. Rats receiving or not lisinopril for 10 weeks, were injected with BrdU 4 days before sacrifice. (**B**) The percentage of BrdU+ claudin1+WT1- cells (white bars), claudin1+WT1+ cells (grey bars), and claudin1-WT1+ cells (black bars), was lower in crescents of ACEi-treated MWF rats in respect with animals given saline. **P<0.05 vs 60w MWF; *P<0.01 vs 60w MWF. (**C**) Representative picture of immunofluorescence staining for claudin1 (red), WT1 (green) and BrdU (white) in 60 week-old MWF rats. DAPI stains nuclei. Scale bar=25 μm

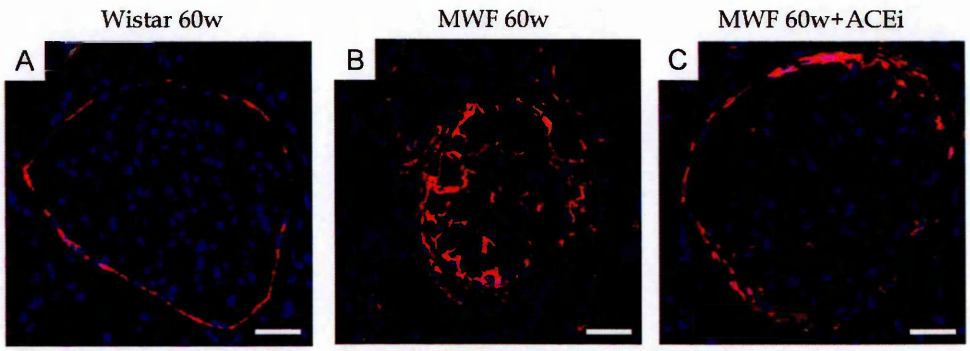

Figure 8. ACE inhibitor limits progenitor cell proliferation and migration.

(A) In Wistar rats, NCAM+ cells were localized along the Bowman's capsule. **(B)** The expression of NCAM increases in glomeruli of 60 week-old MWF rats and localizes in the capillary tuft as well as in crescents. **(C)** ACEi effectively reduced the presence of NCAM+ cells in crescents and restored the distribution of NCAM+ cells in the Bowman's capsule as to the pattern observed in controls. DAPI stains nuclei. Scale bars=25 μm

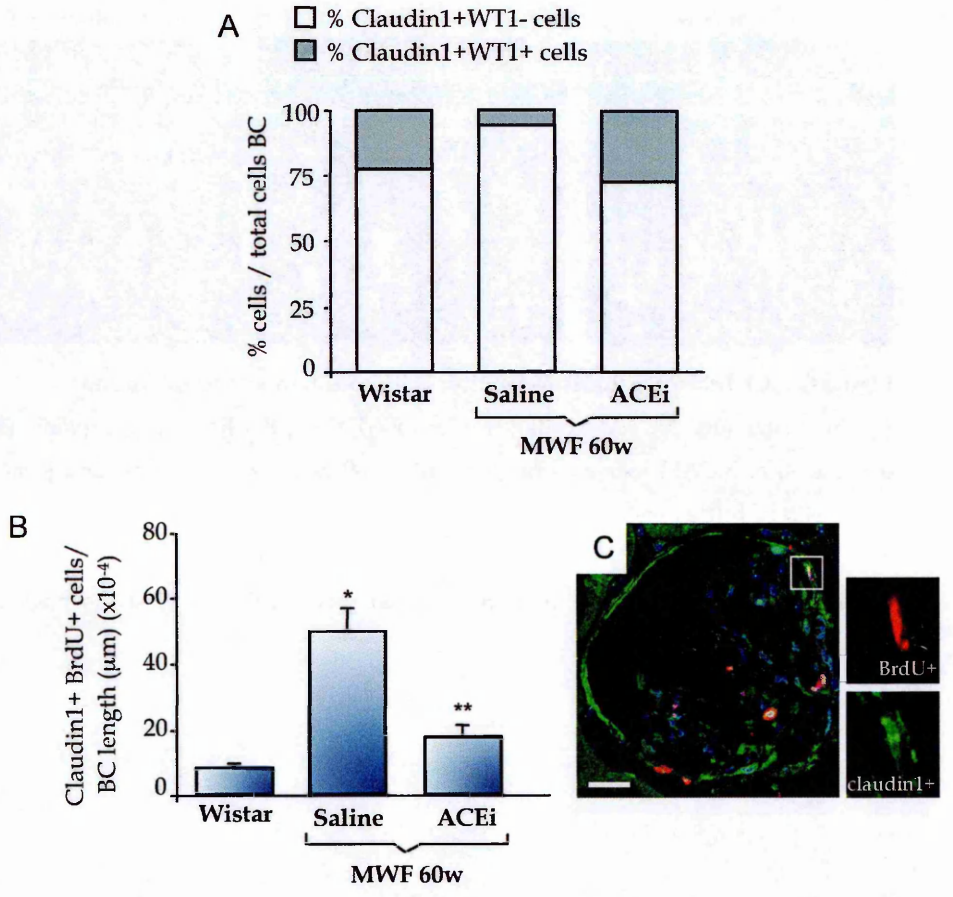

Figure 9. ACE inhibitor reduces proliferation of Bowman's capsule cells. (**A**) In the Bowman's capsule of 60 week-old MWF rats given saline, the percentage of claudin1+WT1- cells is markedly enhanced and claudin1+WT1+ cells is decreased in respect to Wistar rats. ACEi restores the percentage of both cell populations to control levels. (**B**) Cell proliferation of claudin1+ cells along the Bowman's capsule is enhanced in 60 week-old MWF rats given saline as compared with controls. ACEi treatment significantly limits the number of proliferating cells within the Bowman's capsule (claudin1+BrdU+). *P<0.05 vs Wistar; **P<0.01 vs 60w MWF+saline. (**C**) Representative picture of immunofluorescence staining for claudin1 and BrdU in the Bowman's capsule of 60 week-old MWF rats. Inset shows a cell expressing both markers. DAPI stains nuclei. Scale bar=25 μm

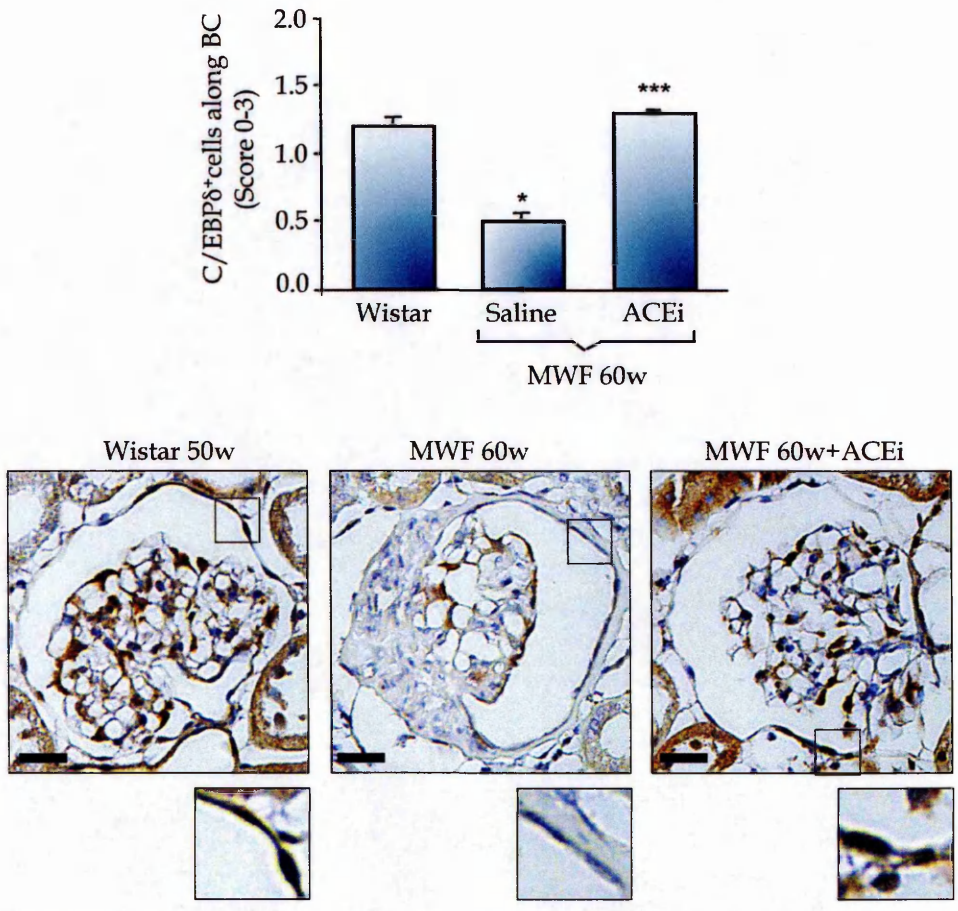

Figure 10. ACE inhibitor regulates the expression of the cell-cycle inhibitor C/EBPδ.

Histogram shows that the expression of C/EBPδ in the Bowman's capsule decreases in MWF rats at 60 weeks of age receiving saline as compared with Wistar rats, and was normalized by ACEi treatment. *P<0.05 vs Wistar; ***P<0.05 vs 60w MWF+saline. In the lower panels and in high-magnification insets, representative pictures show the expression of C/EBPδ in the rat Bowman's capsule. Nuclei were counterstained with hematoxylin. Scale bars=25 μm

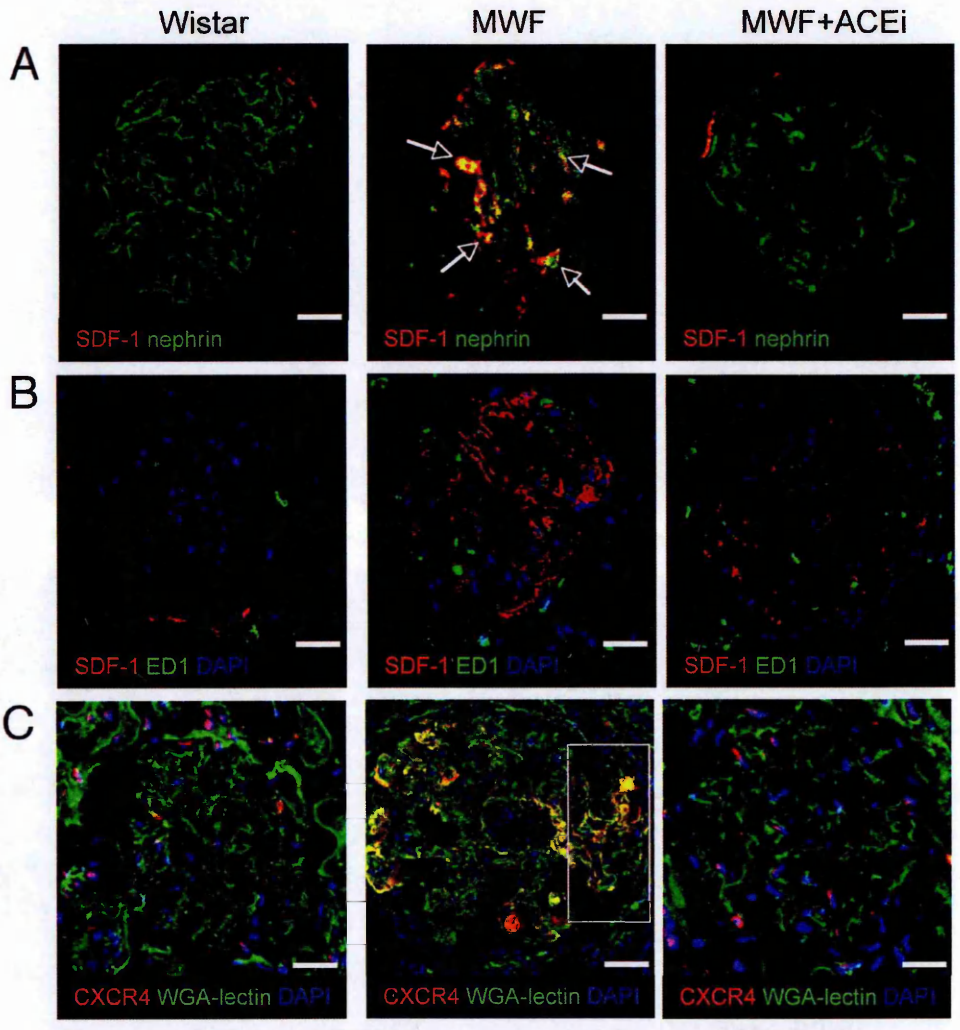

Figure 11. SDF-1 and CXCR4 expression in Wistar and MWF rats

(A) SDF-1 was up-regulated in MWF rats in respect with controls, and co-localized with nephrin (arrows highlighted the double labelled podocytes). ACE inhibitor restored the expression of SDF-1 to control levels. **(B)** Representative photomicrographs of double immunostaining for SDF-1 and ED1 showing that the markers did not overlapped. **(C)** CXCR4 was markedly overexpressed by cells within hyperplastic lesions (inset) in the MWF rat glomerulus. ACE inhibitor treatment normalized the expression of CXCR4 to a level comparable with controls. DAPI (blue) stained nuclei, and renal structures were labelled with fluorescein wheat germ agglutinin (green). Scale bars=25 μm.

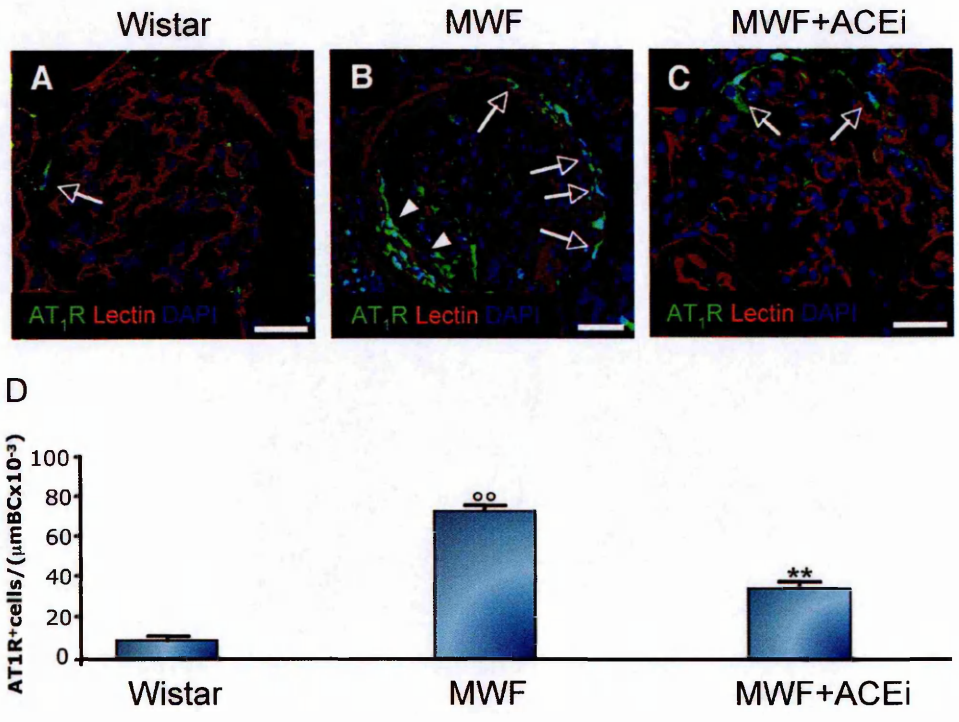

Figure 12. AT_1 receptor expression in PECs of Wistar and MWF rats

(**A**) In Wistar rats used as control, few cells in the Bowman's capsule expressed the AT_1 receptor (arrow). (**B**) In MWF rats given saline, the AT_1 receptor was expressed by the majority of parietal epithelial cells (arrows) as well as by cells within hyperplastic lesions (arrowheads) (**C**) ACE inhibitor treatment reduces the expression of the AT_1 receptor on PECs (arrows). DAPI (blue) stained nuclei, and renal structures were labelled with rhodamine lens culinaris agglutinin (red). Scale bars=25 μm. (**D**) Histogram showing that the number of AT_1 receptor+ cells along the Bowman's capsule was significantly higher in MWF rats given saline as compared with controls. AT_1 receptor over-expression on PECs was reduced by ACE inhibitor treatment. °° $P<0.01$ vs Wistar rats, ** $P<0.01$ vs MWF rats given saline.

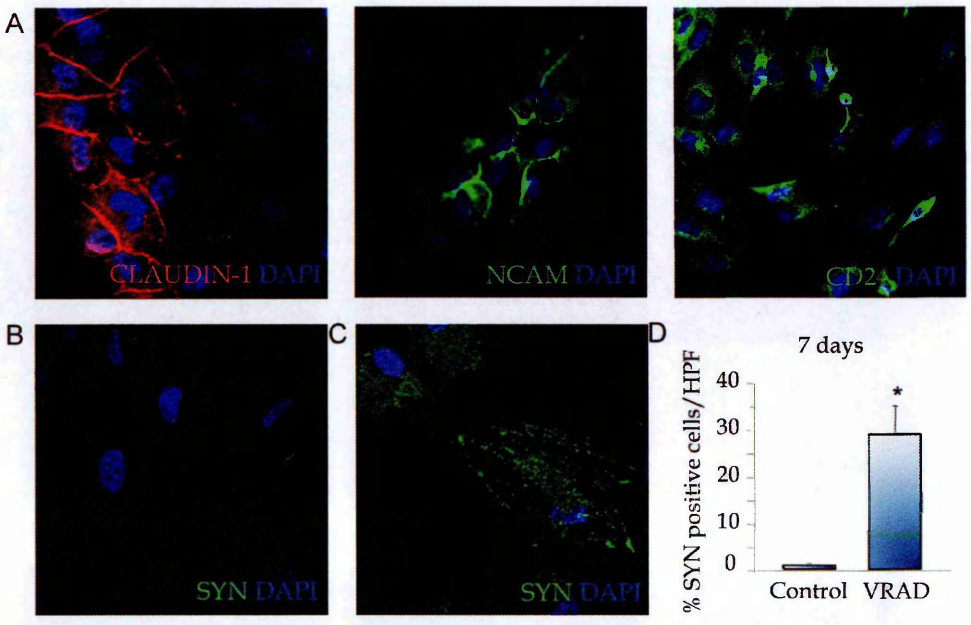

Figure 13. Characterization and differentiation of cultured PECs.

(**A**) Isolated PECs constitutively expressed claudin1, NCAM or CD24. (**B-C**) Representative micrographs of immunoisolated claudin1+ PECs stained with synaptopodin (SYN). No signal for SYN (**B**) was observed in control cells while cells exposed to VRAD medium for 7 days expressed the podocyte marker SYN (**C**). DAPI stains nuclei. Original magnification x630. (**D**) Quantification of the percentage of SYN+ cells in each HPF *P<0.001 vs Control.

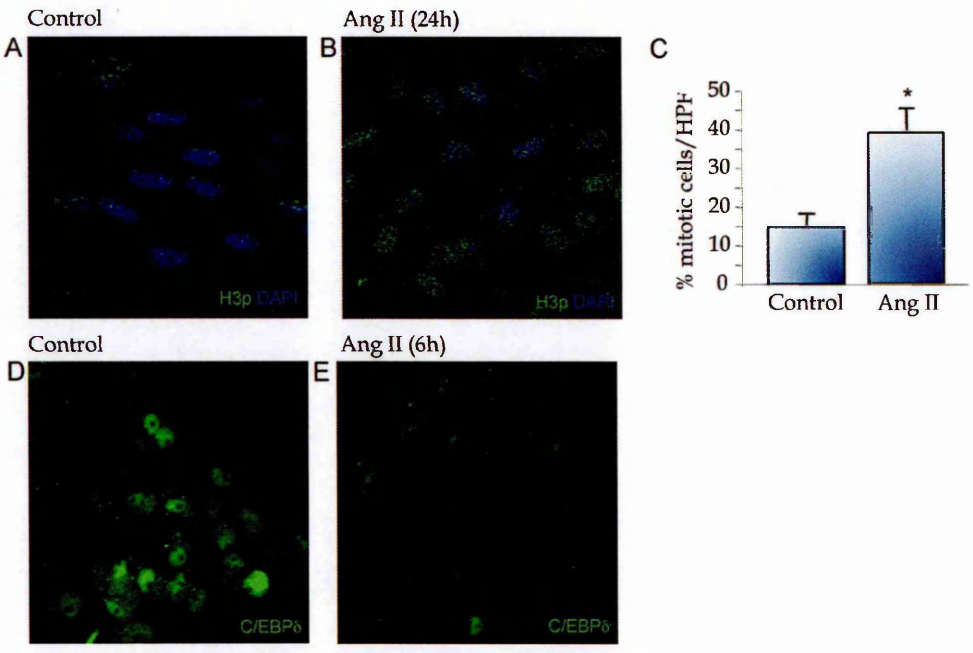

Figure 14. Characterization and differentiation of cultured PECs.

(A-B) Representative images of H3p and DAPI in immunoisolated claudin1+ PECs untreated **(A)** or treated **(B)** with angiotensin II (Ang II) for 24 hours. (I) Quantification of H3p+ cells per each HPF shows that mitotic cells markedly increases when exposed to Ang II in respect to untreated cells. DAPI stains nuclei. *P<0.001 vs control. **(D-E)** Nuclear PECs show a constitutive nuclear expression of the transcription factor C/EBPδ **(E)**, that was markedly reduced after 6 hour-incubation with Ang II **(F)**. Original magnification x630.

CHAPTER 5

RESULTS IN HUMAN TISSUE

5.1 Introduction

Crescentic lesions containing multilayers of cells in the glomerular Bowman's space, are sign of potentially severe injury responsible for evolution to glomerular scarring and chronic renal failure. The most harmful and diffuse crescentic lesions are found in kidneys of patients with inflammatory glomerular diseases, typically crescentic glomerulonephritis, but also other proliferative forms including lupus nephritis, IgA nephropathy, and membranoproliferative glomerulonephritis (Kambham *et al.*, 2012; Jennette *et al.*, 2003).

Although extracapillary lesions are morphologically simple to be recognized, more controversial have been studying their cellular components and their possible pathogenic role. The traditional theories have come largely from immunohistochemical studies that have concluded that multilayered cellular lesions are a mixture of glomerular parietal epithelial cells, macrophages and myofibroblasts (Boucher *et al.*, 1987, Nitta *et al.*, 1999, Jennette *et al.*, 1986). More recent studies also suggested the podocytes as key constituents of the crescents (Moeller *et al.*, 2004, Bariety *et al.*, 2005, Ding *et al.*, 2006, Thorner *et al.*, 2008), but their role remains unclear. Recently, it has been suggested that these extracapillary lesions can be the result of dysregulated proliferation of renal progenitor cells in response to the injured podocytes (Smeets *et al.*, 2009). Nevertheless, the mechanisms and mediators responsible for the intraglomerular accumulation of renal progenitor cells in proliferative

glomerulonephritis remain ill-defined. Evidence in SCID mice with acute renal failure indicates an important role of SDF-1 and its receptor CXCR4 in the therapeutic migration of renal progenitor cells (Mazzinghi *et al.*, 2008). Since activation of the Ang II/AT_1 receptor pathway may contribute to cell proliferation and migration (Kim *et al.*, 2011), we have reasoned that the AT_1 receptor can also play a key role in the abnormal proliferation of renal progenitors underlying the hyperplastic lesions.

Therefore, we have got further insights into the cellular mechanisms and mediators contributing to extracapillary proliferation in humans, by analyzing the contribution of the SDF1/CXCR4 axis and Ang II/AT_1 receptor pathway to the migration and proliferation of renal progenitors, resulting in the progression of extracapillary lesions.

5.2 Clinical and histopathologic characteristics of patient populations

Table 2 showed the clinical and histopathological characteristics of patients whose renal biopsies have been processed and studied. Four diagnostic groups have been considered including extracapillary glomerulonephritis (n=9), IgA nephropathy (n=9), membranous nephropathy (n=7) and diabetic nephropathy (n=11).

The baseline characteristics at the time of biopsy were similar among the different groups. The mean age of the study subjects was 53 years, and there was a slight male predominance, except for patients with

extracapillary glomerulonephritis. There were no differences in baseline systolic and diastolic blood pressure when comparing all the patients, while proteinuria and serum creatinine were slightly lower in patients with IgA nephropathy in respect to the other diagnostic groups.

On the basis of renal histology, glomerular diseases were divided into proliferative and non proliferative pathologies. For each group, the histopathological characteristics including the percentage of partially and totally sclerotic glomeruli, and of glomeruli with some degree of extracapillary proliferation were reported. As shown in table 2, biopsies of patients with extracapillary glomerulonephritis, and at minor extent those with IgA nephropathy, were characterized by an high percentage of glomeruli with extracapillary proliferation. On the contrary, the extracapillary proliferation was absent in biopsies of patients with membranous and diabetic nephropathy. The percentage of glomeruli with global or segmental sclerosis was comparable among all the diagnostic groups, while the number of glomeruli with other glomerular lesions, apart of crescents and sclerosis, was higher in biopsies of patients with non proliferative diseases in respect to patients with extracapillary glomerulonephritis and IgA nephropathy.

Renal biopsies from uninvolved portion of kidney collected for tumor nephrectomy obtained from 10 patients were used as controls.

5.3 CD133$^+$CD24$^+$ renal progenitor cells were major constituents of hyperplastic lesions

According to our previous study (Smeets *et al.*, 2009), crescentic lesions found in biopsies of patients with extracapillary glomerulonephritis were mostly constituted by CD133$^+$CD24$^+$ cells (Figure 15A). To investigate whether migration and accumulation of progenitor cells occurs in renal diseases characterized by active cell proliferation, we also analyzed biopsies of patients with IgA nephropathy, in which abundant CD133$^+$CD24$^+$ cells was consistently found in all segmental lesions between the Bowman's capsule and the glomerular capillary tuft (Figure 15B). To assess whether exuberant progenitor cell accumulation was confined to proliferative disorders, we next evaluated CD133 and CD24 staining in biopsies from patients with membranous nephropathy (Figure 15C) and diabetic nephropathy (Figure 15D). In these latter settings, progenitor cells did not display any sign of migration and were found in the Bowman's capsule, in a manner similar to controls (Figure 15E).

5.4 CXCR4 was overexpressed in progenitor cells within extracapillary lesions

A recent *in vitro* study documents the expression of the chemokine receptor CXCR4 in human renal progenitor cells, which is related to the

migratory property of these cells (Mazzinghi *et al.*, 2008). Here we evaluated the localization of CXCR4 in biopsies of patients with proliferative glomerulonephritis and non proliferative glomerular disorders. In both extracapillary glomerulonephritis and IgA nephropathy, a high CXCR4 expression was observed, which co-localized with CD24 progenitor marker within hyperplastic lesions (Figure 16A).

On the contrary, in biopsies from patients with non proliferative disorders such as membranous nephropathy or diabetes (Figure 16B and C), the expression of CXCR4 was faint and it was restricted to a few $CD24^+$ progenitor cells along the Bowman's capsule, as a pattern similar to those observed in glomeruli from normal kidneys (Figure 16D).

5.5 Podocytes expressed the CXCR4 ligand SDF-1

The increased expression of CXCR4 by renal progenitor cells observed in patients with proliferative disorders in respect to controls, paralleled a significant increase of the CXCR4 ligand SDF-1 (Fig 17A and B). Semi-quantitative evaluation of SDF-1 immunostaining revealed that the difference was statistically significant (Figure 17C, $P<0.05$). A phenotypic characterization of SDF-1-expressing cells by double immunolabelings revealed that podocytes within the glomerular tuft expressed SDF-1, suggesting that they can presumably provide the ligand for CXCR4 in patients with proliferative glomerulonephritis (Figure 17A).

SDF-1 was also expressed by few PECs, at a comparable extent in proliferative diseases and in controls (Figure 17A and B). On the contrast, $CD68^+$ macrophages, which infiltrated the hyperplastic lesions, were not the cellular source of SDF-1 (Figure 17D) as documented by the absence of co-localization between the two markers.

5.6 AT_1 receptor overexpression on progenitor cells in human proliferative disorders

Given the potential role of Ang II/AT_1 receptor pathway to favour cell proliferation and migration (Kim *et al.*, 2011), we then analyzed the localization of AT_1 receptor in proliferative disorders. In both patients with extracapillary glomerulonephritis and IgA nephropathy, AT_1 receptor was abundantly expressed by cells along the Bowman's capsule as well as within cellular synechiae, the early morphological abnormalities preceding extracapillary lesion formation (Figure 18A, arrows). That AT_1 receptor-expressing cells were progenitors, was documented by double immunofluorescence staining with the progenitor cell marker CD24 (Figure 18B). As shown in the inset in Figure 18B, in patients with proliferative diseases AT_1 receptor expression was maintained by progenitor cells forming crescentic lesions. This was not the case in bioptic tissues from patients with non proliferative disorders (Figure 18C) and in normal kidney (Figure 18D), where AT_1 receptor expression was only

restricted to few progenitor cells in the Bowman's capsule (Figure 18C and D, arrows), as also documented by co-localization of the AT_1 receptor with CD24 (inset in Figure 18E).

5.7 ACE inhibitor therapy limited the formation of crescentic lesions in a patient with extracapillary glomerulonephritis

To provide evidence that up-regulation of AT_1 receptor contributes to the formation of glomerular hyperplastic lesions, we took advantage of the case of a 69 year-old patient with ANCA-positive crescentic glomerulonephritis (already included in the cohort of patients studied here) who underwent a repeated renal biopsy after 8 month treatment with an ACE inhibitor (Figure 19A). At the time of the first biopsy, 73.7% glomeruli were affected by florid extracapillary proliferation, while the remnant glomeruli were totally sclerotic and no one glomerulus was intact and free of lesions (Figure 19B and C). Because of high proteinuria (2.60 g/day) and severe renal insufficiency (serum creatinine 6.99 mg/dl), the patient received standard immunosuppressive therapy with steroids and cyclophosphamide. After 7 month treatment, proteinuria worsened (3.70 g/day) despite mild amelioration of renal function (serum creatinine 4.37 mg/dl, Figure 19A). Thus, the therapy was modified and increasing doses of the ACE inhibitor ramipril (from 2.5 to 7.5 mg/day) in association with azathioprine were started (Figure 19A). Eight months later, both

proteinuria and serum creatinine levels were markedly reduced to 1.34 g/day and 1.74 mg/dl respectively (Figure 19A). At this time, a second biopsy revealed that all glomeruli in the tissue specimen were totally free of crescents, suggesting the remission of crescentic lesions observed in the first biopsy (Figure 19B, C and D). Overall 38.5% of glomeruli were normal, while 46.1% showed global sclerosis.

5.8 ACE inhibitor renoprotection occurred via the restoration of CXCR4 and AT_1 receptor expression

Double immunostaining of the first biopsy revealed that the AT_1 receptor was highly expressed and co-localized on $CD24^+$ progenitor cells in the area of hyperplasia (Figure 20A). In the repeated biopsy after ACE inhibitor treatment, AT_1 receptor staining was markedly reduced on $CD24^+$ progenitor cells (Figure 20B), which were no longer present within the extracapillary space, but only localized along the Bowman's capsule, as previously documented in patients with non proliferative diseases as well as in normal kidneys (Figure 15C, D and E).

The decrease of AT_1 receptor after ACE inhibitor paralleled a strong reduction of CXCR4 expression, which in the first biopsy co-localized with the progenitor cell marker CD24 in the majority of cells in crescentic lesions (Figure 20C), while after ACE inhibitor treatment was only faintly expressed (Figure 20D). Of note, CXCR4 immunostaining after

pharmacological treatment was comparable to that previously observed in patients with non proliferative nephropathies and in the normal kidney (Figure 16B, C and D).

	Proliferative		Non proliferative	
	Extracapillary Glomerulonephritis	IgA Nephropathy	Membranous Nephropathy	Diabetic Nephropathy
Patients (*n*)	9	9	7	11
Age (*years-range*)	32-81	32-50	44-66	54-70
Sex (*M:F*)	3:6	7:1	4:3	9:1
SBP (*mmHg*)	135.6±4.7	126.0±8.1	136.8±4.7	145.8±5.4
DBP (*mmHg*)	80.0±1.78	78.8±5.3	80.8±0.8	85.0±2.1
Proteinuria (*g/day*)	5.6±1.4	1.2±0.2	5.6±1.3	4.1±0.6
Serum creatinine (*mg/dl*)	3.9±0.9	1.8±0.6	2.5±0.6	1.2±0.2
Glomeruli with extracapillary proliferation (%)	60.9±8.6	15.0±5.8	0.0±0.0	0.4±0.0
Normal glomeruli (%)	9.4±5.5	16.1±5.6	17.9±4.3	30±7.2
Glomeruli with global sclerosis (%)	17.5±4.3	32.8±9.2	14.8±7.9	15.0±3.8
Glomeruli with segmental sclerosis (%)	4.4±3.0	14.4±3.4	1.9±1.9	27.2±10.2
Other glomerular changes (%)*	21.8±4.2	28.2±4.2	71.4±4.5	49.5±6.4

* capillary loop thickening, mesangial hypercellularity and matrix expansion, epithelial vacuolization

Table 2. Demographic, clinical and histopathologic characteristics of patient populations.

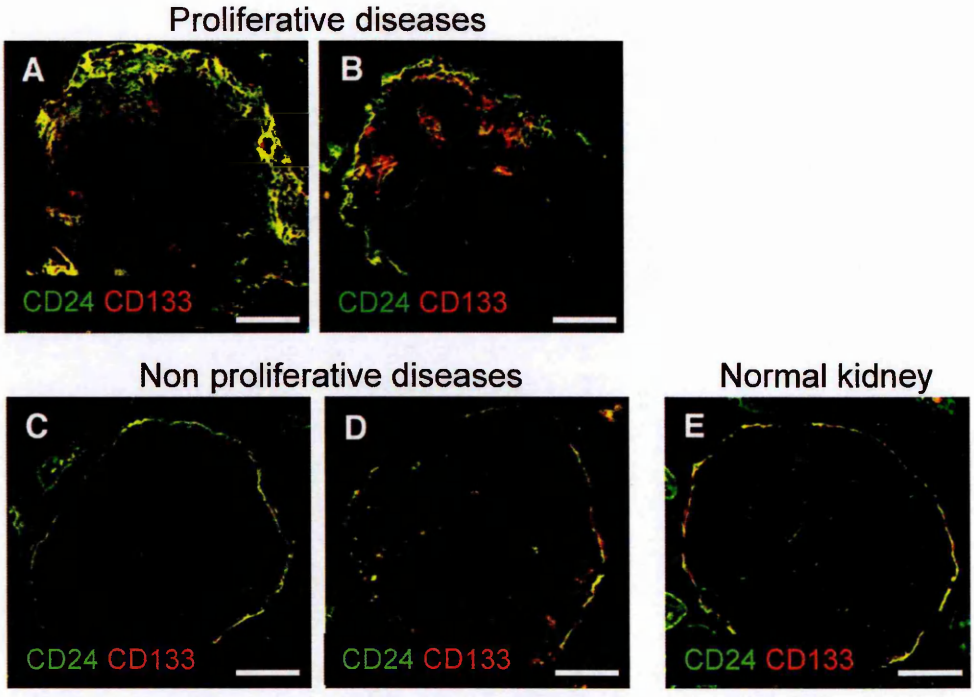

Figure 15. CD24-CD133 expression in patients with proliferative and non proliferative disorders.

Double immunofluorescence staining for CD24 and CD133 revealed that in glomeruli of patients with extracapillary glomerulonephritis (**A**) and IgA nephropathy (**B**) the two antigens co-localized inside crescentic lesions. In membranous nephropathy (**C**) and in diabetic nephopathy (**D**) $CD24^{+}CD133^{+}$ cells were confined to the Bowman's capsule as observed in normal control kidneys (**E**). Scale bars=50 μm.

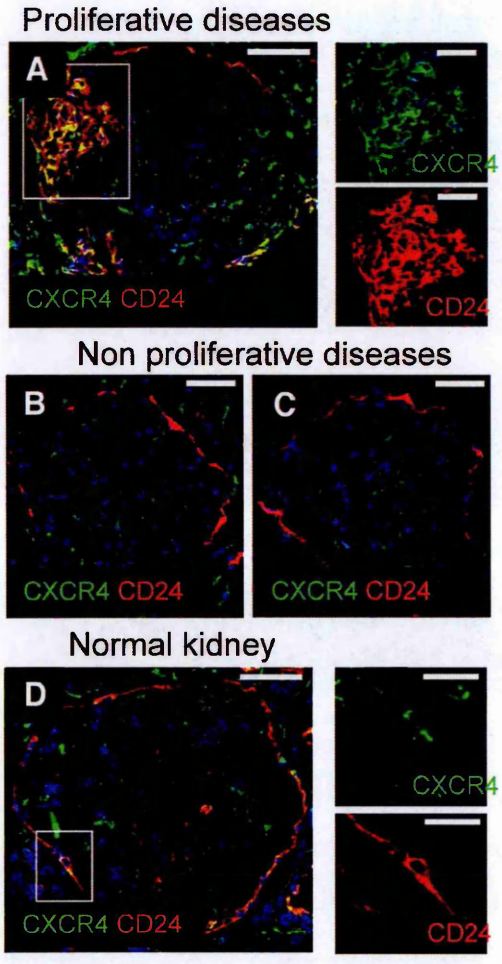

Figure 16. CXCR4 was expressed by CD24$^+$ progenitor cells. **(A)** In patients with extracapillary glomerulonephritis, CXCR4 was expressed by the majority of CD24$^+$ progenitor cells within hyperplastic lesions. (insets). In patients with membranous **(B)** and diabetic **(C)** nephropathies, CXCR4 expression was faint and no cells in the Bowman's capsule co-expressed the CD24 progenitor marker. **(D)** In normal human glomeruli few CD24$^+$ cells in the Bowman's capsule also expressed CXCR4 (insets). DAPI (blue) stained nuclei. Scale bars=50 μm and 25 μm for enlargements.

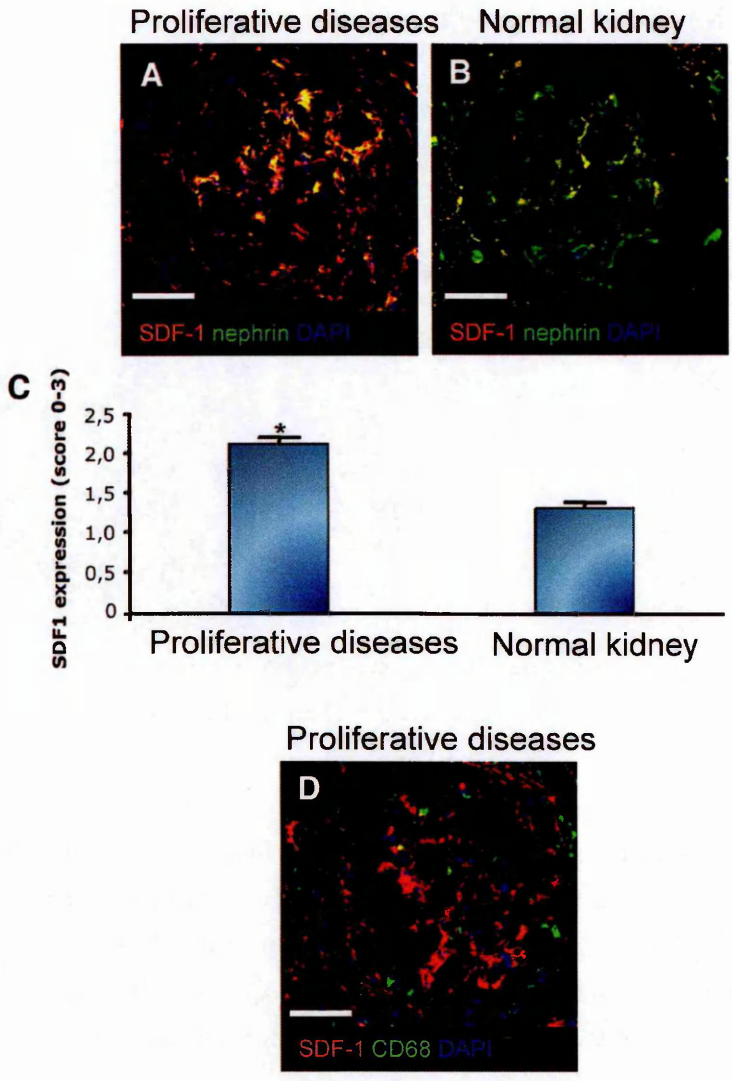

Figure 17. SDF-1 overexpression in proliferative glomerulonephritides. Representative pictures showing SDF-1 and nephrin co-localization in patients with extracapillary glomerulonephritis **(A)** and in control human glomeruli **(B)**. **(C)** Histogram showing that SDF-1 expression was significantly increased in glomeruli of patients with extracapillary glomerulonephritis as compared with normal kidneys. * $P<0.05$ vs normal kidneys. **(D)** Double immunofluorescence staining of SDF-1 and CD68 showed absence of co-localization between the two antigens. DAPI (blue) stained nuclei. Scale bars=50 μm.

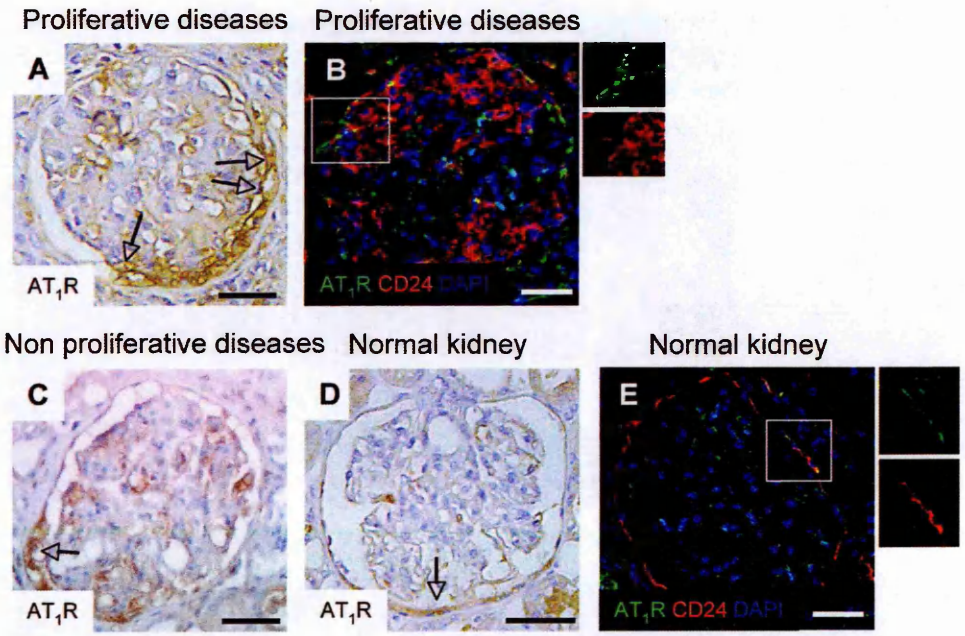

Figure 18. AT_1 receptor expression was up-regulated in proliferative diseases. In patients with extracapillary glomerulonephritis, cells in the area of hyperplasia expressed the AT_1 receptor (arrows) and co-localized with progenitor cell marker CD24 (**B**, insets). Representative photomicrographs of immunoperoxidase staining in non proliferative diseases (**C**) and in a normal human glomerulus (**D**) showing AT_1 receptor expression in a few parietal cells of the Bowman's capsule (arrows). (**E**) Co-localization of AT_1 receptor and CD24 expression showed that in normal human kidneys, the few parietal epithelial cells expressing the AT_1 receptor were progenitor cells (insets). DAPI (blue) stained nuclei. Scale bars=50 μm.

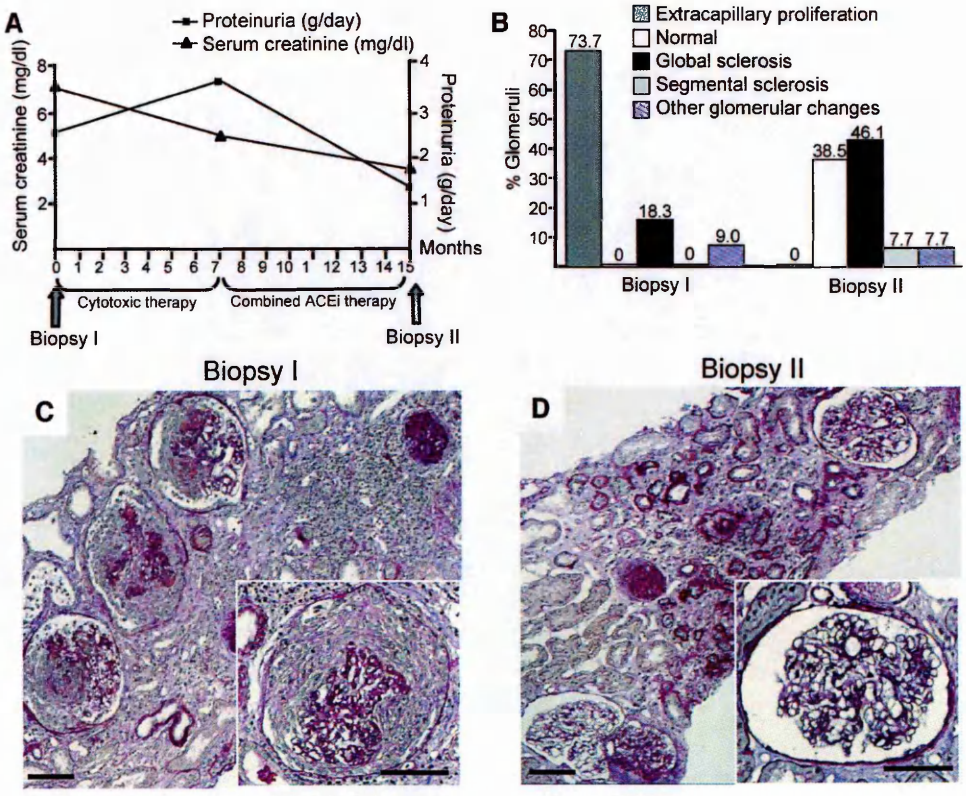

Figure 19. ACE inhibitor therapy ameliorated renal function and morphology in a patient with extracapillary glomerulonephritis.

(A) Study design and clinical findings of a patient with severe ANCA-positive crescentic glomerulonephritis, who underwent renal biopsies before and after ACE inhibitor treatment. (B) Histogram reporting the percentage of glomeruli with different kinds of glomerular lesions observed in renal biopsies obtained before and after ACE inhibitor treatment. (C) PAS-stained biopsy of the patient before ACE inhibitor treatment revealed that the majority of glomeruli were affected by extracapillary proliferation. A representative photomicrograph showing a glomerulus with extracapillary proliferation is illustrated in the high-magnification inset. (D) After ACE inhibitor treatment, all glomeruli of the biopsy were totally free of crescentic lesions, as shown in the representative glomerulus in the high-magnification inset. Scale bars=100 μm.

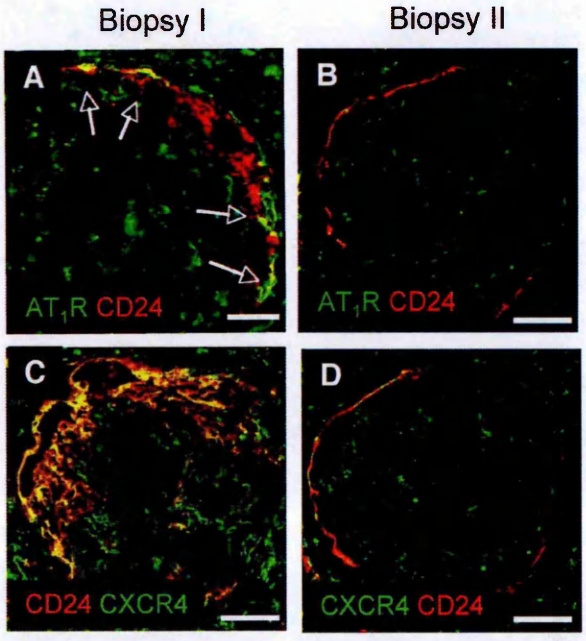

Figure 20. ACE inhibitor therapy limited progenitor cell migration together with normalization of AT_1 receptor and CXCR4 expression in a patient with extracapillary glomerulonephritis.

(A) In patient before ACE inhibitor treatment, AT_1 receptor was overexpressed in $CD24^+$ progenitor cells in the area of hyperplasia (arrows). Scale bar=20 μm. **(B)** Following ACE inhibitor therapy, AT_1 receptor expression was faint and no cells in the Bowman's capsule co-expressed the CD24 progenitor marker. **(C-D)** Double immunostaining for CXCR4 and CD24 showed that, while before ACE inhibitor treatment CXCR4 was expressed by $CD24^+$ progenitor cells in crescents, following the treatment the expression of CXCR4 was strongly reduced. Scale bars=50 μm.

CHAPTER 6

DISCUSSION

In the last years, increasing interest is aroused in determining the pathogenetic role of renal progenitor cells, that are populations of cells with stemness properties which in physiological conditions reside in niches located in different portions of the adult kidney. Among resident renal progenitors, it has been demonstrated that a subset of PECs expressing CD133 and CD24 stem cell markers, normally lying in the Bowman's capsule of healthy human glomeruli, contribute to the formation of hyperplastic lesions in patients with different podocytopathies (Smeets *et al.*, 2009).

Here we confirmed that $CD133^{+}CD24^{+}$ renal progenitor cells proliferate and accumulate into the multilayered crescentic lesions in patients with glomerulonephritides characterized by extracapillary proliferation, including extracapillary glomerulonephritis and IgA nephropathy. Moreover, we have provided evidence that the dysregulated proliferation of $CD133^{+}CD24^{+}$ progenitor cells is a prominent feature of glomerulonephritides with extracapillary proferation, but not of membranous nor diabetic nephropathies, in which progenitor cells line the inner surface of the Bowman's capsule in a manner similar to healthy human glomeruli.

A similar progenitor cell population has been here identified for the first time in rat tissue. In search of a marker of stemness in rats, we have focused on NCAM, normally expressed in rodent and human metanephric mesenchyme, and in the Bowman's capsule of the mature rat kidney

(Abbate *et al.*, 1999; Bard *et al.*, 2001). Here, we show that NCAM is expressed by the large majority of claudin1$^+$ PECs in the Bowman's capsule, and that NCAM$^+$ cells coexpress CD24, a marker of stemness in human and mouse kidneys. Moreover, finding that cultured PECs expressing claudin1 and NCAM, when exposed to an appropriate inductive medium can acquire phenotypic features of differentiated podocytes, further supports the notion that NCAM$^+$ cells represent a progenitor cell population in rats. In agreement with previous findings in humans (Ronconi *et al.*, 2009), co-staining with NCAM and the podocyte marker WT1 allowed to identify three distinct cell populations of epithelial origin in the Bowman's capsule of normal rats: immature progenitor cells expressing only NCAM in absence of podocyte marker WT1, transitional cells expressing markers for both progenitor cells and podocytes (NCAM$^+$WT1$^+$), and more differentiated epithelial cells, the parietal podocytes (NCAM$^-$WT1$^+$).

In parallel with observation in human proliferative diseases, we investigate the contribution of renal progenitor cells during the evolution of glomerular lesions in rats. We have taken advantage of a model of progressive nephropathy characterized by high protenuria and glomerulosclerosis, the MWF rats, in which we have previously demonstrated the effect of ACE inhibitor in reducing glomerular lesions and in regenerating new capillary tufts (Remuzzi A *et al.*, 2006). Here, by studying MWF rats at different weeks of age, the early abnormalities seen

in young rats were bridges between parietal and visceral epithelium, named synechiae, followed by extracapillary crescentic lesions and glomerulosclerosis later on. Accordingly with findings in human biopsies, the majority of cells in crescents are parietal epithelial cells of the Bowman's capsule (claudin1$^+$ PECs), whereas podocytes are present at a lower extent. Claudin1$^+$ PECs within crescents proliferate, as demonstrated by the presence of BrdU-retaining cells in pulsed animals.

Evidence are available that PECs of the Bowman's capsule represent a reservoir of cells that contribute to podocyte physiological turnover (Ronconi *et al.*, 2009). The normal ratio between claudin1$^+$ PECs and parietal podocytes in control rats is altered in old MWF animals, in which claudin1$^+$ PECs increase in number at the expense of parietal podocytes and they actively proliferate, reflecting dysregulation of their ability to generate podocytes and to repair injury. Another possible explanation is that bridges connecting dysfunctional podocytes with the glomerular capsule activate PECs, including NCAM$^+$ progenitor cells, to migrate (Le Hir *et al.*, 2001). Consistent with the low number of BrdU-retaining cells in the Bowman's capsule of control rat is the presence of most PECs expressing the cell cycle inhibitor C/EBPδ (Barbaro *et al.*, 2007). In MWF rats, the scanty expression of C/EBPδ in the Bowman's capsule accounts for the high proliferative rate of claudin1$^+$ PECs. The role of C/EBPδ in maintaining the progenitors in a quiescent state has been confirmed by its marked constitutive expression in cultured NCAM$^+$ PECs

isolated from capsulated glomeruli of control rats. That Ang II decreases C/EBPδ expression and markedly stimulates mitosis of cultured PECs highlights the ability of the peptide to enhance PEC activation status leading to uncontrolled proliferation.

Altogether, these findings indicate that in proliferative diseases in both humans and rats, cells of parietal origin acquired a proliferative phenotype and migrate towards the glomerular tuft contributing to the formation of crescentic lesions. This uncontrolled activation of renal progenitor cells may be triggered by the inflammatory environment, which characterizes the proliferative diseases including the crescentic glomerulonephritis, and by the consequent release of mediators from the glomerular tuft.

In a search of mediators responsible for the abnormal behaviour of progenitor cells in proliferative diseases, we have hypothesized a role for the SDF-1/CXCR4 pathway, due to its property in promoting cell migration and proliferation (Lapidot *et al.*, 2005; Ratajczak *et al.*, 2006). Accordingly, evidence is available that the expression of CXCR4 on cancer cells positively correlates with the metastatic potential of multiple tumors (Reckamp *et al.*, 2008), and that the interaction of CXCR4 with its ligand SDF-1 is the principal effector of hematopoietic stem cell mobilization from the bone marrow (Lapidot *et al.*, 2005). In addition, CXCR4 receptor has been previously found in $CD133^{+}CD24^{+}$ progenitor cells isolated from normal human kidney (Mazzinghi *et al.*, 2008). Based on these studies, we

deepen the possible involvement of CXCR4 in the abnormal migration of progenitor cells in both patients with proliferative diseases and in MWF rat model of progressive nephropathy. In healthy human glomeruli, only few cells in the Bowman's capsule are positive for CXCR4, whereas in proliferative disorders the expression of CXCR4 is markedly increased, especially in $CD24^+$ progenitor cells forming the crescentic lesions. By contrast, the faint expression of CXCR4 in membranous and diabetic nephropathies indicates that progenitor cells have little or no propensity to invade the Bowman's space in non proliferative diseases. A possible explanation of the increased CXCR4 expression exclusively in proliferative diseases is offered by the inflammatory nature of these glomerular disorders. In crescentic glomerulonephritis, immune complex localization in the glomerular capillary wall and mesangium, induces the recruitment of neutrophils and monocytes/macrophages to the glomerular tuft (Sitprija *et al.*, 1980; Lai *et al.*, 1982). Activated cells which infiltrate the glomerulus release soluble cytokines and chemokines that enter the Bowman's space (Sitprija *et al.*, 1974; Lambertucci *et al.*, 1988; Indraprasit *et al.*, 1985), eventually contributing to up-regulation of chemokine receptors located on progenitor cells of the Bowman's capsule (Boucher *et al.*, 1987; Ophascharoensuk *et al.*, 1998, Lan *et al.*, 1992). Here, in patients with proliferative disorders, $CD68^+$ macrophages infiltrating the glomerular tuft (Sanchez-Martin *et al.*, 2011) do not express SDF-1, which is conversely produced by the podocytes activated by the inflammatory microenvironment (Sayyed *et al.*, 2009). The presence of SDF-1 provides

the ligand for the receptor CXCR4 which is up-regulated on $CD133^+CD24^+$ parietal progenitor cells, ultimately promoting their migration and proliferation. Consistently, in MWF rats, the finding of a similar expression pattern of CXCR4 in activated PECs, and of SDF-1 in podocytes, further suggests that SDF-1 production by podocytes is involved in parietal progenitor cell activation leading to crescentic lesion formation.

Besides chemokines, local production of Ang II, the key peptide of the renin-angiotensin system (RAS), is increased in proteinuric glomerulonephritis (Kinoshita *et al.*, 2011). Phlogogenic cells can release enzymes that generate Ang II, including ACE in monocytes/macrophages (Nahmod *et al.*, 2003; Wassmann *et al.*, 2001). The local accumulation of Ang II activates AT_1 receptors further sustaining the inflammatory environment *via* the production of reactive oxygen species, cytokines and adhesion molecules (Brasier *et al.*, 2002). Since Ang II promotes cell migration and proliferation via AT_1 receptor (Kim *et al.*, 2011), we sought to assess whether renal progenitor cells contribute to the progression of hyperplastic lesions as a response to the excessive expression of this receptor on their surface. Here, in patients with proliferative disorders, an high number of progenitor cells located in the Bowman's capsule and within the crescentic lesions expresses AT_1 receptor. By contrast, in patients with membranous and diabetic nephropathies, only rare cells of the Bowman's capsule demonstrate AT_1 receptor immunoreactivity, in a

manner similar to normal human glomeruli. Consistently in MWF rats, the majority of cells lining the Bowman's capsule as well as those constituting the hyperplastic lesions are highly expressive of the AT_1 receptor. These data suggest a contribution of the Ang II/AT_1 receptor pathway to the abnormal behaviour of renal progenitors in proliferative diseases. A schematic representation showing the contribution of SDF-1/CXCR4 and angII/AT1 receptor pathways in crescentic lesion formation is given in Figure 21.

Another unprecedented result of the present study is that ACE inhibitor, beside the well-known effect of lowering blood pressure and proteinuria, limited the formation of crescents in MWF rats with very advanced nephropathy, preventing the accumulation of extracellular matrix and the evolution towards glomerulosclerosis. The reparative process induced by ACE inhibitor parallels a marked reduction of PEC and podocyte proliferation both in crescents and in the Bowman's capsule, as demonstrated by restoration of BrdU and C/EBPδ expression to control levels. Re-establishment of normal glomerular architecture by ACE inhibition associates with reduced activation of $NCAM^+$ progenitors and restoration of their distribution along the Bowman's capsule.

Accordingly with findings in the rat model, we found a patient with extracapillary glomerulonephritis where 8 month-treatment with the ACE inhibitor ramipril induces a complete regression of extracapillary lesions, and possible regeneration of new capillary tufts. In both humans

and rats, the regression of glomerular hyperplasia following ACE inhibitor treatment parallels the normalization of the up-regulated expression of the AT_1 receptor on renal progenitor cells, further suggesting the involvement of AT_1 receptor expression in the development of proliferative disorders. Moreover, a possible link between AT_1 receptor and CXCR4 expression comes from the negligible CXCR4 expression by progenitor cells in the Bowman's space observed in the biopsy specimen collected after ACE inhibitor treatment, as well as in MWF rats treated with lisinopril. This relationship is further supported by findings that RAS inhibition with ACE inhibitors or AT_1 receptor blockers attenuates CXCR4 mRNA expression and protein levels in the left atria in patients with chronic atrial fibrillation and mitral valve disease (Wang *et al.*, 2009).

Altogether, in this study we demonstrated that in presence of an extended renal damage in inflammatory proliferative disesases, renal progenitor cells lose their physiological ability to replace injured podocytes and actively proliferate, thus contributing to renal disesase progression. These data suggest a possible pathway through which the ACE inhibitor reduces crescentic lesions in human and rat proliferative renal diseases, and provide a clue for designing specific molecules targeted to novel players of renal repair that can possibly foster the intrinsic capacity of the kidney to regenerate.

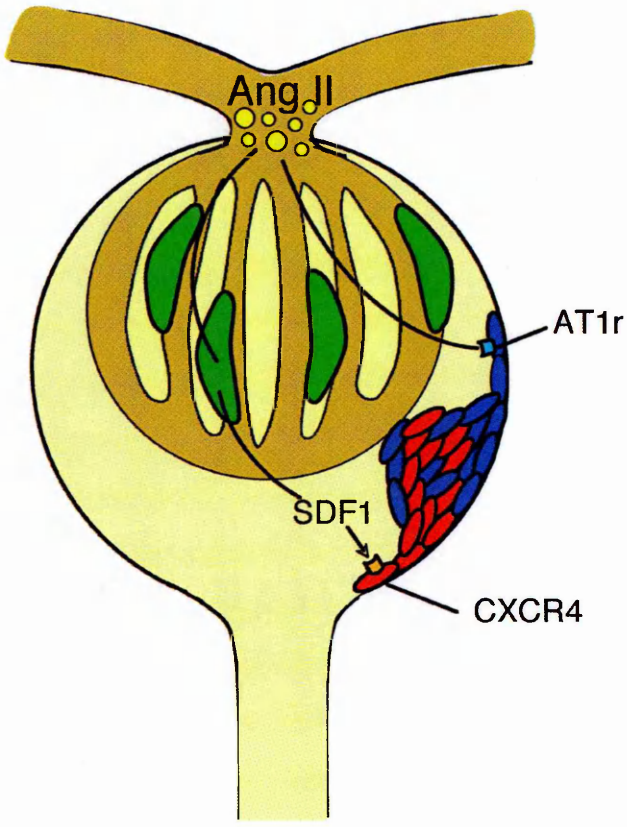

Figure 21. A schematic representation of the pathway involved in crescentic lesion formation.

In humans and animal model of proliferative diseases, ang II (yellow) stimulate visceral podocytes (green) to produce and secrete SDF-1. SDF-1 binds its receptor, CXCR4, expressed by a subset of PECs (red). In parallel, ang II directly activates AT1r-expressing PECs (blue). Both CXCR4 and AT1r promote PEC proliferation and migration towards the capillary tuft, leading to crescent formation.

CHAPTER 7

BIBLIOGRAPHY

Abbate M, Brown D, Bonventre JV. 1999. Expression of NCAM recapitulates tubulogenic development in kidneys recovering from acute ischemia. Am J Physiol. 277:F454-63.

Adamczak M, Gross ML, Krtil J, Koch A, Tyralla K, Amann K, Ritz E. 2003. Reversal of glomerulosclerosis after high-dose enalapril treatment in subtotally nephrectomized rats. J Am Soc Nephrol. 14:2833-2842.

Angelotti ML, Ronconi E, Ballerini L, Peired A, Mazzinghi B, Sagrinati C, Parente E, Gacci M, Carini M, Rotondi M, Fogo AB, Lazzeri E, Lasagni L, Romagnani P. 2012. Characterization of renal progenitors committed toward tubular lineage and their regenerative potential in renal tubular injury. Stem cells. 30:1714-1725.

Appel D, Kershaw DB, Smeets B, Yuan G, Fuss A, Frye B, Elger M, Kriz W, Floege J, Moeller MJ. 2009. Recruitment of podocytes from glomerular parietal epithelial cells. J Am Soc Nephrol 20:333-43.

Barbaro V, Testa A, Di Iorio E, Mavilio F, Pellegrini G, De Luca M. 2007. C/EBP delta regulates cell cycle and self-renewal of human limbal stem cells. J Cell Biol. 177:1037-1049.

Bard JB, Gordon A, Sharp L, Sellers WI. 2001. Early nephron formation in the developing mouse kidney. J Anat. 199:385-392.

Bariety J, Bruneval P, Meyrier A, Mandet C, Hill G, Jacquot C. 2005. Podocyte involvement in human immune crescentic glomerulonephritis. Kidney Int. 68:1109-1119.

Benigni A, Morigi M, Remuzzi G. 2010. Kidney regeneration. Lancet. 375:1310-7.

Benigni A, Morigi M, Rizzo P, Gagliardini E, Rota C, Abbate M, Ghezzi S, Remuzzi A, Remuzzi G. 2011. Inhibiting angiotensin-converting enzyme promotes renal repair by limiting progenitor cell proliferation and restoring the glomerular architecture. Am J Pathol. 179:628-38.

Blau, H.M., T.R. Brazelton, and J.M. Weimann. 2001. The evolving concept of a stem cell: entity or function? Cell. 105: 829-41.

Boffa JJ, Lu Y, Placier S, Stefanski A, Dussaule JC, Chatziantoniou C. 2003. Regression of renal vascular and glomerular fibrosis: role of angiotensin II receptor antagonism and matrix metalloproteinases. J Am Soc Nephrol. 14:1132-1144.

Boucher A, Droz D, Adafer E, Noel LH. 1987. Relationship between the integrity of Bowman's capsule and the composition of cellular crescents in human crescentic glomerulonephritis. Lab Invest. 56:526-533.

Brasier AR, Recinos A, 3rd, Eledrisi MS. 2002. Vascular inflammation and the renin-angiotensin system. Arterioscler Thromb Vasc Biol. 22: 1257-1266.

Cantley LG. 2005. Adult stem cells in the repair of the injured renal tubule. Nat Clin Pract Nephrol.1:22-32.

Cattell V, Jamieson SW. 1974. The origin of glomerular crescents in experimental nephrotoxic serum nephritis in the rabbit. Lab Invest. 39:584-90.

Challen GA, Martinez G, Davis MJ, Taylor DF, Crowe M, Teasdale RD, Grimmond SM, Little MH. 2004. Identifying the molecular phenotype of renal progenitor cells. J Am Soc Nephrol. 15:2344-2357.

Challen GA, Bertoncello I, Deane JA, Ricardo SD, Little MH. 2006. Kidney side population reveals multilineage potential and renal functional capacity but also cellular heterogeneity. J Am Soc Nephrol. 17:1896-912.

Collins AJ, Foley RN, Herzog C, Chavers B, Gilbertson D, Ishani A, Kasiske B, Liu J, Mau LW, McBean M, Murray A, St Peter W, Guo H, Li Q, Li S, Li S, Peng Y, Qiu Y, Roberts T, Skeans M, Snyder J, Solid C, Wang C, Weinhandl E, Zaun D, Arko C, Chen SC, Dalleska F, Daniels F, Dunning S, Ebben J, Frazier E, Hanzlik C, Johnson R, Sheets D, Wang X, Forrest B, Constantini E, Everson S, Eggers P, Agodoa L. 2009. United States Renal Data System Annual Data Report. Am J Kidney Dis. 53:S1-374.

Couser WG, Remuzzi G, Mendis S, Tonelli M. 2011. The contribution of chronic kidney disease to the global burden of major noncommunicable diseases. Kidney Int. 80:1258-70.

Davis BJ, Forbes JM, Thomas MC, Jerums G, Burns WC, Kawachi H, Allen TJ, Cooper ME. 2004. Superior renoprotective effects of combination therapy with ACE and AGE inhibition in the diabetic spontaneously hypertensive rat. Diabetologia. 47:89-97.

De Broe ME. 2005. Tubular regeneration and the role of bone marrow cells: 'stem cell therapy'--a panacea? Nephrol Dial Transplant. 11:2318-20.

Ding M, Cui S, Li C, Jothy S, Haase V, Steer BM, Marsden PA, Pippin J, Shankland S, Rastaldi MP, Cohen CD, Kretzler M, Quaggin SE. 2006.

Loss of the tumor suppressor Vhlh leads to upregulation of Cxcr4 and rapidly progressive glomerulonephritis in mice. Nat Med. 12:1081-1087.

Dinneen SF, Gerstein HC. 1997. The association of microalbuminuria and mortality in non-insulin-dependent diabetes mellitus. A systematic overview of the literature. Arch Intern Med. 157:1413-1418.

Eggers PW. 2011. Has the incidence of end-stage renal disease in the USA and other countries stabilized? Curr Opin Nephrol Hypertens. 20:241-5.

Fang TC, Alison MR, Cook HT, Jeffery R, Wright NA, Poulsom R. 2005. Proliferation of bone marrow-derived cells contributes to regeneration after folic acid-induced acute tubular injury. J Am Soc Nephrol. 16:1723-32.

Fassi A, Sangalli F, Maffi R, Colombi F, Mohamed EI, Brenner BM, Remuzzi G, Remuzzi A. 1998. Progressive glomerular injury in the MWF rat is predicted by inborn nephron deficit. J Am Soc Nephrol. 9:1399-406.

Fioretto P, Steffes MW, Sutherland DE, Goetz FC, Mauer M. 1998. Reversal of lesions of diabetic nephropathy after pancreas transplantation. N Engl J Med. 339:69-75.

Floege J, Jonson R and Feehally J. 2010. Comprehensive Clinical Nephrology, Fourth Edition.

García-Vicuña R, Gómez-Gaviro MV, Domínguez-Luis MJ, Pec MK, González-Alvaro I, Alvaro-Gracia JM, Díaz-González F. 2004. CC and CXC chemokine receptors mediate migration, proliferation, and matrix metalloproteinase production by fibroblast-like synoviocytes from rheumatoid arthritis patients. Arthritis Reum.50:3866-77.

Goodell MA, Brose K, Paradis G, Conner AS, Mulligan RC. 1996. Isolation and functional properties of murine hematopoietic stem cells that are replicating in vivo. J Exp Med.183:1797-806.

Gridelli B, Remuzzi G. 2000. Strategies for making more organs available for transplantation. N Engl J Med. 343: 404-410.

Hackbart H, Gartner K, Alt JM, Stolte H. 1980. A subline of the Munich Wistar strain, response to selection for surface glomeruli. Rat news lett. 7:23.

Hackbart H, Buttner D, Jarck D, Pothmann M, Messow C, Gartner K. 1983. Distribution of glomeruli in the renal cortex of Munich Wistar Fromter (MWF) rats. Renal Physiol. 6:63-71.

Hackbart H, Gwinner W, Alt JM, Hagemann I, Thiemann A, Finke B. 1991. Proteinuria and blood pressure in correlation to the number of superficial glomeruli. Renal Physiol Biochem. 14:246-52.

Hishikawa K, Marumo T, Miura S, Nakanishi A, Matsuzaki Y, Shibata K, Ichiyanagi T, Kohike H, Komori T, Takahashi I, Takase O, Imai N, Yoshikawa M, Inowa T, Hayashi M, Nakaki T, Nakauchi H, Okano H, Fujita T. 2005. Musculin/MyoR is expressed in kidney side population cells and can regulate their function. J Cell Biol. 169:921-8.

Humes HD, Liu S. 1994. Cellular and molecular basis of renal repair in acute renal failure. J Lab Clin Med. 124:749-54.

Imai N, Hishikawa K, Marumo T, Hirahashi J, Inowa T, Matsuzaki Y, Okano H, Kitamura T, Salant D, Fujita T. 2007. Inhibition of histone deacetylase activates side population cells in kidney and partially reverses chronic renal injury. Stem Cells.25:2469-75.

Imgrund M, Gröne E, Gröne HJ, Kretzler M, Holzman L, Schlöndorff D, Rothenpieler UW. 1999. Re-expression of the developmental gene Pax-2 during experimental acute tubular necrosis in mice 1. Kidney Int. 56:1423-31.

Indraprasit S, Boonpucknavig V, Boonpucknavig S. 1985. IgA nephropathy associated with enteric fever. Nephron. 40: 219-222.

Iwatani, H., T. Ito, E. Imai, Y. Matsuzaki, A. Suzuki, M. Yamato, M. Okabe, and M. Hori. 2004. Hematopoietic and nonhematopoietic potentials of Hoechst (low)/side population cells isolated from adult rat kidney. Kidney Int. 65:1604-14.

Jennette JC, Hipp CG. 1986. The epithelial antigen phenotype of glomerular crescent cells. Am J Clin Pathol. 86:274-280.

Jennette JC. 2003. Rapidly progressive crescentic glomerulonephritis. Kidney Int. 63: 1164-1177.

Just PM, Riella MC, Tschosik EA, Noe LL, Bhattacharyya SK, de Charro F. 2008. Economic evaluations of dialysis treatment modalities. Health Policy. 86:163-80.

Kambham N. 2012. Crescentic Glomerulonephritis: an update on Pauci-immune and Anti-GBM diseases. Adv Anat Pathol. 19:111-124.

Kim S. 2011. Molecular and cellular mechanisms of angiotensin II-mediated cardiovascular and renal diseases. Pharmacological Reviews. 52: 11-34.

Kinoshita Y, Kondo S, Urushihara M, Suga K, Matsuura S, Takamatsu M, Shimizu M, Nishiyama A, Kawachi H, Kagami S. 2011. Angiotensin II type I receptor blockade suppresses glomerular renin-angiotensin system activation, oxidative stress, and progressive glomerular injury in rat anti-glomerular basement membrane glomerulonephritis. Transl Res. 158: 235-248.

Lai KN, Aarons I, Woodroffe AJ, Clarkson AR. 1982. Renal lesions in leptospirosis. Aust N Z J Med. 12: 276-279.

Lambertucci JR, Godoy P, Neves J, Bambirra EA, Ferreira MD. 1988. Glomerulonephritis in Salmonella-Schistosoma mansoni association. Am J Trop Med Hyg. 38: 97-102.

Lan HY, Nikolic-Paterson DJ, Atkins RC. 1992. Involvement of activated periglomerular leukocytes in the rupture of Bowman's capsule and glomerular crescent progression in experimental glomerulonephritis. Lab Invest. 67:743-751.

Lapidot T, Dar A, Kollet O. 2005. How do stem cells find their way home? Blood. 106: 1901-1910.

Le Hir M, Keller C, Eschmann V, Hähnel B, Hosser H, Kriz W. 2001. Podocyte bridges between the tuft and Bowman's capsule: an early event in experimental crescentic glomerulonephritis. J Am Soc Nephrol.12:2060-71.

Limesh M, Annigeri RA, Mani MK, Kowdle PC, Rao BS, Balasubramanian S, Seshadri R. 2012. Retarding the progression of chronic kidney disease with renin angiotensin system blockade. Indian J Nephrol. 22:108-115.

Lindgren D, Boström AK, Nilsson K, Hansson J, Sjölund J, Möller C, Jirström K, Nilsson E, Landberg G, Axelson H, Johansson ME. 2011. Isolation and characterization of progenitor-like cells from human renal proximal tubules. Am J Pathol. 178:828-37.

Ma LJ, Nakamura S, Whitsitt JS, Marcantoni C, Davidson JM, Fogo AB. 2000. Regression of sclerosis in aging by an angiotensin inhibition-induced decrease in PAI-1. Kidney Int. 58:2425-2436.

Macconi D, Sangalli F, Bonomelli M, Conti S, Condorelli L, Gagliardini E, Remuzzi G, Remuzzi A. 2009. Podocyte repopulation contributes to regression of glomerular injury induced by ACE inhibition. Am J Pathol. 174:797-807.

Maeshima, A., S. Yamashita, and Y. Nojima. 2003. Identification of renal progenitor-like tubular cells that participate in the regeneration processes of the kidney. J Am Soc Nephrol. 14:3138-46.

Marinides GN, Groggel GC, Cohen AH, Border WA. 1990. Enalapril and low protein reverse chronic puromycin aminonucleoside nephropathy. Kidney Int. 37:749-757.

Martin GB, Harris CA, Dirks JH. 1974. Evidence of GH deficiency in the Munich-Wistar rat. Endocrinology. 94:1359-1363.

Mazzinghi B, Ronconi E, Lazzeri E, Sagrinati C, Ballerini L, Angelotti ML, Parente E, Mancina R, Netti GS, Becherucci F, Gacci M, Carini M, Gesualdo L, Rotondi M, Maggi E, Lasagni L, Serio M, Romagnani S, Romagnani P. 2008. Essential but differential role for CXCR4 and CXCR7 in the therapeutic homing of human renal progenitor cells. J Exp Med. 205:479-490.

Moeller MJ, Soofi A, Hartmann I, Le Hir M, Wiggins R, Kriz W, Holzman LB. 2004. Podocytes populate cellular crescents in a murine model of inflammatory glomerulonephritis. J Am Soc Nephrol. 15:61-67.

Nahmod KA, Vermeulen ME, Raiden S, Salamone G, Gamberale R, Fernandez-Calotti P, Alvarez A, Nahmod V, Giordano M, Geffner JR.

2003. Control of dendritic cell differentiation by angiotensin II. FASEB J. 17: 491-493.

Nitta K, Horita S, Honda K, Uchida K, Watanabe T, Nihei H, Nagata M. 1999. Glomerular expression of cell-cycle-regulatory proteins in human crescentic glomerulonephritis. Virchows Arch. 435:422-427.

Ohse T, Pippin JW, Vaughan MR, Brinkkoetter PT, Krofft RD, Shankland SJ. 2008. Establishment of conditionally immortalized mouse glomerular parietal epithelial cells in culture. J Am Soc Nephrol. 19:1879-90.

Oliver, J.A., O. Maarouf, F.H. Cheema, T.P. Martens, and Q. Al-Awqati. 2004. The renal papilla is a niche for adult kidney stem cells. J Clin Invest. 114:795-804.

Ophascharoensuk V, Pippin JW, Gordon KL, Shankland SJ, Couser WG, Johnson RJ. 1998. Role of intrinsic renal cells versus infiltrating cells in glomerular crescent formation. Kidney Int. 54:416-425.

O'Rourke J, Yuan R, DeWille J. 1997. CCAAT/enhancer-binding proteindelta (C/EBP delta) is induced in growth-arrested mouse mammary epithelial cells. J Biol Chem. 272:6291-6296.

Perico N, Benigni A, Remuzzi G. 2008. Present and future drug treatments for chronic kidney diseases: evolving targets in renoprotection. Nat Rev Drug Discov. 7:936-953.

Pippin JW, Sparks MA, Glenn ST, Buitrago S, Coffman TM, Diffield JS, Gross KW, Shankland SJ. 2013. Cells of the rennin lineage are progenitors of podocytes and parietal epithelial cells in experimental glomerular disease. Am J Pathol. 183:542-57.

Poulsom R, Forbes SJ, Hodivala-Dilke K, Ryan E, Wyles S, Navaratnarasah S, Jeffery R, Hunt T, Alison MR, Cook T, Pusey C, Wright NA. 2001. Bone marrow contributes to renal parenchymal turnover and regeneration. J Pathol. 195:229-35.

Ratajczak MZ, Zuba-Surma E, Kucia M, Reca R, Wojakowski W, Ratajczak J. 2006. The pleiotropic effects of the SDF-1-CXCR4 axis in organogenesis, regeneration and tumorigenesis. Leukemia. 20: 1915-1924.

Reckamp KL, Strieter RM, Figlin RA. 2008. Chemokines as therapeutic targets in renal cell carcinoma. Expert Rev Anticancer Ther. 8: 887-893.

Remuzzi A, Puntorieri S, Mazzoleni A, Remuzzi G. 1988. Sex-related differences in glomerular ultrafiltration and proteinuria in Munich-Wistar rats. Kidney Int. 34:481-6.

Remuzzi A, Puntorieri S, Alfano M, Macconi D, Abbate M, Bertani T, Remuzzi G. 1992. Pathophysiologic implications of proteinuria in a rat model of progressive glomerular injury. Lab Invest. 67:572-9.

Remuzzi A, Imberti B, Puntorieri S, Malanchini B, Macconi D, Magrini L, Bertani T, Remuzzi G. 1994. Dissociation between antiproteinurin and antihypertensive effect of angiotensin converting enzyme inhibitors in rats. 267:F1034-44.

Remuzzi A, Malanchini B, Battaglia C, Bertani T, Remuzzi G. 1996. Comparison of the effects of angiotensin-converting enzyme inhibition and angiotensin II receptor blockade on the evolution of spontaneous glomerular injury in male MWF/Ztm rats. Exp Nephrol. 4:19-25.

Remuzzi A, Fassi A, Bertani T, Perico N, Remuzzi G. 1999. ACE inhibition induces regression of proteinuria and halts progression of renal damage in a genetic model of progressive nephropathy. Am J Kidney Dis. 34:626-632.

Remuzzi A, Gagliardini E, Donadoni C, Fassi A, Sangalli F, Lepre MS, Remuzzi G, Benigni A. 2002. Effect of angiotensin II antagonism on the regression of kidney disease in the rat. Kidney Int. 62:885-894.

Remuzzi G, Ruggenenti P, Perico N. 2002. Chronic renal diseases: renoprotective benefits of renin-angiotensin system inhibition. Ann Intern Med. 136:604-15.

Remuzzi A, Gagliardini E, Sangalli F, Bonomelli M, Piccinelli M, Benigni A, Remuzzi G. 2006. ACE inhibition reduces glomerulosclerosis and regenerates glomerular tissue in a model of progressive renal disease. Kidney Int. 69:1124-1130.

Remuzzi G, Benigni A, Remuzzi A. 2006. Mechanisms of progression and regression of renal lesions of chronic nephropathies and diabetes. J Clin Invest. 116:288-96.

Ronconi E, Sagrinati C, Angelotti ML, Lazzeri E, Mazzinghi B, Ballerini L, Parente E, Becherucci F, Gacci M, Carini M, Maggi E, Serio M, Vannelli GB, Lasagni L, Romagnani S, Romagnani P. 2009. Regeneration of glomerular podocytes by human renal progenitors. J Am Soc Nephrol. 20:322-32.

Ruggenenti P, Perna A, Benini R, Bertani T, Zoccali C, Maggiore Q, Salvadori M, Remuzzi G. Investigators of the GISEN Group. Gruppo Italiano Studi Epidemiologici in Nefrologia. 1999. In chronic nephropathies prolonged ACE inhibition can induce remission: dynamics of time-dependent changes in GFR. J Am Soc Nephrol. 10:997-1006.

Ruggenenti P, Brenner BM, Remuzzi G. 2001. Remission achieved in chronic nephropathy by a multidrug approach targeted at urinary protein excretion. Nephron. 88:254-259.

Ruggenenti P, Perticucci E, Cravedi P, Gambara V, Costantini M, Sharma SK, Perna A, Remuzzi G. 2008. Role of remission clinics in the longitudinal treatment of CKD. J Am Soc Nephrol. 19:1213-1224.

Sagrinati C, Netti GS, Mazzinghi B, Lazzeri E, Liotta F, Frosali F, Ronconi E, Meini C, Gacci M, Squecco R, Carini M, Gesualdo L, Francini F, Maggi E, Annunziato F, Lasagni L, Serio M, Romagnani S, Romagnani P. 2006. Isolation and characterization of multipotent progenitor cells from the Bowman's capsule of adult human kidneys. J Am Soc Nephrol. 17:2443-56.

Sallustio F, De Benedictis L, Castellano G, Zaza G, Loverre A, Costantino V, Grandaliano G, Schena FP. 2010. TLR2 plays a role in the

activation of human resident renal stem/progenitor cells. FASEB J. 24:514-25.

Sanchez-Martin L, Estecha A, Samaniego R, Sanchez-Ramon S, Vega MA, Sanchez-Mateos P. 2011. The chemokine CXCL12 regulates monocyte-macrophage differentiation and RUNX3 expression. Blood. 117: 88-97.

Sayyed SG, Hagele H, Kulkarni OP, Endlich K, Segerer S, Eulberg D, Klussmann S, Anders HJ. 2009. Podocytes produce homeostatic chemokine stromal cell-derived factor-1/CXCL12, which contributes to glomerulosclerosis, podocyte loss and albuminuria in a mouse model of type 2 diabetes. Diabetologia. 52: 2445-2454.

Schena FP. 1998. Role of growth factors in acute renal failure. Kidney Int Suppl. 66:S11-5.

Segerer S, Nelson PJ, Schlöndorff D. 2000. Chemokines, chemokine receptors and renal disease: from basic science to pathophysiologic and therapeutic studies. J Am Soc Nephrol. 11:152-76.

Singh SK, Jeansson M, Quaggin SE. 2011. New insights into the pathogenesis of cellular crescents. Curr Opin Nephrol Hypertens. 20:258-262.

Sitprija V, Pipantanagul V, Boonpucknavig V, Boonpucknavig S. 1974. Glomerulitis in typhoid fever. Ann Intern Med. 81: 210-213.

Sitprija V, Pipatanagul V, Mertowidjojo K, Boonpucknavig V, Boonpucknavig S. 1980. Pathogenesis of renal disease in leptospirosis: Clinical and experimental studies. Kidney Int. 17: 827-836.

Smeets B, Angelotti ML, Rizzo P, Dijkman H, Lazzeri E, Mooren F, Ballerini L, Parente E, Sagrinati C, Mazzinghi B, Ronconi E, Becherucci F, Benigni A, Steenbergen E, Lasagni L, Remuzzi G, Wetzels J, Romagnani P. 2009. Renal progenitor cells contribute to hyperplastic lesions of podocytopathies and crescentic glomerulonephritis. J Am Soc Nephrol. 20:2593-603.

Swetha G, Chandra V, Phadnis S, Bhonde R. 2009. Glomerular parietal epithelial cells of adult murine kidney undergo EMT to generate cells with traits of renal progenitors. J Cell Mol Med. ????

Taal MW, Brenner BM. 2008. Renal risk scores: progress and prospects. Kidney Int. 73:1216-9.

The GISEN Group (Gruppo Italiano di Studi Epidemiologici in Nefrologia). 1997 .Randomised placebo-controlled trial of effect of ramipril on decline in glomerular filtration rate and risk of terminal renal failure in proteinuric, non-diabetic nephropathy. Lancet, 349:1857-1863.

Thorner PS, Ho M, Eremina V, Sado Y, Quaggin S. 2008. Podocytes contribute to the formation of glomerular crescents. J Am Soc Nephrol. 19:495-502.

Tsukamoto O, Kitakaze M. 2011. It is time to reconsider cardiovascular protection afforded by RAAS blockade - overview of RAAS systems. Cardiovasc Drugs Ther.

Van Der Meer IM, Ruggenenti P, Remuzzi G. 2010. The diabetic CKD patient - a major cardiovascular challenge. J Ren Care. 1: 34-46.

Wang XX, Zhang FR, Zhu JH, Xie XD, Chen JZ. 2009. Up-regulation of CXC chemokine receptor 4 expression in chronic atrial fibrillation patients with mitral valve disease may be attenuated by renin-angiotensin system blockers. J Int Med Res. 37: 1145-1151.

Wassmann S, Laufs U, Baumer AT, Muller K, Konkol C, Sauer H, Bohm M, Nickenig G. 2001. Inhibition of geranylgeranylation reduces

angiotensin II-mediated free radical production in vascular smooth muscle cells: involvement of angiotensin AT1 receptor expression and Rac1 GTPase. Mol Pharmacol. 59: 646-654.

Watanabe N, Kamei S, Ohkubo A, Yamanaka M, Ohsawa S, Makino K, Tokuda K. 1986. Urinary protein as measured with a pyrogallol red-molybdate complex, manually and in a Hitachi 726 automated analyzer. Clin Chem. 32:1551-1554.

Witzgall R, Brown D, Schwarz C, Bonventre JV. 1994. Localization of proliferating cell nuclear antigen, vimentin, c-Fos, and clusterin in the postischemic kidney. Evidence for a heterogenous genetic response among nephron segments, and a large pool of mitotically active and dedifferentiated cells. J Clin Invest. 93:2175-88.

Yamashita S, Maeshima A, Nojima Y. 2005. Involvement of renal progenitor tubular cells in epithelial-to-mesenchymal transition in fibrotic rat kidneys. J Am Soc Nephrol. 16:2044-51.

Ysebaert DK, De Greef KE, Vercauteren SR, Ghielli M, Verpooten GA, Eyskens EJ, De Broe ME. 2000. Identification and kinetics of leukocytes after severe ischaemia/reperfusion renal injury. Nephrol Dial Transplant. 15:1562-74.

Zhang Y, Liu T, Yan P, Huang T, Dewille J. 2008. Identification and characterization of CCAAT/Enhancer Binding protein delta (C/EBP delta) target genes in G0 growth arrested mammary epithelial cells. BMC Mol Biol. 9:83.

CHAPTER 8

APPENDICES

8.1 Contribution to the thesis by other researchers

Part of the thesis project was carried on with the collaboration of other researchers of the Istituto di Ricerche Farmacologiche Mario Negri in Bergamo that contributed to the research as follows:

- Animal care and treatments were conducted in collaboration with Dr. Fabio Sangalli, Laboratory of Renal Biophysics, Istituto di Ricerche Farmacologiche Mario Negri. In particular he evaluated proteinuria, serum creatinine and systolic blood pressure in rats, he administered lisinopril and injected BrdU, and finally he sacrificed the animals.
- Daniela Cavallotti, Unit of Advanced Microscopy, Istituto di Ricerche Farmacologiche Mario Negri, gave me technical assistance for sample observation with electron microscopy.
- Dr. Cinzia Rota, Laboratory of Cell Biology and Regenerative Medicine, Istituto di Ricerche Farmacologiche Mario Negri, helped me in conducting in vitro experiments.

All the other techniques and experiments described in this thesis (sample preparation and cutting, immunofluorescence/immunoperoxidase/ immunogold experiments, in vitro experiments, morphological evaluations, immunolabelling quantifications, statistical analysis) were performed by the PhD student, Paola Rizzo.

8.2 Publications concerning the work described in this thesis

Smeets B, Angelotti ML, Rizzo P, Dijkman H, Lazzeri E, Mooren F, Ballerini L, Parente E, Sagrinati C, Mazzinghi B, Ronconi E, Becherucci F, Benigni A, Steenbergen E, Lasagni L, Remuzzi G, Wetzels J, Romagnani P. Renal progenitor cells contribute to hyperplastic lesions of podocytopathies and crescentic glomerulonephritis. *J Am Soc Nephrol* 2009 Dec;20(12):2593-603.

Benigni A*, Morigi M*, Rizzo P*°, Gagliardini E, Rota C, Abbate M, Ghezzi S, Remuzzi A, Remuzzi G. Inhibiting angiotensin-converting enzyme promotes renal repair by limiting progenitor cell proliferation and restoring the glomerular architecture. *American Journal of Pathology* 2011 Aug;179:628-638. * equally contributing to the work, ° correspoding author

Rizzo P*, Perico N*, Gagliardini E, Novelli R, Alison MR, Remuzzi G, Benigni A. Nature and mediators of parietal epithelial cell activation in glomerulonephritides of human and rat. *American Journal of Pathology* 2013 Dec;183(6):1769-78. * equally contributing to the work

8.3 Full list of publications by the candidate on topics not associated with the work described in the thesis

Guidetti GF, Bernardi B, Consonni A, Rizzo P, Gruppi C, Balduini C, Torti M. Integrin alpha2beta1 induces phosphorylation-dependent and phosphorylation-independent activation of phospholipase Cgamma2 in platelets: role of Src kinase and Rac GTPase. *J Thromb Haemost* 2009 Jul;7(7):1200-6.

Perico N, Casiraghi F, Introna M, Gotti E, Todeschini M, Cavinato RA, Capelli C, Rambaldi A, Cassis P, Rizzo P, Cortinovis M, Marasà M, Golay J, Noris M, Remuzzi G. Autologous mesenchymal stromal cells and kidney transplantation: a pilot study of safety and clinical feasibility. *Clinical J Am Soc Nephrol* 2011 Feb;6:412-422.

Macconi D, Tomasoni S, Romagnani P, Trionfini P, Sangalli F, Mazzinghi B, Rizzo P, Lazzeri E, Abbate M, Remuzzi G, Benigni A. MicroRNA-324-3p promotes renal fibrosis and is a target of ACE inhibition. *J Am Soc Nephrol* 2012 Sep;23(9):1496-505.

Xinaris C, Benedetti V, Rizzo P, Abbate M, Corna D, Azzolini N, Conti S, Unbekandt M, Davies JA, Morigi M, Benigni A, Remuzzi G. In vivo maturation of functional renal organoids formed from embryonic cell suspensions. *J Am Soc Nephrol* 2012 Nov;23(11):1857-68.

Gagliardini E, Perico N, Rizzo P, Buelli S, Longaretti L, Perico L, Tomasoni S, Zoja C, Macconi D, Morigi M, Remuzzi G, Benigni A. Angiotensin II

contributes to diabetic renal dysfunction in rodents and humans via Notch1/Snail pathway. *American Journal of Pathology* 2013 Jul;183(1):119-30.

Perico N, Casiraghi F, Gotti E, Introna M, Todeschini M, Cavinato RA, Capelli C, Rambaldi A, Cassis P, Rizzo P, Cortinovis M, Noris M, Remuzzi G. Mesenchymal stromal cells and kidney transplantation: pretransplant infusion protects from graft dysfunction while fostering immunoregulation. *Transplant International* 2013 May 20.

Buelli S, Rosanò L, Gagliardini E, Corna D, Longaretti L, Pezzotta A, Perico L, Conti S, Rizzo P, Novelli R, Morigi M, Zoja C, Remuzzi G, Bagnato A, Benigni A. β-arrestin-1 drives ET-1-mediated podocyte activation and sustains renal injury. Accettato alla rivista *J Am Soc Nephrol.*

8.4 Congress presentations related to the work described in this thesis

Poster presentation

"*American Society of Nephrology*" congress, Denver (Colorado, USA), 17-21 November 2010.

Rizzo P, Morigi M, Gagliardini E, Rota C, Remuzzi G, Benigni A. Dysregulated glomerular stem/progenitor cells participate in crescent formation in Munich Wistar Fromter (MWF) rats, ACEi modulates stem cell activation and preserves the niche.

ACKNOWLEDGMENTS

I would like to express my sincere gratitude to Professor Silvio Garattini, Director of the Istituto di ricerche farmacologiche Mario Negri, and Professor Giuseppe Remuzzi, Researcher Coordinator of the Mario Negri laboratories of Bergamo. I would thank them for their total commitment to scientific research and for the possibility they give to young researchers to growth in this Institute.

I am indebted to Dr. Ariela Benigni, my Director of the Studies, for her help in supervising my work over these years and for her unique scientific support.

I am grateful to Professor Malcolm Alison, my external supervisor, for his willingness and competence in supervising my PhD project. I feel honoured to have worked with him.

A heartfelt thanks goes to Dr. Elena Gagliardini, head of the Unit of Advanced Microscopy, and Dr. Susanna Tomasoni, head of the Laboratory of Gene Therapy and Cellular Reprogramming, for their trust in my work, and to all the people of my laboratory, Sara, Daniela and in particular Daniela and Rubina, that always stand me!

Special thanks to all the researchers who contributed to this study: Marina Morigi, Cinzia Rota, Fabio Sangalli, Norberto Perico, Mauro Abbate, Andrea Remuzzi, Rubina Novelli, Elena Gagliardini and Daniela Cavallotti.

Finally thanks to my loving family, my mother Loretta, my father Flavio and my sister Laura. To my beloved Paolo and to my little sweet Giulia that thirteen months ago had changed my life...